Insulation co-ordination —

Part 4: Computational guide to insulation co-ordination and modelling of electrical networks

ICS 29.080.30

BSI British Standards

National foreword

This Published Document reproduces verbatim IEC TR 60071-4:2004.

The UK participation in its preparation was entrusted to Technical Committee GEL/28, Insulation coordination, which has the responsibility to:

— aid enquirers to understand the text;

— present to the responsible international/European committee any enquiries on the interpretation, or proposals for change, and keep the UK interests informed;

— monitor related international and European developments and promulgate them in the UK.

A list of organizations represented on this committee can be obtained on request to its secretary.

Cross-references

The British Standards which implement international or European publications referred to in this document may be found in the *BSI Catalogue* under the section entitled "International Standards Correspondence Index", or by using the "Search" facility of the *BSI Electronic Catalogue* or of British Standards Online.

This publication does not purport to include all the necessary provisions of a contract. Users are responsible for its correct application.

Compliance with a British Standard does not of itself confer immunity from legal obligations.

This Published Document was published under the authority of the Standards Policy and Strategy Committee on 17 August 2004

Summary of pages

This document comprises a front cover, an inside front cover, the IEC TR title page, pages 2 to 118, an inside back cover and a back cover.

The BSI copyright notice displayed in this document indicates when the document was last issued.

© BSI 17 August 2004

Amendments issued since publication

Amd. No.	Date	Comments

ISBN 0 580 44284 5

TECHNICAL REPORT

IEC
TR 60071-4

First edition
2004-06

Insulation co-ordination –

**Part 4:
Computational guide to insulation co-ordination
and modelling of electrical networks**

CONTENTS

INSULATION CO-ORDINATION –

Part 4: Computational guide to insulation co-ordination and modelling of electrical networks

FOREWORD

1) The International Electrotechnical Commission (IEC) is a worldwide organization for standardization comprising all national electrotechnical committees (IEC National Committees). The object of IEC is to promote international co-operation on all questions concerning standardization in the electrical and electronic fields. To this end and in addition to other activities, IEC publishes International Standards, Technical Specifications, Technical Reports, Publicly Available Specifications (PAS) and Guides (hereafter referred to as "IEC Publication(s)"). Their preparation is entrusted to technical committees; any IEC National Committee interested in the subject dealt with may participate in this preparatory work. International, governmental and non-governmental organizations liaising with the IEC also participate in this preparation. IEC collaborates closely with the International Organization for Standardization (ISO) in accordance with conditions determined by agreement between the two organizations.

2) The formal decisions or agreements of IEC on technical matters express, as nearly as possible, an international consensus of opinion on the relevant subjects since each technical committee has representation from all interested IEC National Committees.

3) IEC Publications have the form of recommendations for international use and are accepted by IEC National Committees in that sense. While all reasonable efforts are made to ensure that the technical content of IEC Publications is accurate, IEC cannot be held responsible for the way in which they are used or for any misinterpretation by any end user.

4) In order to promote international uniformity, IEC National Committees undertake to apply IEC Publications transparently to the maximum extent possible in their national and regional publications. Any divergence between any IEC Publication and the corresponding national or regional publication shall be clearly indicated in the latter.

5) IEC provides no marking procedure to indicate its approval and cannot be rendered responsible for any equipment declared to be in conformity with an IEC Publication.

6) All users should ensure that they have the latest edition of this publication.

7) No liability shall attach to IEC or its directors, employees, servants or agents including individual experts and members of its technical committees and IEC National Committees for any personal injury, property damage or other damage of any nature whatsoever, whether direct or indirect, or for costs (including legal fees) and expenses arising out of the publication, use of, or reliance upon, this IEC Publication or any other IEC Publications.

8) Attention is drawn to the Normative references cited in this publication. Use of the referenced publications is indispensable for the correct application of this publication.

9) Attention is drawn to the possibility that some of the elements of this IEC Publication may be the subject of patent rights. IEC shall not be held responsible for identifying any or all such patent rights.

The main task of IEC technical committees is to prepare International Standards. However, a technical committee may propose the publication of a technical report when it has collected data of a different kind from that which is normally published as an International Standard, for example "state of the art".

IEC 60071-4, which is a technical report, has been prepared by IEC technical committee 28: Insulation co-ordination.

The text of this technical report is based on the following documents:

Enquiry draft	Report on voting
28/156/DTR	28/158/RVC

Full information on the voting for the approval of this technical report can be found in the report on voting indicated in the above table.

This publication has been drafted in accordance with the ISO/IEC Directives, Part 2.

The committee has decided that the contents of this publication will remain unchanged until the maintenance result date indicated on the IEC web site under "http://webstore.iec.ch" in the data related to the specific publication. At this date, the publication will be

- transformed into an International standard
- reconfirmed;
- withdrawn;
- replaced by a revised edition, or
- amended.

A bilingual version of this technical report may be issued at a later date.

INSULATION CO-ORDINATION –

Part 4: Computational guide to insulation co-ordination and modelling of electrical networks

1   Scope and object

This technical report gives guidance on conducting insulation co-ordination studies which propose internationally recognized recommendations

– for the numerical modelling of electrical systems, and

– for the implementation of deterministic and probabilistic methods adapted to the use of numerical programmes.

Its object is to give information in terms of methods, modelling and examples, allowing for the application of the approaches presented in IEC 60071-2, and for the selection of insulation levels of equipment or installations, as defined in IEC 60071-1.

2   Normative references

The following referenced documents are indispensable for the application of this document. For dated references, only the edition cited applies. For undated references, the latest edition of the referenced document (including any amendments) applies.

IEC 60060-1:1989, *High-voltage test techniques – Part 1: General definitions and test requirements*

IEC 60071-1:1993, *Insulation co-ordination – Part 1: Definitions, principles and rules*

IEC 60071-2:1996, *Insulation co-ordination – Part 2: Application guide*

IEC 60076-8:1997, *Power transformers – Part 8: Application guide*

IEC 60099-4:1991, *Surge arresters – Part 4: Metal-oxide surge arresters without gaps for a.c. systems* [1]

IEC 61233:1994, *High-voltage alternating current circuit-breakers – Inductive load switching*

3   Terms and definitions

For the purposes of this document, the following terms and definitions, in addition to those contained in IEC 60071-1, apply.

NOTE   Certain references are taken from the IEC Multilingual Dictionary[1] [2].

---

[1]   A consolidated edition exists, published in 2001, which incorporates the current edition, plus its amendment 1 (1998) and amendment 2 (2001).

[2]   References in square brackets refer to the bibliography.

**3.1
backfeeding**
refers to the conditions of supplying a high-voltage overhead line or cable through a transformer from the low-voltage side

**3.2
back flashover**
flashover of phase-to-earth insulation resulting from a lightning strike to towers and shielding wires [1]

**3.3
back flashover rate**
number of back flashovers of a line per 100 km per year

**3.4
closing of capacitive load**
essentially closing of capacitor banks but also closing of any other capacitive load

**3.5
critical current**
minimum lightning current that induces a flashover on a line

NOTE   The critical current of the line is the smallest critical current among all injection points.

**3.6
direct lightning strike**
lightning striking a component of the network, for example, conductor, tower, or substation equipment [1]

**3.7
energization**
connecting or reconnecting to a source an element of a power system which has no stored energy

**3.8
fault clearing**
interruption of the short-circuit condition on a system

**3.9
limit distance**
distance from the substation after which no overvoltage resulting from a lightning stroke gives rise to an impinging surge dangerous for the substation's equipment

**3.10
line dropping**
disconnection of the line by opening the last circuit-breaker

**3.11
line fault application**
application of a line short-circuit on a system

**3.12
load rejection**
opening of a line breaker during normal power flow causing a certain amount of load to be unsupplied

NOTE   From a temporary overvoltage point of view, the worst case occurs when the remote circuit-breaker of a long line transmitting a significant part of the supply of a power station is opened.

3.13
line re-energization
opening and fast closing of the line circuit-breaker as the consequence of a fault or a relay maloperation

NOTE   With respect to line energization, trapped charges should be taken into account.

3.14
maximum shielding current
maximum lightning current that can hit a phase conductor on a line protected by shielding wires

3.15
parallel line resonance
overvoltage appearing on an unenergized shunt reactor compensated circuit due to capacitive coupling with a parallel energized circuit

3.16
point-on-cycle controlled switching
energization of capacitive load at the instant that the voltage is zero across the circuit-breaker contacts thus eliminating the switching transient

NOTE   De-energization of inductive load ensures a long and weak power arc at zero-current crossing thus eliminating the risk of re-strike and re-ignition.

3.17
representative lightning stroke current
minimum value of lightning current at a specific point of impact which produces overvoltages that the equipment has to withstand; it is deduced from experience

3.18
slow-front overvoltage flashover rate
number of flashovers of a line per 100 km per year due to slow-front overvoltages

3.19
switching resistor
resistance inserted to match the surge impedance of the line in order to limit the switching surge magnitude launched from the source

3.20
switching of inductive and capacitive current
includes interruption of starting current of motors, interruption of inductive current when interrupting the magnetizing current of a transformer or when switching off a shunt reactor, switching and operation of arc furnaces and their transformer, switching of unloaded cables and of capacitor banks, interruption of current by high-voltage fuses

(See 2.3.3.4 in IEC 60071-2)

3.21
uneven breaker pole operations
operation caused by one or two breaker poles stuck during opening or closing of the circuit-breaker

4 List of symbols and acronyms

AIS	Air-insulated substation
BFO	Back flashover
BFR	Back flashover rate
EGM	Electro-geometric model
FACTS	Flexible alternating current transmission systems
FFO	Fast-front overvoltages
GIS	Gas-insulated system
HVDC	High-voltage d.c.
LIWV	Lightning impulse withstand voltage
MOA	Metal oxide surge arrester
SFO	Slow-front overvoltages
SIWV	Switching impulse withstand voltage
SFOFR	Slow-front overvoltage flashover rate
TOV	Temporary overvoltages
TRV	Transient recovery voltage
VFFO	Very-fast-front overvoltages
Z_s (or Z_c)	Surge (or characteristic) impedance
I_c	Critical current
I_m	Maximum shielding current

In addition, refer to 1.3 of IEC 60071-2 as well as the list of symbols in [4].

5 Types of overvoltages

Table 1, extracted from IEC 60071-1, and Figure 1, detail the characteristics of all types of overvoltages.
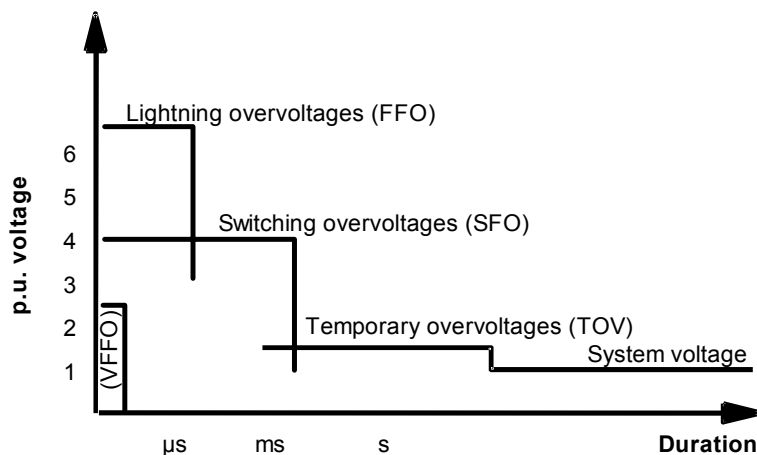
IEC   763/04

Figure 1 – Types of overvoltages (excepted very-fast-front overvoltages)

Table 1 – Classes and shapes of overvoltages – Standard voltage shapes and standard withstand tests

Class	Low frequency		Transient		
	Continuous	**Temporary**	**Slow-front**	**Fast-front**	**Very-fast-front**
Voltage or over-voltage shapes					
Range of voltage or over-voltage shapes	f = 50 Hz or 60 Hz $T_t \geq 3\,600$ s	10 Hz < f < 500 Hz $0,03$ s $\leq T_t \leq 3\,600$ s	20 μs < T_p $\leq 5\,000$ μs $T_2 \leq 20$ ms	$0,1$ μs < T_1 ≤ 20 μs $T_2 \leq 300$ μs	3 ns < $T_f \leq 100$ ns $0,3$ MHz < f_1 < 100 MHz 30 kHz < f_2 < 300 kHz
Standard voltage shapes	f = 50 Hz or 60 Hz T_t [1]	48 Hz $\leq f$ ≤ 62 Hz T_t = 60 s	T_p = 250 μs T_2 = 2 500 μs	T_1 = 1,2 μs T_2 = 50 μs	[1]
Standard withstand test	[1]	Short-duration power frequency test	Switching impulse test	Lightning mpulse test	[1]

[1] To be specified by the relevant apparatus committees.

6 Types of studies

For range I voltage level (U_m up to 245 kV), SFO are generally not critical while the FFO due to lightning have to be carefully considered. However, for higher voltage levels, SFO become of major importance, specifically in the UHV range, while FFO become in many cases less critical.

TOV have to be studied for all system voltage levels. Table 2 provides a list of events and the most critical types of overvoltages generated.

**Table 2 – Correspondence between events and most critical types
of overvoltages generated**

	Temporary overvoltages TOV	Transient overvoltages		
		Slow-front overvoltages SFO	Fast-front overvoltages FFO	Very-fast-front overvoltages VFFO
Load rejection (see 2.3.2.2 in IEC 60071-2)	X			
Transformer energization	X	X		
Parallel line resonance	X			
Uneven breaker poles	X			
Backfeeding	X			
Line fault application (see 2.3.3.2 in in IEC 60071-2)	X	X		
Fault clearing (see 2.3.3.2 in in IEC 60071-2)	X	X		
Line energization (see 2.3.3.1 in in IEC 60071-2)	X	X		
Line re-energization	X	X		
Line dropping	X	X		
AIS busbar switching			X	[1]
Switching of inductive and capacitive current (see 2.3.3.4 in IEC 60071-2)	X	X	X	
Back flashover			X	
Direct lightning stroke (see 2.3.3.5 in IEC 60071-2			X	
Switching inside GIS substation				X
SF_6 circuit-breaker inductive and capacitive current switching	X	X	X	[1]
Flashover in GIS substation				X
Vacuum circuit-breaker switching			X	X
[1] In the case of short distance busbars and low damping, very-fast-front overvoltages can also occur.				

6.1   Temporary overvoltages (TOV)

Temporary overvoltages are of importance when determining stresses on equipment related to power-frequency withstand voltage in particular for the energy capability of MOA. TOV can stress transformers and shunt reactors as a consequence of over fluxing. Ferro-resonance is a particular type of TOV which is not studied in this report.

6.2   Slow-front overvoltages (SFO)

Slow-front overvoltages play a role in determining the energy duty of surge arresters and in the selection of required withstand voltages of equipment as well as the air gap insulation for transmission line towers.

SFO studies require the investigation of possible network configurations and switching conditions that result in overvoltages exceeding the withstand values mentioned above. In decreasing order of importance, events which have to be considered typically are line re-energization, line energization, line fault application, fault clearing, capacitive load closing and inductive load opening (from the reactor's point of view). In reactive current switching, the

circuit-breaker may break down after the final clearance due to excessive dv/dt. A dielectric breakdown across the circuit-breaker before a quarter cycle of the power frequency after the final clearance is known as re-ignition, but a dielectric breakdown across the CB after the quarter cycle of the power frequency following the final clearance is known as restrike. Circuit-breaker restrike generates high SFO.

NOTE   There is no withstand value specified for range I equipment.

6.3   Fast-front overvoltages (FFO)

They are essentially produced by lightning strokes. Their magnitude is much larger than other kinds of overvoltages.

FFO are therefore critical for all voltage levels, and it is essential to mitigate them with protective devices, i.e. mainly surge arresters. Fast-front overvoltages are studied to determine the risk of equipment failure and therefore to select their required withstand level in relation to protective device configuration and tower earthing, and to evaluate line and station performance.

NOTE   Vacuum breakers can cause overvoltages in the fast-front range because of current chopping and restrike.

6.4   Very-fast-front overvoltages (VFFO)

Very-fast-front overvoltages are important for protection against high-touch voltages and internal flashover in GIS enclosures. VFFOs appear under switching conditions in GIS (see [3]) or when operating vacuum circuit-breakers in medium-voltage systems.

Pre-striking GIS disconnector and SF_6 circuit-breaker re-ignition would produce VFFO. Normally, these VFFOs can be avoided by point-on-cycle (POC) switching but analysis is required to cater for the control relay malfunction.

7   Representation of network components and numerical considerations

7.1   General

Simplified methods for the evaluation of each type of overvoltage are presented briefly in 8.1, 9.1 and 10.1, respectively. They do not require a precise modelling of each component. However, when it is necessary to determine accurately overvoltages or overvoltages for which simplified methods cannot deal, detailed analysis with detailed models are required. These models representing the components of the system to be used in studies depend on the type of overvoltage being considered. After numerical considerations, this clause presents, for each type of overvoltage, the models which are adequate for representing each component.

7.2   Numerical considerations

7.2.1   Initialization before calculation of transients

The solution of a transient phenomenon is dependent on the initial conditions with which the transient is started. Some simulations may be performed with zero initial conditions, i.e. with some particular cases of lightning surge studies, but there are many cases for which the simulation must be started from power-frequency steady-state conditions. In most cases, this issue is solved internally by simulation tools.

However, there is presently no digital tool which can calculate the initial solution for the most general case, although some programmes can perform an initialization with harmonics for some simple cases. The initial solution with harmonics can be obtained using simple approaches. The simplest one is known as the "brute-force" approach: the simulation is started without performing any initial calculation and carried out long enough to let the transients settle down to steady-state conditions. This approach can have a reasonable accuracy, but its convergence will be very slow if the network has components with light damping.

A more efficient method is to perform an approximate linear a.c. steady-state solution with non-linear branches disconnected or represented by linearized models.

7.2.2 Time step

The time step has to be coherent with the highest frequency phenomenon appearing in the system during the transient under consideration. A value of one-tenth of the period corresponding to the highest frequency is advised.

The time step has to be lower than the travel time of any of the propagation elements of the network. A value of half this travel time is advised.

The correctness of the time step may be verified by the method presented in [5] which involves comparing the result given with the time step and half of the time step. If the two results are equivalent, the first value of the time step is considered small enough.

7.2.3 Duration of the simulation

The duration time must be sufficiently long to ensure that the maximum overvoltages are recorded in the simulation results. In particular, propagation times and reflections must be taken into account. For TOV, it is necessary to cover a time interval sufficient to permit an accurate calculation of energy in surge arresters.

7.2.4 Numerical oscillations

Numerical oscillations can be related to:

– numerical methods applied for the calculation of the transient, particularly the integration method applied in the solver in the case of time-domain calculation,
– the intrinsic unstable character of the modelling of the system for given values of parameters.

When oscillations occur in a simulation case, one has to check if they are related to physical phenomena or not. If the oscillations depend on the time step or are not damped, they may be numerical.

In programmes using the trapezoidal rule, a resistance may be included in parallel with inductances (Figure 2) to damp numerical oscillation which may occur when a current is injected into it, as shown in the following diagrams [29].

According to [29], this resistance may not have a detrimental effect on the amplitude-frequency response of the inductance but introduces a phase error. Based on an acceptable phase error at power frequency, [38] proposes to use the following criteria:

$$5,4 \times \frac{2 \times L}{\Delta t} \leq R_{\text{dampL}} \leq 9,4 \times \frac{2 \times L}{\Delta t}$$

Numerical oscillations can also appear in a capacitance current if an abrupt change is applied to the voltage between the terminals of the capacitor, in a programme using trapezoidal rule but is seldom a problem in practical studies. To damp these oscillations a resistance may be included in series with the capacitance (Figure 3).

Reference [29] proposes using

$$R_{\text{dampC}} = 0,15 \times \frac{\Delta t}{2 \times C}$$
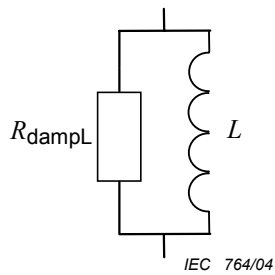
**Figure 2 – Damping resistor
applied to an inductance**
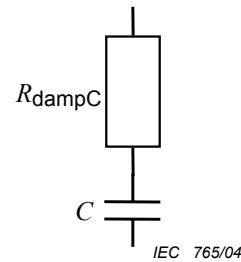
**Figure 3 – Damping resistor
applied to a capacitance**

It is also possible to apply the backward Euler rule for a few time steps to damp the oscillation [29].

7.2.5   Data representation for output

Care should be taken to avoid inopportune filtering of the results of calculation during preparation of these results for output. This may happen, for example, if the time step used for the representation of the output is not small enough and hides some oscillations occurring between two samples.

7.2.6   Non-linear elements

The number of elements representing the piecewise non-linearity must be large enough to accurately represent the element, especially for the data around the "knee point" and produce credible results. Non-linear elements can cause numeric inaccuracies due to methods used for time-domain resolution.

Attention must be paid to the assumptions made for values during steady state, as one can see in the following example (Figure 4).
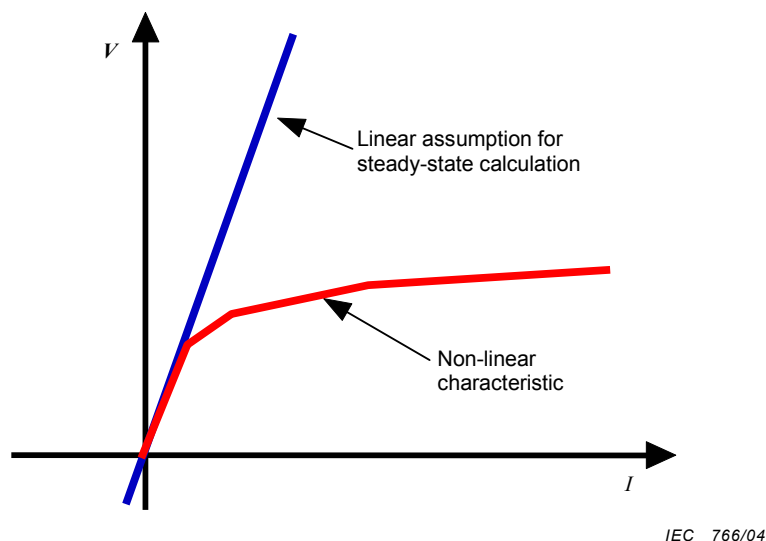
**Figure 4 – Example of assumption for the steady-state calculation
of a non-linear element**

7.3 Representation of overhead lines and underground cables

Many alternatives exist to represent overhead lines and underground cables. Table 3 gives a summary of the models which are most commonly used. Details on modelling are given in Annex A.

Table 3 – Application and limitation of current overhead line and underground cable models

Name	Applications	Limitations
1 – Exact Pi model	Initialization	
2 – Nominal Pi model	Initialization Transients	• Initialization at one frequency only • Choice of number of cells • Trapezoidal rule problem, due to first capacitance
3 – Travelling wave model with constant transform matrix	Transients	• Choice of frequency for calculation of model • Reflections due to lumped impedances representing the losses • In most cases discrepancies due to real approximation of the coefficients of the transfer matrix • Approximations in calculation of historical terms due to time step $$\frac{\text{Time step}}{\text{Propagation time for each mode}} \leq 1/2$$
4 – Frequency-dependent model with constant transform matrix	Transients	• Transfer matrix is frequency-dependent for cables and multiphase conductors at low frequencies • Coefficients of the transfer matrix are in many cases approximated as real coefficients • Time-step limitations
5 – Frequency-dependent model with frequency-dependent transform matrix	Transients	• Coefficients of the transfer matrix are in many cases approximated as real coefficients • Time-step limitations
6 – Phase domain model	Transient and initialization	• Phase-domain line modelling is currently not very popular. One advantage may be to avoid approximating the co-efficients of the transfer matrix as real

When modelling cables, care should be taken to represent carefully cross-bonding (more generally sheath arrangements of cables). Damping of oscillations are in general difficult to simulate in the case of cables, particularly because of the representation of the shunt losses.

7.4 Representation of network components when computing temporary overvoltages

Most of the models described in this subclause are presented in more detail in [2].

7.4.1 Power supply

a) Positive- and zero-sequence RLC circuit

IEC 767/04
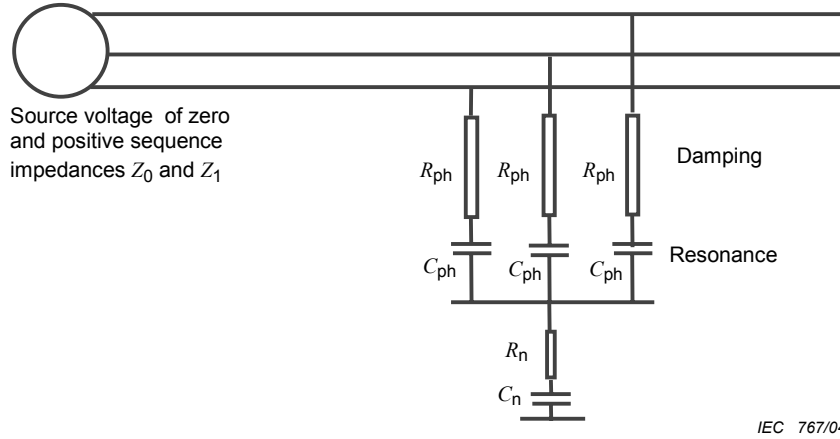
Figure 5 – AC-voltage equivalent circuit

In Figure 5, Z_0 and Z_1 are respectively the zero and positive-sequence impedance of the source.

$$Z_0 = R_0 + \mathrm{j}L_0 \times 2\pi f, \qquad \text{and} \qquad Z_1 = R_1 + \mathrm{j}L_1 \times 2\pi f,$$

To compute Z_0 and Z_1, one can assume that they are mostly inductive, i.e. $Z_0 \approx \mathrm{j}L_0 \times 2\pi f$, and $Z_1 \approx \mathrm{j}L_1 \times 2\pi f$, with f the power frequency. L_0 and L_1 are calculated from the values of single-phase and three-phase short-circuit currents and by the formula:

$$\frac{Z_0}{Z_1} = \frac{3 \times I_{3\text{ph}-\text{sc}}}{I_{1\text{ph}-\text{sc}}} - 2$$

R_0 and R_1 are then computed from the inductances by the relationship $L/R = \tau$, the time constant. Resonance capacitors are determined from the zero- and positive-sequence resonance frequencies (both of these frequencies are obtained from measurements) by:

$$\begin{cases} C_1 = \dfrac{1}{L_1\omega_1^2} \\[2mm] C_0 = \dfrac{1}{L_0\omega_0^2} \end{cases} \qquad\qquad \begin{cases} C_\text{ph} = \dfrac{1}{L_1\omega_1^2} \\[2mm] C_\text{n} = \dfrac{3}{L_0\omega_0^2 - L_1\omega_1^2} \end{cases}$$

Zero- and positive-sequence values   Phase and neutral values

Then the damping resistors are given by:

$$\begin{cases} R_1 = k\sqrt{\dfrac{L_1}{C_1}} \\[2mm] R_0 = k\sqrt{\dfrac{L_0}{C_0}} \end{cases}$$

$$\begin{cases} R_{ph} = kL_1\omega_1 \\[2mm] R_n = \dfrac{k}{3}\left(L_0\omega_0 - L_1\omega_1\right) \end{cases}$$

Zero and positive sequence values   Phase and neutral values

The factor k defines the level of attenuation and is deduced from measurements.

The pulsations ω_0 and ω_1 are estimated from measurements. Reference [63] proposes for instance to evaluate the resonance frequencies of the network from the overvoltages obtained when energizing a transformer. When a transformer is energized its magnetic core saturates and therefore highly distorted currents occur, which provide harmonic peaks on the overvoltage.

b) Synchronous machine

Modelling is based on the simulation of the equations in the direct and quadrature axes. Saturation, excitation and mechanical torque must be represented. It is also important to represent voltage and speed control. The parameters are frequency-dependent, but this dependency is complex to model and for the transients considered is often not important. The effect of the capacitances is negligible.

c) Dynamic source model [55]

This model is adapted to represent a source with a fluctuating frequency. It permits the representation of a network bypassing the difficulty of modelling the synchronous machine by using the results of a transient stability programme (see Figure 6).

IEC   768/04
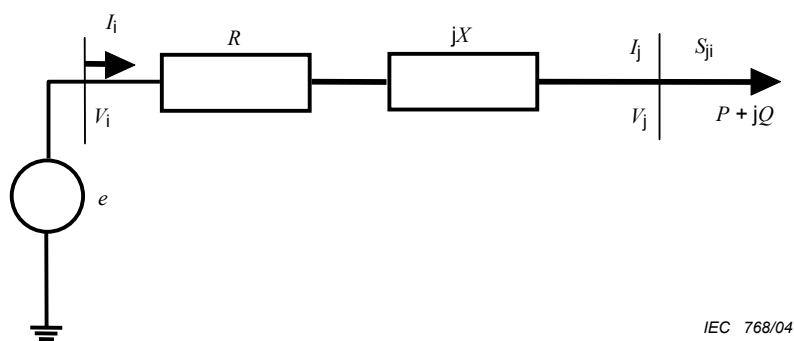
Figure 6 – Dynamic source modelling

The quantities P, Q, V_j and δ_j are functions of time. They are obtained from measurements or from transient stability studies. This model provides a way to calculate for each time step the amplitude and the phase of the Thevenin equivalent source of the system.

We have

$$Z = R + jX$$

$$S_{ji} = -(P + jQ) = P_{ji} + jQ_{ji}$$

$$P = -P_{ji} = (R\ x\ V_i\ V_j\ \cos\delta - X\ V_i\ V_j\ \sin\delta - R\ V_j^2)/(R^2 + X^2)$$

$$Q = -Q_{ji} = (X x V_i V_j \cos\delta - R_i V_j \sin\delta - X V_j^2)/(R^2 + X^2)$$

where

$\delta = \delta_i - \delta_j$

$\delta_I = \angle V_i$ and $\delta_j = \angle V_j$

$R_e(V_i) = x = V_i \cos\delta$

$I_m(V_i) = y = V \sin\delta$

$R x + X y = a = (R^2 + X^2)(P/V_j) + R V_j$

$X x - R y = b = (R^2 + X^2)(Q/V_j) + X V_j$

$x = (a R + b X)/(R^2 + X^2)$

$y = (a X - b R)(R^2 + X^2)$

$V_i = (x^2 + y^2)^{0,5}$

$\delta = \arctan(y/x)$ with $-\pi < \delta < \pi$

The voltage of the equivalent source is given by $e = V_i(t) \cos[2\pi f t + \delta_i(t)]$.

7.4.2 Linear network equivalent

A linear portion of the network can be reduced in order to gain calculation speed by network reduction routines. The fitting between the real network and the reduced one may be made up to 1 kHz, which is the frequency range of interest for TOV. The aim is to calculate an equivalent circuit which has the same frequency response as the detailed network (typically up to 1 kHz), from the nodes connected to the portion of the system represented in detail (see Figure 7).
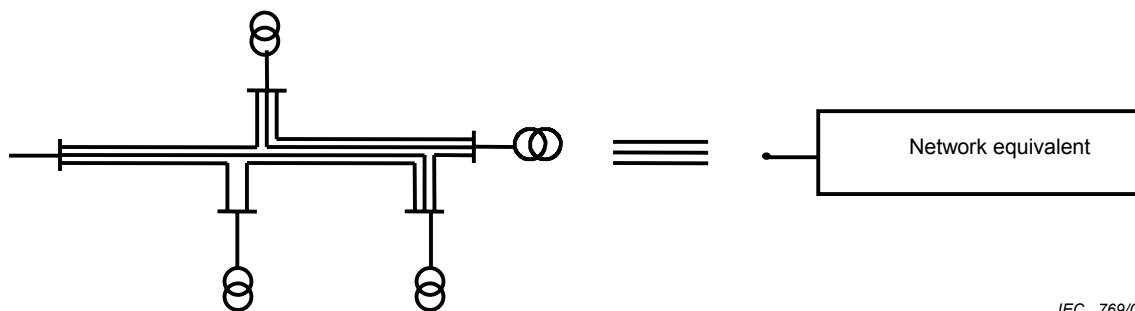
IEC   769/04

Figure 7 – Linear network equivalent

7.4.3 Overhead lines and underground cables

When representing overhead lines it is of importance to take into account the frequency dependence of the zero-sequence parameters. Asymmetry has to be considered as well. Shielding wires may be eliminated assuming zero voltage on these wires.

It is possible to use models 2, 3, 4 and 5 of 7.3. When using model 2 (nominal Pi model) the recommendations of the subclause above have to be taken into consideration.

7.4.3.1 Recommendations for the use of the Pi-model

The number of Pi-sections required to represent the line correctly is directly related to the frequency of the oscillation which can be expected during transient. The highest frequency [17] which can be represented by a Pi-cell, the corresponding length of which is l, is given by the following formula:

$$f_{\max} = \frac{1}{\pi l \sqrt{LC}}$$

where L and C are respectively the inductance and the capacitance per unit length.

Reference [5] considers that if a frequency f has to be represented, the line length corresponding to a Pi-cell should be smaller than:

$$l = \frac{v}{5 \times f_{\max}}$$

where v is the velocity of electromagnetic wave given by:

$$v = \frac{1}{\sqrt{LC}}$$

If the line is switched immediately in parallel to a capacitance of the feeding system side, this leads to an infinite current due to the direct connection of two capacitors if the two initial voltages are different. To avoid this problem, a resistor in the order of the surge impedance of the line should be connected in series with the first shunt capacitance of the first Pi-cell.

7.4.4 Tower

When analysing a fault application overvoltage, overhead line towers are represented as a single electrical node because of their small impedance and admittance.

Towers can be neglected.

7.4.5 Corona effect

A corona effect is not represented in most of the TOV studies because overvoltages observed in these studies are too small and do not reach the ionization threshold, except for very long lines and bad environmental conditions, for example, humidity and altitude.

7.4.6 Air gap, line insulator

It is not common to represent air gaps when studying TOV.

7.4.7 Busbar

Busbars are not represented individually because their length is negligible compared with wave lengths involved in this type of study. Major busbars can be represented by lump capacitances.

7.4.8 Transformers and shunt reactors

At TOV frequencies, transformers react as inductive elements. Capacitances do not have to be considered. Saturation of the magnetizing inductance, residual flux and losses (copper and magnetizing) play an important role in TOV generation and damping. Inductance and resistance are obtained from measurements or estimated from computer programmes. See IEC 60076-8 or [8].

Non-saturated shunt reactors are easy to represent by an inductance, since losses which are very low can be neglected. If TOV amplitude is large enough to lead to the saturation of the shunt reactors, then the remarks about transformers can be applied.

The design of the core plays a fundamental role since it affects the zero sequence of the transformer. A three-limbed design involves a lower zero-sequence impedance. In fact, in a three-leg transformer the zero-sequence flux closes its path through the tank, and therefore the relevant zero-sequence reluctance is higher with respect to the five-leg transformer (or the shell-type core).The inductance is in inverse proportion with respect to reluctance, thus the zero-sequence inductance of a three-leg transformer is lower than that of a five-leg one.

The above depends on the winding connection, i.e. on the vector group and the earthing of the neutral. The zero sequence is open for both unearthed star- and delta-winding connection, since these kinds of connection do not allow the flow of zero-sequence current. Thus, in practice, the different performance of a three-leg transformer with respect to a five-leg one is of concern for a star-earthed winding connection.

In this particular configuration, when, for instance, a transformer is seen from its star-earthed winding terminals and, on the other side, there is only a star-unearthed winding, the three-leg transformer has a performance which is markedly different to a five-leg one, since, from a modelling point of view, the three-leg transformer acts as a five-leg transformer but is equipped with an additional fictitious delta winding which takes into account the low zero-sequence inductance (for a five-leg transformer the zero sequence is open in this case). When a transformer is seen from its star-earthed winding terminals, yet there is only a delta winding, the three-leg transformer has a performance which is slightly different from a five-leg one, since, from a modelling point of view, the three-leg transformer acts as a five-leg transformer but equipped with an additional fictitious delta winding which takes into account the slightly lower zero-sequence inductance. Reference to this aspect can be found in [50] or in [66].

7.4.9 Unoperated circuit-breaker and disconnector

An open circuit-breaker is generally represented as a dead-end element, but in some studies circuit-breaker grading capacitance may be required for open-circuit breakers, especially if ferro-resonance is considered. A closed circuit-breaker is represented as a single electric node.

7.4.10 Substation and tower earthing electrodes

If the representation of an earthing electrode is required, it may be modelled as a resistor representing the low-frequency earth resistance for small current.

7.4.11 Lightning stroke

If it is necessary to simulate a short-circuit (or flashover) caused by lightning, it can be modelled by a short-circuit with a closing switch.

7.4.12 Surge arresters

There are some cases where surge arresters have to be modelled:

– if their damping effect has to be taken into account;

– if their energy withstand is analysed;

– if TOV amplitude exceeds the rated voltage of a metal-oxide arrester or the sparkover voltage of an arrester with gap;

– if the studied TOV is associated with a slow front transient overvoltage;

– when sacrificial arresters are used to limit the amplitude of TOV.

In these cases, a non-linear resistor is enough to represent the influence of the arrester on TOV.

7.4.13 Loads

The main problem for the representation of loads is to know their parameters. If the only known parameters are active and reactive powers, then it is advised (see [2]) to perform two TOV studies, one with series-RL loads, one with parallel-RL loads. If the two studies show a big difference between the two models, then more data about loads should be obtained in order to use a more accurate model.

The presence of motors in loads may modify short-circuit power and frequency response.

IEC 770/04
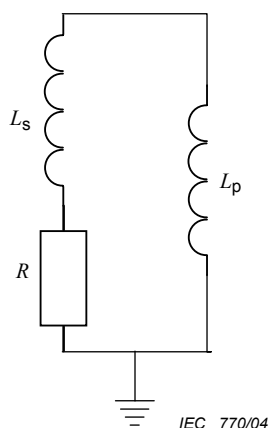
Figure 8 – Representation of load in [56]

Reference [56], which deals with harmonics calculation, proposes approaching the issue of load modelling using three methods:

- Method 1 – The equivalent reactance of the load is neglected, by considering it infinite. The load is equivalent to a resistance $R = U^2/P$, where U is the nominal voltage and P the active power controlled by the load.

- Method 2 – The equivalent resistance of the load is calculated as above but it is associated with an inductance in parallel with it. The reactance is estimated based on the number of motors in service, their installed unitary power and their installed reactance.

- Method 3 – Over a frequency range corresponding to frequencies between the 5th and the 20th harmonics, the load can be represented by an inductance L_s in series with a resistance R, the two of them being connected in parallel with an inductance L_p such that

$$R = \frac{U^2}{P_{50}}$$

$$L_s = 2{,}3 \times 10^{-4}\, R$$

$$L_p = \frac{R}{100 \times \pi (6{,}7 \times \tan\varphi_{50} - 0{,}74)}$$

with $\varphi_{50} = Q_{50}/P_{50}$.

P_{50} and Q_{50} are respectively the active and reactive power absorbed at nominal frequency by the overall load.

7.4.14 Filters and capacitors

It is important for TOV to represent them. They are represented by lumped R, L, C elements. Examples of installations can be found inIEC 60071-5 [64] for HVDC applications.

7.4.15 Other equipment

Devices such as FACTS or HVDC that can modify power flows or inject harmonics have to be accurately represented, especially their control. The action of protection systems has to be taken into account in order to get realistic scenarios.

7.5 Representation of network components when computing slow-front overvoltages

7.5.1 Power supply

7.5.1.1 Source network representation

According to [57], the characteristics listed below have a major effect on the overvoltages and must be modelled correctly.

- Power-frequency impedance.
- Surge impedance as seen from the energizing bus.
- Behaviour of the source at the major natural frequencies of the whole system (switched lines included).

Reference [57] makes the following general recommendations to model the sources adequately in line energization and line re-energization studies.

- Parts of the source network at a lower voltage level with respect to that of the switched line may be disregarded apart from their contribution to the short-circuit power.
- It is generally sufficient to represent the lines, at least in meshed systems, up to two busbars back from the energizing bus; the remaining part of the system may be represented by its short-circuit reactance in parallel with its surge-impedance.

7.5.1.2 Synchronous machine

For slow front overvoltage computation, synchronous machines are modelled as shown in Figure 9.

C (external capacitance of the overall system) must be calculated, taking into account what is connected to the machine. This capacitance is of secondary importance in the case of slow-front overvoltage computing.

The transition from subtransient to transient and to synchronous reactance is only of importance for the decay of short-circuit current [5].

When modelling the external behaviour of a synchronous machine only, $R(f)$ can often be represented by a constant, independent of frequency.
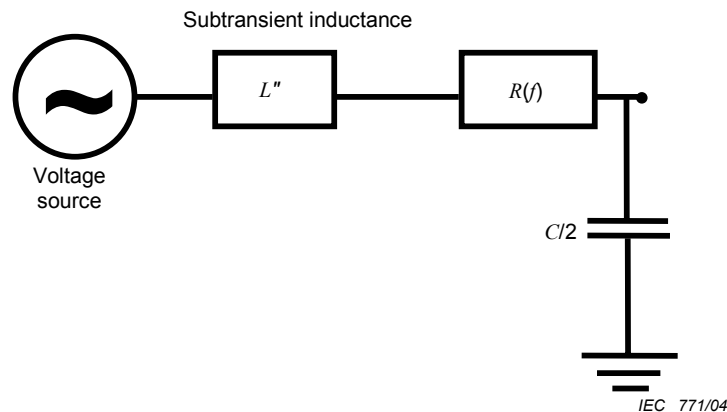
Figure 9 – Representation of the synchronous machine

7.5.2 Overhead lines

7.5.2.1 Trapped charge

This is used to simulate a high-speed reclosure condition. Completely different behaviour is expected when the line is equipped with shunt reactors, which implies a free oscillation of the trapped charges, in contrast with uncompensated lines without magnetic transformers for which trapped charges decay exponentially without free oscillations.

When a circuit-breaker opens an overhead line sequentially without current chopping, polarity of trapped charges on each phase is positive, negative and positive, or negative, positive and negative. Magnitude of trapped charge on the last phase to open corresponds to 1 p.u. However, the voltage magnitude corresponding to trapped charge on the first phase to open becomes larger than 1 p.u. and can reach more than 1,3 p.u. This voltage increase is caused by capacitive coupling between phases [53]. For single-circuit OHL, this voltage rise is a function of C_1/C_0. For double-circuit OHL, the voltage rise is a function of C_1/C_0 and of the coupling from the adjacent circuit. On the other hand, magnitude of the voltage on the second phase to open is smaller than 1 p.u. This phenomena has been confirmed by field tests. Of course, trapped charges decay with time. To simplify the simulation for high-speed reclosing, it is assumed in many cases that the trapped charges are +1 p.u. −1 p.u. and +1 p.u. or −1 p.u. +1 p.u. and −1 p.u. However, care should be taken that in the case of reclosing after a single phase-to-earth fault, trapped charges on the healthy phases may be higher than 1 p.u., depending on the earthing of the neutral. In the case of a single-phase reclosing, the trapped charge is smaller than 1 p.u.

7.5.2.2 Line model

Models 3, 4 and 5 of 7.3 may be used.

7.5.3 Tower

As the tower's equivalent capacitance to the line can be considered negligible when compared to the capacitance of the line, they need not be represented in the study, except when a flashover occurs at a tower. In this case the tower is represented by a resistance equal to the tower footing resistance for SFO studies, if necessary (because a fault application overvoltage is little affected by the tower footing resistance).

7.5.4 Corona effect

In most of the cases, slow-front overvoltages are too low to induce corona effects.

7.5.5 Underground cable

Models 3, 4 and 5 of 7.3 may be used.

Cross-bonding and earthing have to be carefully taken into account. All conductors (core, sheath, armour and additional conductors) must be represented. Reference [58] provides a large presentation of solutions generally adopted for underground cable cross-bonding and earthing.

7.5.6 Air gap, line insulator

7.5.6.1 Flashover trigger

For a first approximation, one can assume that the gap flashes as soon as its voltage reaches a given value. Once the flashing condition has been verified, several possibilities exist to represent the flashover process.

7.5.6.2 Flashover process

7.5.6.2.1 Ideal switch

An air gap, once the flashing condition has been verified, can be simply represented by an ideal switch which closes in one time step. If the time step is not too small, this model is quite representative.

7.5.6.2.2 Voltage source

In the case of a study using a very small time step, the last model can lead to excessively high overvoltages due to a value too high of dV/dt. One can then model the flashing of an air gap by a voltage source which decays progressively from the initial voltage to zero in a given time, equal to several time steps.

7.5.6.2.3 Use of inductance

For a study using a small time step, the air gap may be represented by a small inductance (for example, 1 μH/m) in a series with an ideal switch which closes in one time step.

7.5.7 Busbar

Busbars are not represented individually because their impedance and admittance are too small to influence the transient response. Important sets of busbars can be represented as a single lumped capacitance. Small busbar sections (the travel time of which represents few time steps) can be represented as a lumped capacitance.

7.5.8 Transformer

A power-frequency model must be used, taking into account non-linearity, losses, remnant flux and primary-secondary stray capacitances. In some cases it is important to model accurately the capacitances to get a correct resonant behaviour (energization of a transformer from a short line). A frequency-dependent transformer model would be of interest but in most practical cases the knowledge of the transformer parameters does not permit an accurate representation of the transformer.

7.5.9 Open circuit-breaker

An open circuit-breaker is represented as a dead-end element. A grading capacitor, in parallel with the breaker contacts, can also be included when possible.

7.5.10   Circuit-breaker

Breakers are important in SFO as most of these are generated during switching operations. Depending on the type of phenomena that are being studied, a different model for the breaker should be used.

7.5.10.1   Ideal switch (closing and opening)

As a first approximation, a breaker can be considered as either an infinite resistance (open breaker) or a null resistance (closed breaker), changing from one to the other in a time step in case of closing, as well as when its current reaches zero in case of opening.

Several improvements have been proposed to this model:

- The possibility to chop non-zero current when the current drops under a given value. This data is difficult to obtain; it depends on the current value and the characteristics of the load. This feature can be very useful when simulating the interruption of inductive currents [14].

- A high-frequency current property (see IEC 61233). A value of dI/dt which is too high prevents the breaker from opening. This data is also difficult to obtain.

- Restriking possibility. This model includes a computation routine to determine when the breaker will restrike after it has opened. The routine may be a simple comparison of the longitudinal voltage versus time and a TRV shape.

- Statistical switch. The closing times of the three phases of the breaker have a great influence on the generated overvoltage. Two parameters are taken into account. First, the closing command may happen at any time, which means anywhere on the power-frequency sine. Then the three phases, which are supposed to receive the command at the same time, respond to this command with a random delay due to mechanical dispersions and pre-strikes. The strategy the most commonly adopted is as follows: the closing command is supposed to be uniformly distributed on the sine and real closing times are supposed to be around it, with a Gaussian probability. This double distribution is illustrated in Figure 10. If the transient behaviour of the system is symmetric in terms of polarities, one can limit the excursion of the switching order time to under one-third of a power voltage period. Concerning the Gaussian distributions, the standard deviation of the inter-phase time distribution is not always known. A value of 0,8 ms to 2 ms may be used as a typical value. IEC 62271-100 [65]. allows 5 ms.

IEC 772/04
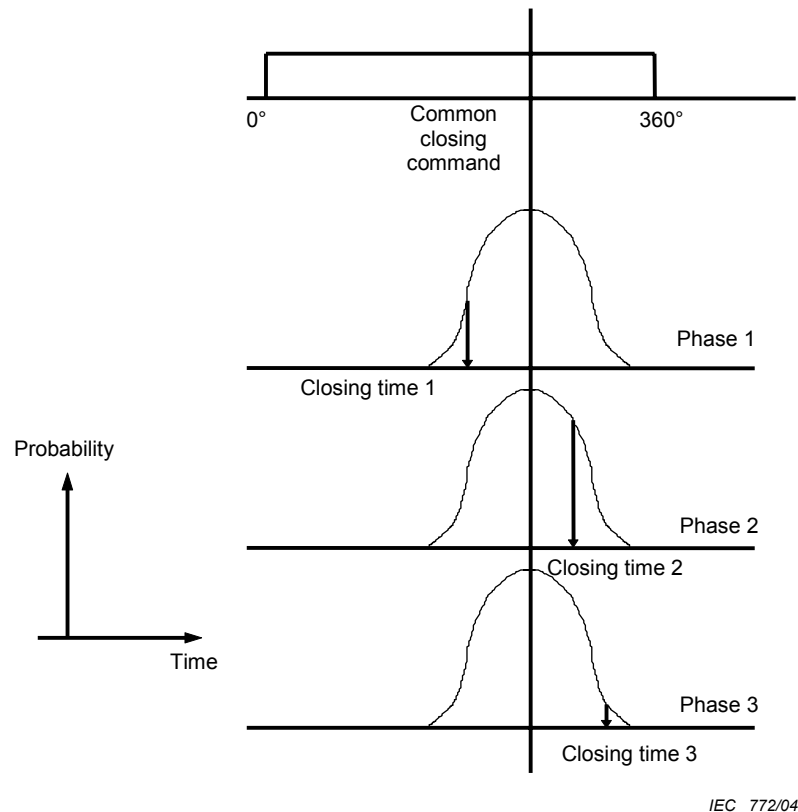
Figure 10 – Diagram showing double distribution used for statistical switches

It is a simplification to assume that the closing command is unique for the three phases. If a particular breaker is studied and if data are available, three different closing commands can be given, as described in [20].

7.5.10.2   Arc model based on the physics of the circuit-breaker

This sophisticated model tries to simulate the physics of the circuit-breaker as closely as possible. It is much more complicated than the ideal switch, and its parameters can be difficult to obtain. It is not required for most studies but it is useful for an accurate representation of restrike phenomena in cases such as breaker explosion investigations.

Most mathematical models are based on energy balances between the electric arc and the surrounding environment when the current drops to zero. The two equations most used are the Mayr and Cassie equations [13]. More details are given in Annex B.

A simplified model may be used if the effect of arc voltage only is considered [5]. Statistical characteristics can be added to this model in the same manner as above.

7.5.11   Metal-oxide surge arrester

A MOA is represented as a non-linear resistor, using its 30/80 µs characteristics (IEC 60060-1). The surge arrester's benchmarks are 0,5 kA, 1 kA and 2 kA.

7.5.12   Substation and tower earthing electrodes

If the representation of the earthing electrode is required, it may be modelled as a resistor representing the low-frequency earth resistance for small current.

7.5.13 Network equivalent

A model similar to the one given in 7.4.2 may be used but covering a higher frequency range (up to 20 kHz).

7.6 Representation of network components when computing fast-front transients

7.6.1 Power supply – voltage source

The power-frequency voltage, at the inception time of a lightning stroke, can be represented as a power-frequency voltage source and an adaptation resistor in series (value $[R] = [Z_s]$, surge impedance matrix).

The relative polarities of the lightning stroke and the initial line voltage are of importance. It is necessary to investigate both polarities. In some specific configurations, several values of initial line voltage need to be considered.

7.6.2 Overhead transmission line and underground cable

7.6.2.1 Line or cable close to the lightning stroke inception point

If a complex model is to be implemented, approximately 2 000 m of overhead line must be accurately modelled. In the case of underground cables, especially when the remote end of the cable is under open-circuit conditions, invaded surge may produce high overvoltages due to positive multi-reflections at both ends. Therefore, use of a cable model with full length is recommended.

7.6.2.2 Line or cable far from the lightning stroke inception point

If reflections are not to be considered, the line can be terminated in its equivalent characteristic surge impedance in the phase domain.

7.6.3 Tower

A tower is commonly represented as a radiating structure [4]; as a lossless propagation line with constant characteristics; as a propagation line with damped inductance; or as an equivalent inductance.

7.6.3.1 Lossless propagation line with constant parameters

Wagner and Hileman [15] have proposed the expression below to calculate the surge impedance of a cone:

$$Z_{\text{pyl}} = 60 \times \ln \frac{H\sqrt{2}}{r_{\text{pyl}}}$$

where:

H is the height of the cone equivalent to the tower;

r_{pyl} is the tower base radius.

Chisholm, Chow and Srivastava have discovered that the impedance depends on the direction of injection. However, they propose the use of an average impedance Z_{av} [18]:

$$Z_{\text{av}} = 60 \times ln(\cot\theta/2)$$

where $\theta = \tan^{-1}(r(h)/h)$, h is the height along the tower and $r(h)$ is the tower radius at a height of h.

They propose the following practical simplification:

$$Z_{av} = 60 \times ln[\cot(0{,}5 \times \tan^{-1}(r_{avg}/H_t))]$$

with:

$$r_{avg} = \frac{r_1 h_2 + r_2(h_1 + h_2) + r_3 h_1}{h_1 + h_2}$$

where:

r_1 is the tower top radius;

r_2 is the tower mid-section radius;

r_3 is the tower base radius;

h_1 is the height from base to mid-section;

h_2 is the height from mid-section to top;

$H_t = h_1 + h_2$.

7.6.3.2 Propagation line with damped inductance
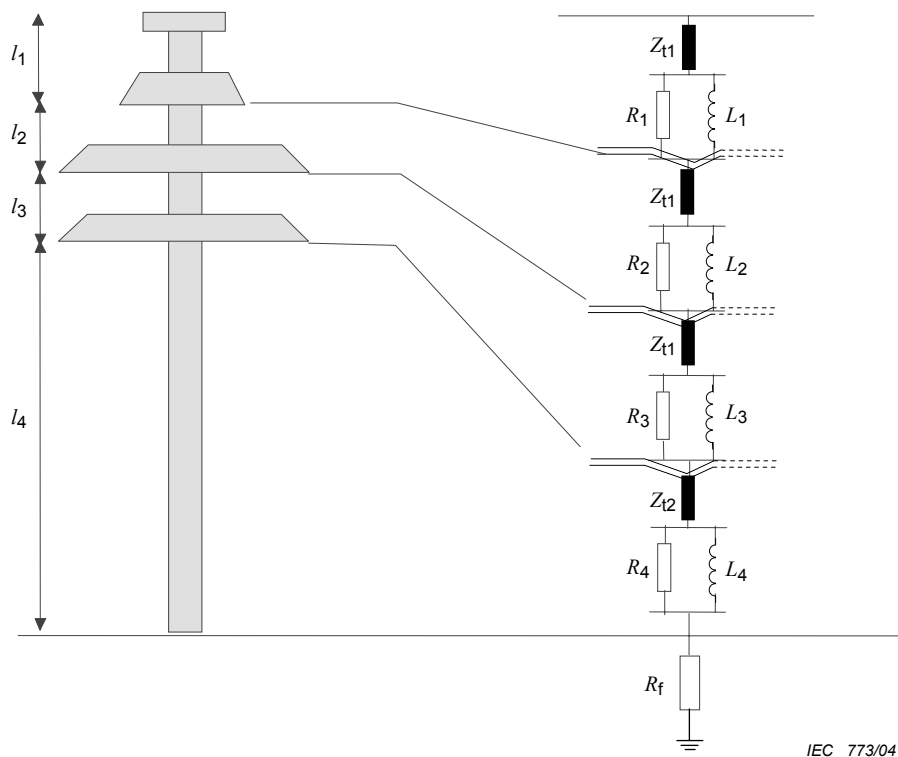
Figure 11 – Multi-story transmission tower [16], $H = l_1 + l_2 + l_3 + l_4$

A model for a multi-story transmission tower [16] has been developed on the basis of measurements on a 500 kV transmission tower equipped with shield wires (see Figure 11). This model consists of four sections divided at the upper, middle and lower phase cross-arm positions. Each section consists of a lossless transmission line in series with an inductance in parallel with a damping resistance. The impedance depends on the direction of the lightning current in air. The model considers the most severe condition. The parameters of the corresponding electrical model are calculated using the following rules:

Surge impedance: (upper part) $Z_{t1} = Z_{t2} = Z_{t3} = 220 \ \Omega$ (lower part) $Z_{t4} = 150 \ \Omega$

Surge propagation velocity: $v_t = v_{t1} = v_{t2} = v_{t3} = v_{t4} = 300$ m/µs

Time constant (travel time on tower $\times$ 2): $\tau = 2 \times H/v_t$

Attenuation is constant along the tower: $\gamma = 0{,}8944$

Damping resistance per unit length of upper part: $r_1 = 2 \times Z_{t1} \ln(\gamma/(l_1 + l_2 + l_3)$

Damping resistance per unit length of lower part: $r_2 = 2 \times Z_{t4} \ln(\gamma/l_4)$

$R_1 = r_1\, l_1$, $R_2 = r_1\, l_2$, $R_3 = r_1\, l_3$, $R_4 = r_2\, l_4$ where l_1, l_2, l_3 and l_4 are real length.

Inductance in parallel with a damping resistance: $L_1 = R_1\ \tau$, $L_2 = R_2\ \tau$, $L_3 = R_3\ \tau$, $L_4 = R_4\ \tau$.

7.6.3.3   Inductive branch

A value of 1 μH per metre can be used.

7.6.3.4   Cross-arm representation

Because of their short length, propagation in cross arms cannot be represented easily in FFO studies. Cross arms have been represented as short, electrical transmission lines with open-circuit ends [4], [18], including the effect of doubling of the overvoltage at the end of the cross arm.

Therefore, in this respect, a cross arm may be modelled as a lossless propagation line with constant parameters or an equivalent inductance (1 μH/m); this last representation does not give the effect of doubling of the overvoltage at the end of the cross arm before flashover.

7.6.3.5   Travel time

Some experiments [18], [19] have shown that travel time is longer than the tower height divided by the speed of light in a vacuum but it is reasonable to ignore the additional path length in practical studies. The additional contribution due to the propagation from the shield wire may be considered [4].

7.6.4   Corona effect

The corona effect [45] [4] involves an increase in the line capacitance due to the ionization of the air around the conductor. This effect appears both between phase and ground and between phases. Most of the models account for the phase-to-ground corona effect.

Since this effect tends to reduce the steepness of the impinging surge, it is a conservative approximation to neglect it. There are many proposals on the methods to simulate corona effect. The next subclause presents one of them.

7.6.4.1   Discrete components model

The corona effect can be represented using discrete classical components. This is achieved by dividing the line into sections of a given length and connecting one or two branches containing a diode, a capacitor and a d.c. voltage source to each section. The source represents the voltage above which the corona begins to appear, the capacitor represents the additional capacitance of the line due to the corona and the diode is an artifice which facilitates the connection of the capacitor only when the voltage reaches the d.c. source value. This model is only valid for one polarity of overvoltages, i.e. positive, in the example shown in Figure 12.

IEC 774/04
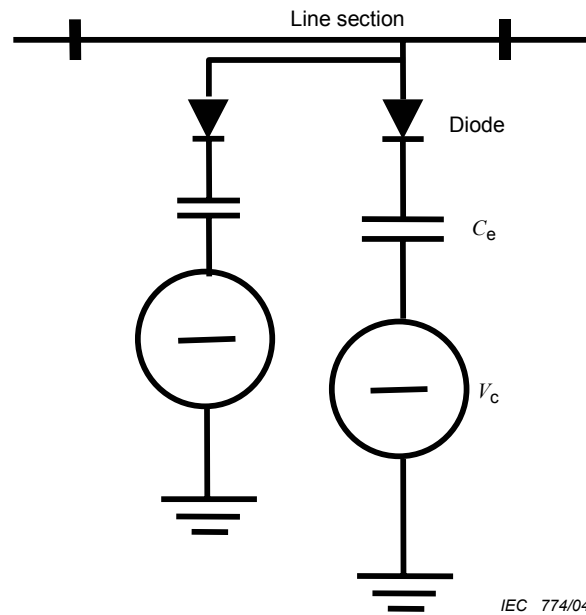
Figure 12 − Example of a corona branch model

For the computation process, this model is both time- and memory-consuming because it requires dividing the line into many small lengths. For this reason, it is recommended that the model only be used in the most stressed part of the network, i.e. 500 m from the stroke inception point.

7.6.4.2 Parameter values

Parameter values can be found in Clause F.1 of IEC 60071-2, in [21], [24] and in 5.6 of [4]. It must be noted that parameters for the corona effect depend on the geometry of the line (i.e. conductor radius, number of sub-conductors per bundle), polarity and even on the waveform of the transient. Reference [4] proposes a method to evaluate the reduction of steepness due to the corona effect of an impinging surge.

7.6.5 Air gap, line insulator

7.6.5.1 Flashover trigger

7.6.5.1.1 Voltage threshold

An assumption that the gap flashes as soon as its voltage reaches a given value is not recommended for this type of studies.

7.6.5.1.2 Volt-time curve [4], [10] (Figure 13)

The instant of breakdown is considered as being the point of intersection of $U(t)$ with the volt-time curve of the insulation. $U(t)$ is the voltage between the two terminals of the air gap versus time. The knowledge of the performance of insulation under the stress of the standard lightning impulse is, however, not sufficient to predict the performance of the insulation exposed to any non-standard impulse. Furthermore, it is not always correct to assume that flashover will occur when a voltage wave just exceeds the volt-time curve at any time. The experimental volt-time characteristic is only adequate for relating the peak of the standard impulse voltage to the time of flashover. For a non-standard impulse, a more accurate determination of the time of flashover may be obtained using the two models presented below.
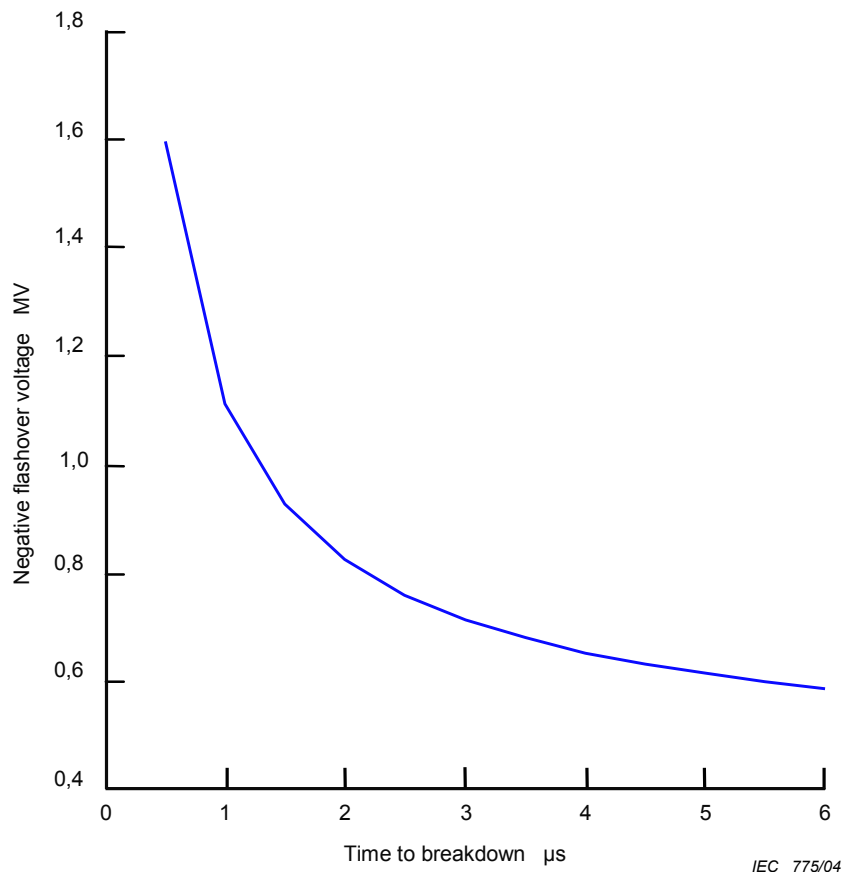
Figure 13 –Example of volt-time curve

7.6.5.1.3 Air gap model using the area criterion [4], [30]

The area criterion involves determining the instant of breakdown using a formula of the type described below. The method allows the applied waveform to be taken into account.

$$Integrate\,(t) = \int_{T_0}^{t} \left(U(\tau) - U_0 \right)^{k} d\tau$$

Flashover occurs when *Integrate*(*t*) becomes equal to *DE* (constant):

> $U(t)$ is the voltage applied at time t, to the terminals of the air gap.
> U_0 is a minimum voltage to be exceeded before any breakdown process can start or continue.
> k and U_0 and DE are constants corresponding to an air-gap configuration and overvoltage polarity.
> T_0 is the time from which $U(\tau) > U_0$.
> The parameters U_0, k and DE are determined by using the voltage-time curve.
> This model is valid for impulses of either positive or negative polarity but does not apply in case of oscillation, when the voltage between the terminals decreases below U_0 after having being greater than U_0.

The model is recommended for air gaps smaller than 1,2 m.

In [59] standard impulse tests have been used to evaluate some sets of parameters U_0, k, DE which were used to predict the performance of the insulation stressed by non-standard data and to make some comparison with experimental data. The sets of parameters corresponding to the different configurations considered are presented in Table 4 below.

Table 4 – Values of U_0, k, DE for different configurations proposed by [59]

Gap (cm) – Test object – Polarity			k	U_0 kV	DE
56	– rod-rod –	+	1	306	4,9
56	– rod-plan –	+	1	252,2	306,5
114	– rod-rod –	+	1	577,5	641,2
8	– insulators[1] –	+	1	643	369,3
56	– rod-rod –	–	1	391,6	240,1
56	– rod-plan –	–	0,47	590	7,947
114	– rod-rod –	–	1	825,8	427,5
8	– insulators –	–	1	638,7	525,4
NOTE An eight-unit string of 254 mm $\times$ 146 mm suspension insulators mounted in a geometry similar to that of a steel tower.					

7.6.5.1.4 Air-gap model based on the leader propagation representation [4], [30]

The physics of discharge in large air gaps, i.e. air gaps greater than 1 m, has proved that the breakdown in large air gaps involves three successive phases: corona inception (t_i), streamer propagation (t_s) and leader propagation (t_l).

Leader propagation models are based on the numerical representation of these three stages.

a) Breakdown process

When the voltage applied to the air gap exceeds the corona inception voltage, streamers propagate and cross the gap after a time t_s, if the voltage remains high enough.

When the streamers have crossed the gap, the leaders develop rapidly, with speed being dependent on the applied voltage. The streamers and the leaders can develop from one or two electrodes. The breakdown occurs when the leader has crossed the gap or when the two leaders have met. The time to breakdown can be calculated by:

$$t_c = t_i + t_s + t_l$$

t_i being the time before streamers exist. It can be neglected for practical purposes.

b) Calculation of t_s (streamer propagation time)

An approximation made in most models is that the streamer phase is completed when the voltage applied reaches a value leading to an average gradient E equal to E_{50} (average field for U_{50}).

c) Calculation of tl (leader propagation time)

The leader velocity $v_l(t)$ can be calculated using the following formula [4]:

$$v_l(t) = g(u(t),d_g)\ (u(t) - U_0(d_g - l_l))/(d_g - l_l)$$

Where g and U_0 are some functions, d_g and l_l correspond to the gap length and the leader length respectively; $u(t)$ is the absolute value of the actual voltage in the gap. The model considers an equivalent leader propagating from one electrode even if two leaders exist in reality.

It is considered that the leader stops if $u(t)$ drops below $U_0(d_g - l_l)$. As a practical application, two types of formula have been proposed for the calculation of the velocity of the leader:

$$v(t) = 170 \times d_g \ (u(t)/(d_g - l_l) - E_0) \ \exp(0{,}0015 \times u(t)/d_g)$$

and

$$v(t) = k \ u(t) \ (u(t)/(d_g - l_l) - E_0)$$

The parameters k and E_0 depend on gap configuration and voltage polarity and values can be found in [4].

Formula to calculate t_c for the realistic impulse voltage waveform with a fast front and a short tail, which is generated on the air gap of the tower, is proposed in [31], [32].

d) Leader current

Because of synchronization problems, it is difficult to determine a relation between the leader current and the velocity of the leader. A linear relation of the type $i_l(t) = qv_l(t)$ seems to be acceptable with a value of q ranging from 300 µC/m to 400 µC/m.

The leader model works for long air gaps.

NOTE   Other models also exist [28].

7.6.5.2   Flashover process

7.6.5.2.1 Ideal switch

An air gap, once the flashing condition has been verified, can be simply represented by an ideal switch which closes in one time step. If the time step is not too small, this model is fairly representative. For this type of study the time step may be too small.

7.6.5.2.2 Voltage source

In the case of a study using a very small time step, the last model can lead to excessively high overvoltages due to a high dV/dt. One can then model the flashing of an air gap by a voltage source which decays progressively from the initial voltage to zero in a given time, equal to several time steps.

7.6.5.2.3 Use of inductance

The air gap is represented as a small inductance (1 µH/m) connected to an ideal switch. This inductance corresponds to the inductance of the arc. A physical background of this model is given in [47].

7.6.6   Busbar

Busbars are represented as propagation elements. Where certain busbars are too short, compared to a time step (a few time steps), they can be represented as a single propagation element, the length of which is the total length of all busbars being considered. For a very short busbar, a lumped inductance can be used.

7.6.7   Transformer

Where the transformer's internal voltage or the transferred voltage from LV-HV, HV-LV is required, a capacitance may be used in a simplified approach. A more rigorous approach requires the determination of the matrix of frequency-dependent impedances in order to use it to calculate the parameters of a model [12], [43], [54]. This matrix is calculated from the internal structure of the transformer [12] or from measurements [43].

If only the transformer voltages to earth are required, the transformer can be represented by its capacitances to earth.

Capacitances of autotransformers can be computed by the following formula [8] which is valid for a Y connection transformer. For a D connection transformer, C has to be divided by 2.

$$C = 0{,}52 \times P^{0,4}$$

Where:

C is the capacitance in nF;

P is the rated power in MVA.

The following set of values, as shown in Table 5, is recommended in Japan as the minimum capacitance to earth [44].

Table 5 – Minimum transformer capacitance to earth taken from [44]

Nominal voltage kV	Capacitance nF
500	3
187-220-275	2,5
110-155	1,5
66-77	1

Reference [28] proposes the following set of values, as shown in Table 6, for typical capacitance to earth of various types of transformer.

Table 6 – Typical transformer capacitance to earth taken from [28]

Voltage kV	115	400	765
Capacitive potential transformer (pF)	8 000	5 000	4 000
Magnetic potential transformer (pF)	500	550	600
Current transformer (pF)	250	680	800
Autotransformer (pF)	3 500	2 700	5 000

If the transfer of overvoltage from one side to the other has to be calculated, it is necessary to represent the longitudinal capacitance of the transformer (see IEC 60071-2). It is also required to add an inductance, whose value is determined according to the size of the transformer.

Transformer parameters can also be found in [8].

7.6.8 Circuit-breaker and disconnector

These are represented as capacitances between contacts and between contacts and earth. Table 7 shows an example of the capacitance value.

Table 7 – Circuit-breaker capacitance to earth taken from [28]

Voltage kV	115	400	765
Disconnecting switch (pF)	100	200	160
Circuit-breaker/Dead tank (pF)	100	150	600

7.6.9 Lightning stroke

Lightning statistics are considered as being the same all over the world. Regions are characterized by their ground flash density. It is the number of strokes per year and per unit area, which is usually expressed as an annual average. The valid information on statistics is presented in [4] but it is possible to use detection systems to evaluate lightning statistics. However, up to now, there is no agreement on the accuracy of the data provided by such systems.

7.6.9.1 Electrical model

An ideal current source is used most widely. For the representation of distant strokes, a voltage source whose maximum value is equal to withstand voltage of air gaps of transmission lines can be used, but a current source is preferred.

7.6.9.2 Waveshape

The current waveshape shown in Figure 14 has been widely used. This shape is simple and easy to use.

IEC   776/04
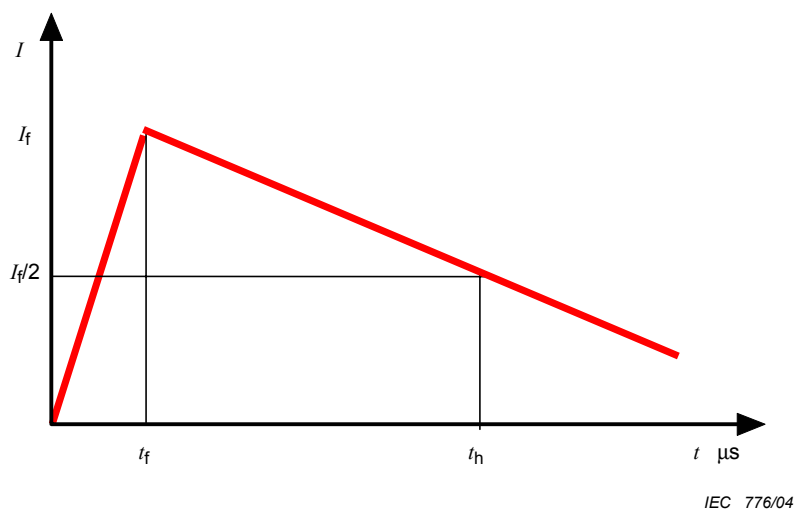
Figure 14 – Double ramp shape
(t_f is the front time, $_h$ is the time to half-value and I_f the crest value of the current)
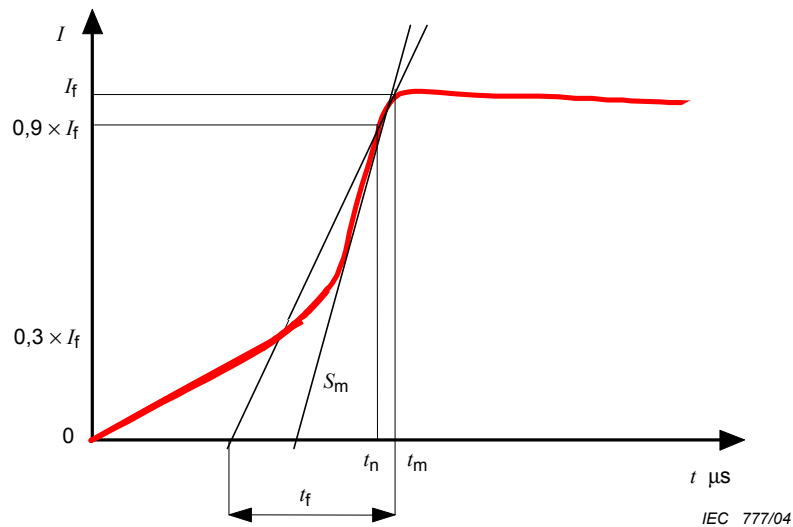
Figure 15 – CIGRE concave shape

(I_f is the crest current, S_m is the maximum front steepness, t_f is the equivalent front duration
(source: from Figure 13 [4]))

The CIGRE concave shape shown in Figure 15 represents more accurately the concave front of a lightning stroke and usually gives more realistic results. Reference [4] proposes a method to evaluate, from lightning statistics data, the parameters of a corresponding analytical expression.

7.6.9.3   Probabilistic distributions for the representation of the first negative downward strokes

Table 8 summarizes parameters of log-normal representation for the first negative downward strokes which have been extracted from [4]. The data have been collected from recording to structures. The probability density of a log normal distribution is given by the following equation.

$$f(x) = \frac{1}{\sqrt{2\pi}\,\beta x}\,\mathrm{e}^{-\frac{z^2}{2}} \quad \text{where} \quad z = \frac{\ln(x/M)}{\beta}$$

M is the median parameter value and β is the slope parameter; x is the variable log normally distributed (in Table 8, it represents I_f, S_m).

We have, for a log normal distribution, $E(X) = M \times \exp(\frac{\beta^2}{2})$ and

$$\sigma(X) = M \times \exp(\frac{\beta^2}{2})\sqrt{\exp(\beta^2) - 1}$$

$E(X)$ is the mean value and $\sigma(X)$ is the standard deviation.

Table 8 – Representation of the first negative downward strokes

Parameter	3 kA < I < 20 kA		I > 20 kA	
	M	β	M	β
I_f, final crest current (kA)	61,1	1,33	33,3	0,605
Derived distributions				
S_m/I_f, conditional (kA/µs)	12,0 $I_f^{0.171}$	0,554	6,5 $I_f^{0.376}$	0,554
NOTE The notations used in Table 8 are presented in Figure 15.				

Other derived distributions may be found in [4].

IEEE proposes a simplified formula (see in [10] and [11] for the distribution of the crest current:

$$P(I_f) = \frac{1}{1 + \left(\dfrac{I_f}{31}\right)^{2.6}}$$

This formula and the CIGRE representation with two domains give very close figures except at the extremities of the distribution.

Some experience formulae exist in some countries and may also be used.

For the duration parameter (time to half-value) reference [4] proposes the following data, as shown in Table 9:

Table 9 – Time to half-value of the first negative downward strokes

Stroke duration (t_h) (µs)	30	77,5	200
Cases exceeding tabulated value (%)	95	50	5

7.6.9.4   Probabilistic distributions for the representation of the negative downward subsequent strokes

Table 10 gives parameters of log-normal representation for subsequent strokes. The notations are the same as for the first stroke. They have been extracted from [4].

Table 10 – Representation of the negative downward subsequent strokes

Parameters	M	β
Crest current (kA)	12,3	0,53
Max front steepness (kA/µs)	39,9	0,852

For the duration parameter (time to half-value) reference [4] proposes the following data, as shown in Table 11.

Table 11 – Time to half-value of negative downward subsequent strokes

Time to half-value (th)(µs)	6,5	30,2	140
	95	50	5

7.6.9.5 Representation of the positive lightning strokes

According to [4], there is no comprehensive source of information for the parameters of the positive lightning strokes. Being very rare (less than 10 % of the total number of lightning strokes are positive), they are usually not considered in lightning studies, even if they are of larger energy.

7.6.10 Metal-oxide surge arrester [60]

Non-linear resistor using 8/20 μs characteristics (see IEC 60099-4) equipped with stray capacitance (only required for GIS) and inductances (linear inductance L' is about 1 μH/m). An inductance can be added to represent delay. Reference [49] proposes a model representing the surge arrester as two non-linear resistors in parallel.

The surge arrester benchmarks are 5 kA, 10 kA, 20 kA and 40 kA.

7.6.11 Earthing electrode of towers

Physical phenomena involved when current is circulating through an earthing electrode is quite complex, except for simplified idealistic configurations. It is therefore quite difficult to accurately represent at the same time propagation and ionization. The domain of validity of the models presented below is difficult to assess.

7.6.11.1 Simplified model

The footing impedance is represented in Figure 16.

IEC 778/04
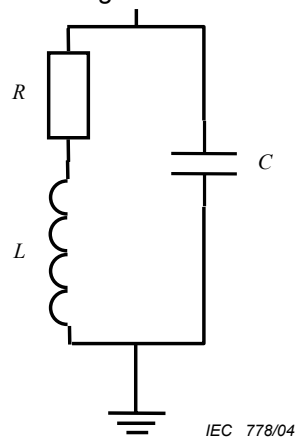
Figure 16 – Simplified model of earthing electrode

Typical values for L and C are respectively several μH and a few pF. The footing impedance may also be represented by only a resistance.

7.6.11.2 Ionization model

Because of the high value of earth current during a lightning strike, ionization may be taken into account and earth connections may be represented as non-linear resistors, the value of which can be determined as follows (see [4] and IEC 60071-2).

$$\text{if } I < I_g \quad R = R_0$$

$$\text{if } I > I_g \quad R(I) = \frac{R_0}{\sqrt{1 + \dfrac{I}{I_g}}}$$

with:

$$I_\mathrm{g} = \frac{E_0\,\rho}{2\pi R_0^2}$$

where:

R_0 is the low-current and low-frequency resistance (Ω);

I is the lightning current through the footing impedance (A);

I_g is the limit current (A);

ρ is the soil resistivity ($\Omega{\times}$m);

E_0 is the soil ionization gradient (recommended value: $E_0 \approx 400$ kV$\times$m^{-1}).

According to IEC 60071-2, the model is only valid when the tower footing resistance is within a radius of 30 m.

7.6.11.3   HF-model

Reference [26] proposes to represent each earthing network segment as a propagation element. This type of modelling is still limited and complex and excludes the representation of ionization.

7.6.12   Earthing electrode of substations

Earthing electrodes of substations being extended, the ionization phenomenon, if such an effect exists, is very local and is likely to produce a very limited effect. It is therefore not to be taken into account. The simplified model presented previously (7.6.11.1) is usually considered as adequate.

7.6.13   Counterpoise

In terms of modelling, a counterpoise is equivalent to a propagation line.

7.6.14   Network equivalent

It is not important for fast-front overvoltages but care should be taken to avoid unrealistic reflection of waves.

7.7   Representation of network components when computing very-fast-front overvoltages

7.7.1   Equivalent circuit for components

Table 12 presents the equivalent circuit which may be used to represent components. Most of the information included in this table has been taken from [33].

Table 12 – Representation of components in VFFO studies

Component	Equivalent	Notes
Bus duct	Loss-free distributed parameter transmission line	• Surge impedance is calculated from the physical dimension • Propagation velocity taking into account the effect of spacers is close to 0,95 of the speed of light in vacuum
Spacer	Capacitance	C = 10 pF to 30 pF
Elbow, closed disconnector, closed switch, closed breaker	Loss-free distributed parameter transmission line	Propagation velocity is close to 0,95 of the speed of light
Open switch, open breaker	• The breaker is divided into as many sections as there are interrupters, all connected by the grading capacitors • Two equal lengths of bus connected by a capacitor equivalent to the series combination of all the grading capacitors	The parameters of the sections are calculated from the physical dimensions of the breaker
Open disconnector	A capacitor	
Power transformer	See IEC 60071-2, Annex E	
Current transformer	Can be represented by a Pi section	Can often be neglected due to the flashover of their protective air gap
Gas filled bushing	Can be represented by a lossless transmission line terminated by a capacitance (on the air side) between terminal and earth	C = a few tens of pF Z_s approx. 250 Ω
Bushing (capacitive type)	Several transmission lines in series with a lumped resistor representing losses	It may be possible to represent the increase of the surge impedance as the location goes up the bushing [46] but a lumped capacitance is adequate for a normal study
Power transformer (termination)	An equivalent network whose parameters are evaluated from the frequency response of the transformer	
Aerial line or cable (termination)	A resistance	Its value is equal to the value of the surge impedance of the line or cable
Surge arrester	A capacitance especially if overvoltages are lower than the protective level	Switching operations in GIS generally do not cause surge arresters to conduct

The lossless propagation lines of the table take into account the internal mode (conductor enclosure) and do not take into account the external mode (enclosure-earth), supposing the enclosure perfectly earthed. If transient enclosure voltages have to be considered the external mode has to be taken into account because at high frequencies earthing connections may have a significant impedance.

Because duration time of this kind of overvoltage is very short, components that influence this kind of overvoltage are those of substations. Outgoing transmission lines act only as surge impedances.

7.7.2   Rise time of the wave during breakdown in SF$_6$ [33]

During a phase-to-earth fault, the voltage drop at the location of default is similar to the one between the two terminals of a disconnector.

The rise time of the overvoltage is approximated by

$$t_r = 13{,}3 \frac{k_T}{\Delta u/s}$$

where

t_r is the rise time (ns);

k_T is the breakdown constant of Toepler = 50 kV ns/cm;

s is the breakdown distance (cm);

Δu is the voltage level just before breakdown (kV).

By using the approximation $\Delta u/s = (E/p)_0 \, p \, \eta$ with $(E/p)_0$ = 860 kV/(cm×Mpa), p = gas pressure (Mpa) and $\eta = E_{mean}/E_{max}$ = 0,5 .. 0,8 of a normal GIS, the minimum value of the rise time may be approximated by

$$t_{r,min} \text{ (ns)} = (1 .. 1{,}5)/p \text{ (Mpa) .}$$

Roughness and particles can increase the value of the rise time.

8   Temporary overvoltages analysis

8.1   General

Temporary overvoltages originate from the following events:

–   earth faults;
–   system faults leading to switching operations such as load rejection and/or system separation;
–   switching a non-linear component such as an unloaded transformer in a system having low-frequency poles;
–   shunt-compensated line resonance caused by uneven breaker pole operation;
–   shunt-compensated parallel line resonance;
–   other events.

Usually the selection of the rated voltage of surge arresters is based upon the envelope of the temporary overvoltage expected, taking into account the energy capability of the surge arrester (see IEC 60071-2).

Subclause 2.3.3 of IEC 60071-2 gives some general information on the determination of the corresponding representative overvoltage in the case of earth fault, load rejection, resonance and ferro-resonance and synchronization, which can cause longitudinal temporary overvoltages.

8.2 Fast estimate of temporary overvoltages

Annex B of IEC 60071-2 proposes a simplified method for the evaluation of temporary overvoltages due to earth faults only which neglects the effect of non-linearities associated with the magnetizing impedance of transformers.

In many cases, load flow and system stability analysis (i.e. phasor analyses) are performed in order to evaluate power-frequency overvoltages and then to select the rated voltage of the surge arresters which will be used in the system considered. This approach does not permit the consideration of temporary overvoltages due to resonance and ferro-resonance which may reach high values but are not normally considered when selecting the surge arrester rated voltage and for the insulation design (see IEC 60071-2).

8.3 Detailed calculation of temporary overvoltages [2], [9]

8.3.1 Presentation of the method

Detailed calculation of temporary overvoltages is needed when the effect of non-linearities cannot be neglected, such as for weak systems.

The same comment applies when temporary overvoltages originated by events different from earth faults are to be evaluated.

More generally, a sophisticated method of calculation of temporary overvoltages, as shown hereunder, is recommended in case of risk of resonance, related also to non-linearities, and in case of risk of uncontrolled power frequency voltage due to the dynamic performance of the synchronous machines and their associated regulators.

The method consists in detecting the particular events which may lead to TOV and eventually the corresponding condition, and then in evaluating, by using simulation tools, the overvoltages existing when each of these event occurs.

The successive steps of the method are as follows:

a) selection of the events to be simulated by performing a load flow and a frequency domain analysis;

b) determination of the portion of the system to be simulated in the time domain;

c) simulation, in the time domain, of the electromagnetic transients associated to the events in the relevant configurations;

d) analysis of results.

8.3.2 Required data

For load flow:

– power-frequency parameters of elements,

– loads (active and reactive),

– power exchange among areas.

For frequency domain analysis:

– transformers.

For the determination of the portion of the system to be represented in detail:

– non-linear behaviour of transformers, reactors, loads,

– SVAR compensation.

For time-domain simulations:

– control system of generators,

– equivalent circuits of the portions of the network not to be represented in detail,

– the same information as in the previous steps for the portion of the network to be represented in detail.

8.3.3 Computational tools

The evaluation of TOV is performed by means of simulation. To this end, three kinds of tools are available:

– digital computer programmes devoted to time-domain simulation and, as an auxiliary approach, to impedance versus frequency analysis;

– TNA (transient network analyser), which are analogue (or hybrid) simulators;

– RTDS (real time digital simulators), which are fully based on a digital model of the system, as for conventional digital programmes, but run in real time.

The accuracy of the simulation is practically the same for the three tools; the main difference lies in their efficiency.

Other digital programmes, based on the space state approach, are suitable for determining the behaviour of non-linear systems: for instance, by using the theory of bifurcations, the evolution of a state variable as a function of another state variable (for example, overvoltage at a transformer as a function of the pre-existent residual flux) can be drawn.

Such programmes can be a valuable aid mainly in finding the initial conditions that give rise to the worst overvoltages, which are then to be simulated in the time domain.

8.3.4 Guideline to perform studies

8.3.4.1 Selection of the events to be simulated in the time domain

At first, load flow and system stability analysis are applied after a switching event to ascertain roughly power frequency overvoltages at all nodes of the network. Frequency domain analysis studies are the conducted to determine the poles of the positive- and zero-sequence impedances of the network as seen from the transformers. The frequency domain analysis is performed from the critical buses detected during load flow and from the nodes connected to power electronics converters. The poles are critical when they are near fundamental or harmonic frequencies. Weak systems typical of developing countries show low-frequency poles near fundamental frequency or low harmonics.

The range of interesting harmonics is up to the 13th. In case of asymmetry, the impedance of the system can be evaluated on a single-phase base. Eigen-value analysis, if available, is also suitable to give valuable information.

The portion of the system where overvoltages are detected by load flow and/or stability post-event analysis must be represented in detail. Weak systems are generally not strongly meshed and can be represented in complete detail.

The typical events to be investigated are as follows:

– load rejection when long lines, low short-circuit level and system stability are concerned;

– transformer energization for poorly interconnected systems having low-frequency poles and when load flow analysis detects overvoltages before switching;

– parallel line resonance for double-circuit lines with a high percentage of shunt compensation;

- highly shunt-compensated line resonance – uneven breaker pole operation for long and highly shunt-compensated lines (more than 100 km) and long cables (in excess of 10 km);

- backfeeding;

- fault application especially in the case of high earth-fault factor;

- fault clearing and line dropping mainly when a nearby transformer has proved to give rise to critical TOV following its energization;

- line energization: this is particularly interesting for long lines when the post-event load-flow analysis detects high voltages on transformers. Line energization of a long line by a weak system should be carefully investigated;

- line re-energization: the same conditions as for line energization apply;

- closing of capacitive loads: usually not of interest except if high post-event overvoltages arise, as shown by load-flow analysis.

- switching of inductive current: usually the overvoltages do not last for a long time and are not critical from a TOV point of view.

For strong systems, the events to be usually considered, in decreasing order of priority, are load rejection, transformer energization, fault clearing, fault application and backfeeding.

For weak systems, the events considered for strong systems have to be considered, but line energization and line re-energization have to be considered as well.

In order to obtain realistic TOV scenarios, all actions associated with the most relevant protection and automatic switching systems in the network should be predicted and simulated.

8.3.4.2 Determination of the portion of the system to be simulated

In general, all the network where the prime event occurs, is to be modelled in detail, whereas networks (at different nominal voltage) which are interconnected through transformers can be represented by equivalent circuits with the same impedance versus frequency seen by the transformer terminals.

Weak systems, i.e. systems with low short-circuit currents which are often not (or poorly) meshed, are typically risky from the point of view of TOV; even if these systems have long lines, they are relatively simple and have few components. Therefore, in this case, the modelling of all the network at the voltage level where the event occurs is relatively easy.

Strong systems, i.e. systems with high short-circuit currents, are typically meshed and are therefore complex to model. Such systems, however, are less risky from the point of view of TOV, since any event in general causes a small voltage variation in any bus. If the complete representation of a whole system of this type is too cumbersome, the detailed model of the network can be limited to a portion near the prime event.

A simple criterion to select this portion consists of the calculation of the steady-state (load-flow) solution after the event with the simplifying hypothesis that all components be linear; the portion of the system where the voltage goes over the "highest voltage of the system" and where non-linear inductive components (transformers, saturable reactors) are connected, is to be represented in detail; the remaining part of the system can be represented by equivalent circuits.

In these equivalent circuits, both positive- and zero-sequence impedances versus frequency have to be covered. The important factor is the frequency of the poles, while the residues are of less importance.

8.3.4.3   Analysis of configurations and events by simulation in the time domain

This analysis is compulsory because it gives the amplitude and the duration of the transient. An adequate duration of the simulation is required (not less than 200 ms and up to 1 s). This long duration obliges the control systems of FACTS devices and the synchronous machine mechanical dynamic to be represented with an automatic voltage regulator (AVR) and governor. The worst configurations and associated events are to be detected by a deterministic approach (usually a probabilistic approach is not necessary).

Therefore, several simulations have to be performed to detect the worst configurations. All the possible configurations, even black-start, have to be considered.

9   Slow-front overvoltages analysis

9.1   General

9.1.1   Origin of SFO

SFO generally arise from (see 2.3.3 in 60071-2):

–   line energization and re-energization;

–   fault and fault clearing;

–   load rejection;

–   switching of capacitive or inductive currents;

–   distant lightning strokes to the conductor of overhead lines

but this last cause of overvoltage is not considered critical and is therefore not considered in insulation co-ordination procedures.

9.1.2   The particular case of phase-to-phase overvoltages [61]

The study of phase-to-phase overvoltages poses a particular problem for insulation configurations in which the dielectric strength between phases depends on its subdivision between components. Such is the case for large air clearances (corresponding to range 2) or three-phase, enclosed gas-insulated substations.

In order to simplify the study of this type of overvoltage, Annex D of IEC 60071-2 proposes to take into account insulation characteristics by considering two instants:

a)   the instant of phase-to-phase overvoltage peak – it gives the highest phase-to-phase overvoltage value;

b)   the phase-to-phase overvoltage at the instant of the phase-to-earth overvoltage peak.

The dependency between the dielectric strength of the insulation and the voltage components leads to the consideration of two variables which are the positive component and the absolute value of the negative component at each of the instants specified above.

In insulation co-ordination studies, it is necessary to consider globally the phase-phase-earth system (it is not possible to treat separately the phase-phase insulation and the phase-to-earth insulation) and the representative overvoltage is determined based on the two variables.

9.2   Fast methodology to conduct SFO studies

IEC 60071-2 gives in 2.3.3 some indication as to which of the events listed previously have to be taken into account when performing an insulation co-ordination study. It also gives some fast estimates of slow-front overvoltages.

a) Figure 1 of 2.3.3.1 (IEC 60071-2) gives the range of the 2 % overvoltage values which may be expected between phase and earth at the receiving end of a line energized or re-energized, taking into account the effect of most of the factors determining the overvoltages. This figure may be used as an indicator to know in a given situation whether the overvoltages are to be taken into account or not.

b) Simplified methods exist. Subclause 2.3.3.2 of IEC 60071-2 presents formulae enabling the calculation of a conservative estimate of the assumed maximum phase-to-earth overvoltage occurring at fault initiation or fault clearing.

c) Annex D of IEC 60071-2 proposes a general approach including several levels of simplification to determine the representative slow-front overvoltage due to line energization and reclosing. This approach allows the case of a phase-phase-earth over-voltage to be treated, taking into account the dependency of the phase-phase withstand of the air insulation with the subdivision of the phase-to-phase overvoltage into two phase-to-earth components. It does not require the use of a simulation tool.

However, a deterministic approach may also be implemented, using a simulation tool, in order to have a quick estimate of the maximum overvoltage that can be generated in a network subjected to a switching operation or a fault. Only a small amount of electrical simulation is required. The user has to guess the network configuration that will give rise to the highest overvoltages and determine the breaker switching times or fault occurrence time that will induce the highest overvoltages. The limit of the approach is that the risk cannot usually be assessed. The user should take care to avoid too optimistic conclusions.

9.3 Method to be employed

Studies are usually based on an estimation of the probability distribution of the representative overvoltages obtained by a series of time-domain simulations, from which the risk is calculated. For instance, in the case of line energization, different closing times of the breaker may be chosen randomly, applying the Monte-Carlo method, one time-domain simulation being performed for each closing time. The next subclause is a guideline to implement such studies and describes two methods. The first one is called full statistical because it takes into account all variables that have an influence on the overvoltage (closing times of breaker but also network configuration) considering their probability of occurrence. The second one is a semi-statistical one. In this one, the configuration of the network is considered as fixed.

Practical experience from the participating members indicates that the semi-statistical method is preferred for "line operations": line re-energization, line energization, fault application. The deterministic method should not be used if phase coupling exists. The deterministic method (with several values of chopped currents) is used for reactive device operations (reactor switching and capacitor bank closing), but semi-statistical methods can also be implemented.

9.4 Guideline to conduct detailed statistical methods

9.4.1 Application of a full statistical method

9.4.1.1 What is evaluated

The results of this method are overvoltage distributions from which the risk is calculated as described in IEC 60071-2. The statistical behaviour of insulation can be included, and, in this case, the result obtained is directly the risk of failure.

9.4.1.2 Principles

This method most closely resembles the real configuration. All variables that may influence the overvoltages are taken into account. These variables are principally closing times of a breaker, time of fault occurrence, location/type of fault, network configurations and short-circuit power. With this method, none of these variables are considered as a constant. Once all variable parameters have been identified, their range of possible values and the probability of each value (or sub-range of values) has to be known.

Electrical simulations are performed. The risk is evaluated using the probability associated with variables and the results of the electrical simulations. For instance, Monte Carlo can be applied.

9.4.1.3 Required data

The required data is as follows:

– list of all possible configurations and operations;

– probability of each configuration;

– location of the fault;

– number of operations per year;

– main breaker probabilistic data:

  • mean time of closing,

  • standard deviation of closing time,

  • type of distribution of closing time,

  • pre-strike information;

– auxiliary breaker statistical data (if present):

  • mean insertion time,

  • insertion time standard deviation,

  • type of distribution of insertion time;

– insulation behaviour:

  • withstand voltage,

  • standard deviation of withstand voltage;

– electrical parameters of all elements.

9.4.2 Semi-statistical method

9.4.2.1 What is evaluated

This method gives an estimation of the overvoltage distributions, taking into account certain configurations. Afterwards, risk of failure can be calculated with the methodology explained in IEC 60071-2.

If the insulation statistical behaviour is included, the risk of failure can be calculated directly (this is seldom performed).

9.4.2.2 Principles

This method is similar to the full statistical method except that only some configurations are considered. Several strategies are possible. The most probable configurations are often considered but it is sometimes valuable to consider only the worst case.

9.4.2.3 Required data

This method requires the same data sets as those required for the full statistical method except that only variables associated with few considered configurations are necessary.

9.4.3   Modelling aspects

9.4.3.1   How far to represent the network

The network surrounding the event that is the cause of the slow front transient has to be represented. The depth of modelling is one or two substations. The following schemes (Figures 17 and 18) show two examples of network representation.
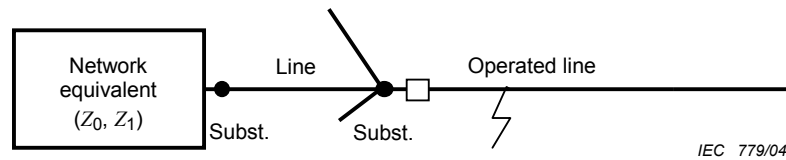
Figure 17 – Example of a one-substation-deep network modelling
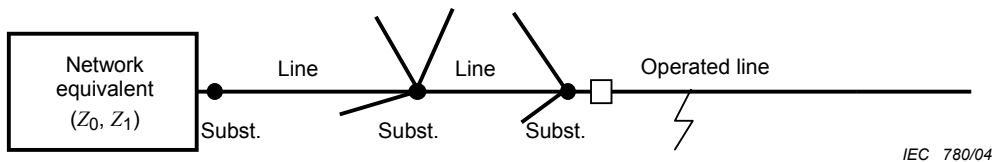
Figure 18 – Example of a two-substation-deep network modelling

This last scheme is called two-substation deep because, besides the substations directly connected to the line on which the transient appears, two other substations are represented. After these two substations, the rest of the network is modelled as a Thevenin equivalent based on positive- and zero-sequence impedances.

The more extensively the network is represented, the more accurate the results will be. Generally, the more deeply the network is represented, the more damped the overvoltages are. So a one-substation deep network will generally give higher maximum values than a two-substation one. However, in the case of switching of capacitive current, a two-substation-deep network may lead to higher overvoltages because the switched capacitive charge may resonate with another capacitive charge. It should also be pointed out that a two-substation network will give more information about harmonic resonance.

Usually, for "line operations" (line re-energization, line energization, fault application), the network is represented up to two substations from the operated line. For reactive device operations (reactor switching and capacitor bank closing), the network is represented very simply, but the reactive device has to be precisely modelled.

9.4.3.2   The modelling of breakers

The statistical switch described in 7.5.10.1 must be used in statistical methods.

The deterministic method may be used as a first and quick estimation. In this case, an ideal switch may be used according to 7.5.10.1.

To study the opening of reactive elements, it is recommended that the arc model described in 7.5.10.2 which can predict the possibility for a given breaker to open such currents be used. An ideal switch may be used if there is some means of estimating the chopping current.

If the relevant data is available from experiment, TRV studies should be carried out with the restriking breaker presented in 7.5.10.1.

As a simplification, an ideal switch can be used and the TRV calculated can be compared with the TRV withstand level of the breaker.

10 Fast-front overvoltages analysis

10.1 General

Fast-front overvoltages are mainly due to lightning but they can also occur when equipment is connected to, or disconnected from, the system via short connections (IEC 60071-2) or when external insulations flash over. These two cases are not considered in this subclause.

Approaches to perform FFO studies may be classified according to two criteria:

– the use or not of an electromagnetic transient programme;
– the application or not of a statistical approach.

This is illustrated in Table 13.

Table 13 – Types of approach to perform FFO studies

	Use of an electromagnetic transient programme	No use of an electromagnetic transient programme
Statistical approach	1 Semi-statistical method and 2 Statistical method described in 10.2	------------
No statistical approach	3 Deterministic approach described below	-------------
Simplified statistical approach	4 Method described in Annex F of IEC 60071-2	5 Method described in Annex F of IEC 60071-2

The following is a brief description of the approaches.

10.1.1 Semi-statistical method

This method presented in 10.2 gives an estimation of the risk of failure of equipment in a system with a predetermined configuration. An electrogeometric model is used to evaluate the lightning incidence on the aerial part of the system and an electromagnetic transient programme is used to evaluate the overvoltages generated by the lightning strokes.

10.1.2 Statistical method

This method presented in 10.2 gives an estimation of the risk of failure of equipment in a system taking into account all the possible configurations of the system.

10.1.3 Deterministic approach

Applications of this type of approach are used at present in Japan [52] and in many other countries. From experience, the minimum value of lightning current at a specific point of impact has been determined, which produces overvoltages that the equipment has to withstand. This is called the representative lightning stroke current and it usually depends on the system voltage and the type of equipment considered (GIL).

10.1.4 Method described in Annex F of IEC 60071-2

The method consists in:

a) calculating a lightning current with the desired return rate using lightning data and the back-flashover rate or the shielding failure rate within the limit distance, whether shielding penetration or back flashovers are considered,

b) calculating the amplitude of the impinging surge at substation based on several simplified assumptions,

c) using the impinging voltage surge evaluated previously to perform a travelling wave calculation within the substation.

10.1.5 Method described in Annex F of IEC 60071-2

A complete analytical approach is proposed assuming that the configuration of the substation is very simple, a surge arrester or a spark gap is installed only at the substation entrance and the overvoltage at a tower is generated by the tower footing resistance, neglecting further increase due to the tower surge impedance.

The use of an electromagnetic transient programme allows a more accurate estimation of the overvoltages. For this reason, the methods presented below will be based on the use of such a programme.

10.2 Guideline to apply statistical and semi-statistical methods

10.2.1 General

The application of such methods in summarized in Figure 19.
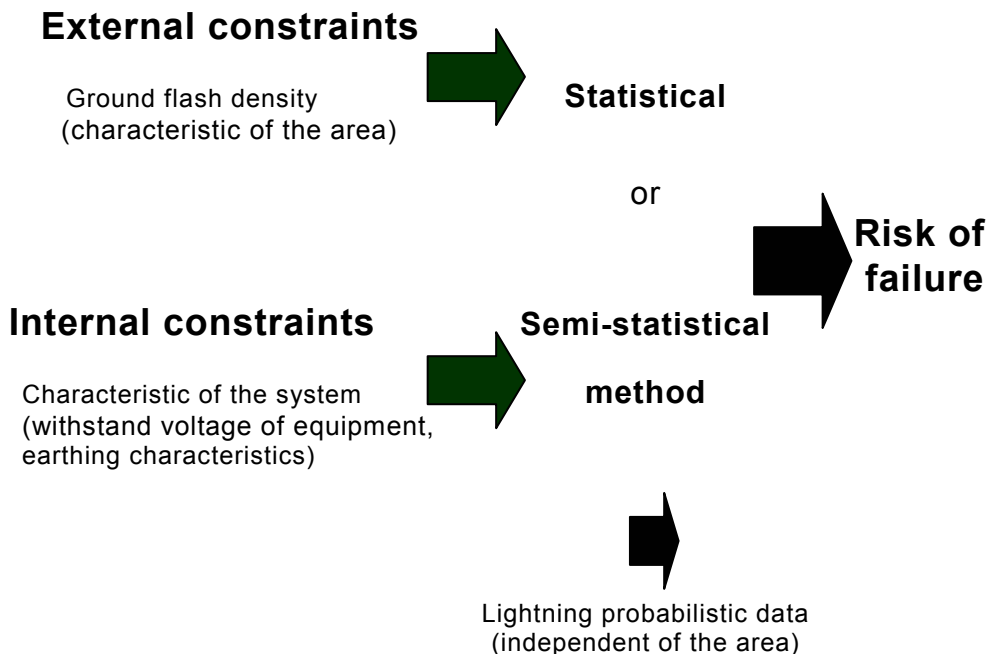
Figure 19 – Application of statistical or semi-statistical methods

In both methods, the random nature of lightning is considered. The difference between the two methods is related to the accounting of the possible configurations of the system. In the semi-statistical method, the system is considered as fixed. For example, the number of circuits of the line connected to the substation and the configuration of the substation are deemed as fixed. On the contrary, when applying a statistical method, all the configurations of the system which may exist are taken into consideration. For example, the number of circuits connected to the substation and the different possible configurations of the substation will need to be taken into account.

The main successive steps of these methods are as follows:

- Determination of the limit distance: the attenuation of the overvoltages generated by a lightning stroke increases with the travelling distance of the travelling wave. When the distance between the point of impact and the equipment is sufficient, the lightning stroke will not provoke an overvoltage of sufficient amplitude between the terminals of the equipment and the earth to be considered. So for distances larger than the limit distance, lightning strokes do not have to be considered.

- Evaluation of the number of lightning strikes impacting the aerial parts, within the limit distance, per year, and evaluation of the probabilities corresponding to the point of impact and crest value of the lightning current.

- Determination of the risk of failure of equipment for one configuration of the system.

- Estimation of the risk of failure of equipment, taking into account all the possible configurations of the system in the case of statistical methods, or only one configuration in the case of semi-statistical methods.

10.2.2   Required data

The application of these methods requires the following data:

- Configuration of substations (location and characteristics of equipment) and, more generally, of the system to be protected against FFO (cable);
- Withstand voltage of equipment (transformer, circuit-breaker and others);
- Characteristic of protection equipment (surge arrester, air gap);
- Number of circuits of the line;
- Characteristics of phase conductors;
- Sag of conductors and shielding wires;
- Geometry of towers (position of conductors and shield wires);
- Characteristic of shield wires;
- Tower footing arrangement;
- Flashover characteristics of insulator strings and arcing horns;
- Characteristic and position of line surge arresters;
- Ground flash density.

10.2.3   Determination of the limit distance

IEC 60071-2 proposes a simplified formula to determine the limit distance based mainly on the assertion that the steepness of the impinging surge is reduced significantly by the number of overhead lines connected to the substation and the damping due to corona effect.

It is generally more accurate to determine the limit distance using a simulation tool.

10.2.4 Evaluation of the number of lightning stokes impacting the line, within the limit distance, per year, and evaluation of the random distributions of peak current associated with these lightning strokes

10.2.4.1 Average attractive radius – strokes impacting the towers and the shield wires

Reference [4] proposes an expression to evaluate the number of lightning strikes impacting 100 km of line per year, based on a notion of attractive radius R_a, which relates on a simplified leader model and on observations on practical transmission lines:

$$R_a(m) = 14 \times H_T^{0,6} \qquad \text{and} \qquad N_L = N_g \, (2 \times R_a + b)/10$$

where

H_T is the average tower height (m);

N_L is the number of lightning strikes per year and per 100 km;

N_g is the ground flash density (flashes/km^2/year);

b is the distance between shield wires (m).

The probabilistic distributions to be used for the electrical representation of the lightning stroke are detailed in 7.6.9.3. The results are usually considered as conservative.

For a line equipped with shield wires, it is commonly considered that 40 % of the strokes terminate within the span and 60 % terminate at the tower.

10.2.4.2 Attractive radius versus crest value of the stroke current: strokes impacting the towers and the shield wires

The following formula can be applied to evaluate the number of lightning strikes per year and per 100 km, N_L:

$$N_L \approx \frac{N_g}{10} \int\limits_{3}^{300} (2 \times R(I) + b) f_g(I) \mathrm{d}I$$

where

N_g is the ground flash density (flashes/km^2/year);

I is the crest value of the lightning current (kA);

$R(I)$ is the attractive radius of the line for I (m);

b is the distance between shielding wires (m);

f_g is the probability density function of the lightning current striking the ground.

10.2.4.3 Direct application of an electro-geometric model

The probabilistic distributions to be used for the electrical representation of the lightning stroke that are given in the 7.6.9.3 are valid for this one (see Figure 20).

Input data

- Ground flash density

- Probabilistic repartition
  of the crest value of the
  lightning current on the ground

Application of the

electrogeometric

model

Output data

For each tower within
the limit distance:
- the number of lightning
  strokes impacting

For each span within
the limit distance:
- the number of
  strokes impacting
- their repartition
  along the span

The conditional probabilistic
repartition
$f(l/\text{point of impact})$

Geometrical structure
of the overhead line

IEC   782/04

Figure 20 – Application of the electro-geometric model

10.2.5   Determination of the risk of failure for one configuration of the system [22]

The probability density function corresponding to the failure of an equipment $F(u)$ is the probability of insulation breakdown at a stress of u given by $P(u)$ times the density of probability of observing an overvoltage of maximum amplitude u given by $f_U(u)$, that is to say:

$$F(u) = P(u)\, f_U(u)$$

Therefore, the probability of failure, considering all overvoltages, is (see IEC 60071-2):

$$P_F = \int_0^\infty f_U(u) P(u)\,\mathrm{d}u$$

$P(u)$ can be also considered as the probability to have a voltage u_d lower than the voltage u:

$$P(u) = P(U_d < u)$$

By definition U_d is called the disruptive voltage. U_d and U are independent probabilistic variables.

$$P_F = \int_U f_U(u)(\int_o^u f_{U_d}\mathrm{d}u_d)\,\mathrm{d}u$$

Therefore, an equivalent formulation can be used for the risk of failure:

$$P_F = \iint_{u_d < u} f_U(u) f_{U_d}(u_d)\,\mathrm{d}u\mathrm{d}u_d$$

U is a function of basic variables X, namely lightning current parameters, point of impact of the lightning stroke, instantaneous angle of the operative phase voltage:

$$P_F = \iint\limits_{u_d < u(x)} f_X(x) f_{U_d}(U_d) \, du_d \, dx$$

We can define the state of the system:

- $[u_d - u(x) > 0]$ provides the safe state;
- $[u_d - u(x) < 0]$, the failure state, which is the domain of integration for probability;
- and the boundary $[g(x) = 0]$ is the limit state surface. See Figure 21.

IEC 783/04
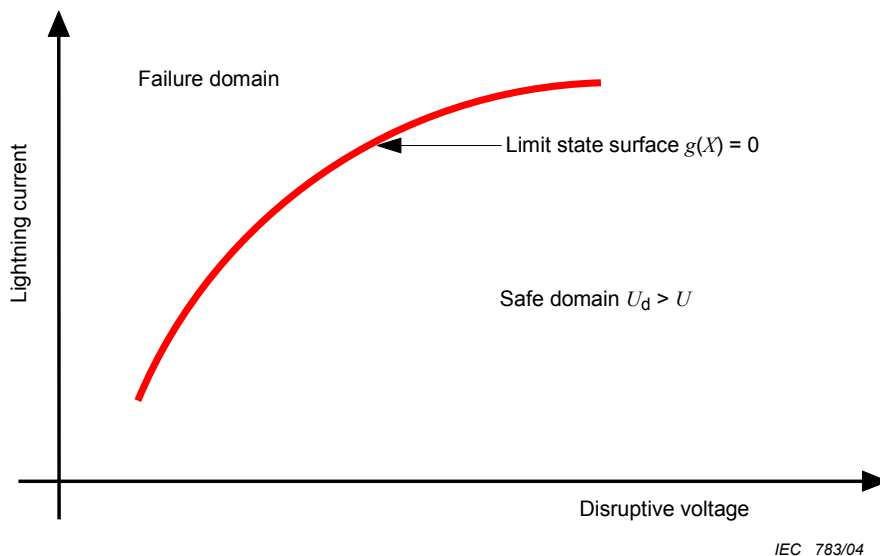
**Figure 21 – Limit function for the two random variables considered:
the maximum value of the lightning current and the disruptive voltage**

The procedure to determine the probabilistic representative overvoltage is the following: the function f_X has been determined in the previous steps:

- the limit distance defines the domain of variation of X;
- f_X has been defined using the electro-geometrical model.

An approximation of the limit state surface is performed, using an electromagnetic transient programme. The waveshape obtained by numerical simulations may not correspond to the standard shape (see IEC 60071-1). However, the overvoltages calculated are usually considered as the representative overvoltages. The approximation of the limit state surface may be restricted to a domain of interest based mainly on the assumption that only the configurations of basic variables having a sufficient probability of occurrence are of interest for the evaluation of the risk. The probability of failure is calculated and then the risk of failure is determined using the ground flash density which has been associated to that particular configuration of the system. The final calculation of the probability of failure can be performed using Monte Carlo methods or other methods like FORM/SORM [42]. The risk of failure is estimated by multiplying the probability of failure by the average number of occurrences per year of overvoltages due to lightning.

10.2.6 Determination of the risk of failure for all the configurations

The risk of failure is the sum of the partial risks of failure determined in the previous step.

11 Very-fast-front overvoltage analysis

11.1 General

VFFO arise within a gas-insulated substation (GIS) any time there is an instantaneous change in voltage. Most often this change occurs as the result of the opening or closing of a disconnector switch, but other events, such as the operation of a circuit-breaker (for instance, the de-energization of a shunt reactor), the closing of an earthing switch or the occurrence of a fault can also cause VFFO. Surge arresters are not effective to control these overvoltages due to their extreme rate of rise.

Their generation and propagation from their original location throughout a GIS can produce internal and external overvoltages. The main concern is internal overvoltages between the centre conductor and the enclosure. However, external transients can be dangerous for secondary and adjacent equipment. These external transients include transient voltages between the enclosure and earth at GIS-air interfaces, voltages across insulating spacers in the vicinity of GIS current transformers when they do not have a metallic screen on the outside surface, voltages on the secondary terminals of GIS instrument transformers and radiated electromagnetic fields (EMF) which can be dangerous to adjacent control or relay equipment.

VFFO generally have a very short rise time, in the range of 4 ns to 100 ns, and are normally followed by oscillations having amplitude values in the range of 1,5 to 2,0 per unit of the line to neutral voltage crest, but they can also reach values as high as 2,5 per unit. These values are generally below the LIWV of the GIS and connected equipment. VFFO in GIS are of greater concern for range 2 equipment, for which the ratio of the LIWV to the system voltage is lower. Some equipment failures and arcing problems between earthed parts have occurred at systems voltages above 420 kV, they have been correlated with disconnector switch and circuit-breaker operation.

11.2 Goal of the studies to be performed

A breakdown of a GIS due to VFFO not being acceptable, studies consist in detecting configurations leading to flashover due to VFFO. This matter has been covered by IEC 62271-102 [66]. Usually a deterministic approach is applied to find the worst VFFO. In general, the worst configurations correspond to the ones with the minimum number of bays connected.

11.3 Origin and typology of VFFO

VFFO are mainly due to

a) disconnector operation,

b) circuit-breaker operation,

d) internal fault including both a.c. and d.c. flashover,

e) earthing switch operation,

f) disconnector switch operation.

These are the main causes of VFFO. During a disconnector operation a number of prestrikes or restrikes occur due to the relatively low speed of the moving contact. During closing, as the contacts approach, the electric field between them will rise until sparking occurs. The first strike will almost inevitably occur at the crest of the power-frequency voltage, due to the slow operating speed. Thereafter, current will flow through the spark and charge the capacitive load to the source voltage. As it does so, the potential difference across the contacts falls, the spark will eventually extinguish and trapped charges may be left on the insulated busbar. The VFFO of the subsequent strike may lead to higher voltage magnitude.

11.3.1 Circuit-breaker operation

Physical phenomena appearing during this type of operation may be the same as for the disconnector switch operation but the stress is usually less severe. One particular case is circuit-breaker re-ignition when switching small inductive loads (see IEC 61233).

11.3.2 Internal faults

This is not usually a critical aspect, except for external overvoltages (see 11.3.5).

11.3.3 Earthing switch operation

This is the same mechanism as for internal fault but the stress is less severe.

11.3.4 Internal transients

Internal transients are transients between inner conductors and the encapsulation. The propagation of VFFO throughout GIS can be analysed by representing GIS sections as low-loss distributed parameter transmission lines. The internal damping of the transients influencing the highest frequency components is determined by the spark resistance. Skin effects due to the aluminium enclosure can be neglected. The main portion of the damping of the very-fast-front transients occurs by out-coupling at the transition to the overhead line. The trapped charge remaining on the load side of the disconnector has a strong influence on the level of VFFO. For a normal disconnector, the maximum trapped charge reaches 0,5 p.u. and results in overvoltages in the range of 1,7 p.u. and reach 2,0 p.u. for specific cases.

11.3.5 External transients

The mechanism that generates the external transients from the internal transients can be analysed by considering GIS–air interface to be a connection of three transmission lines as shown in Figure 22. GIS internal transients arriving at the GIS-air interface are then partly transmitted to overhead lines, partly transmitted to enclosure and also partly reflected in the GIS.

a) Actual configuration   b) Schematic configuration
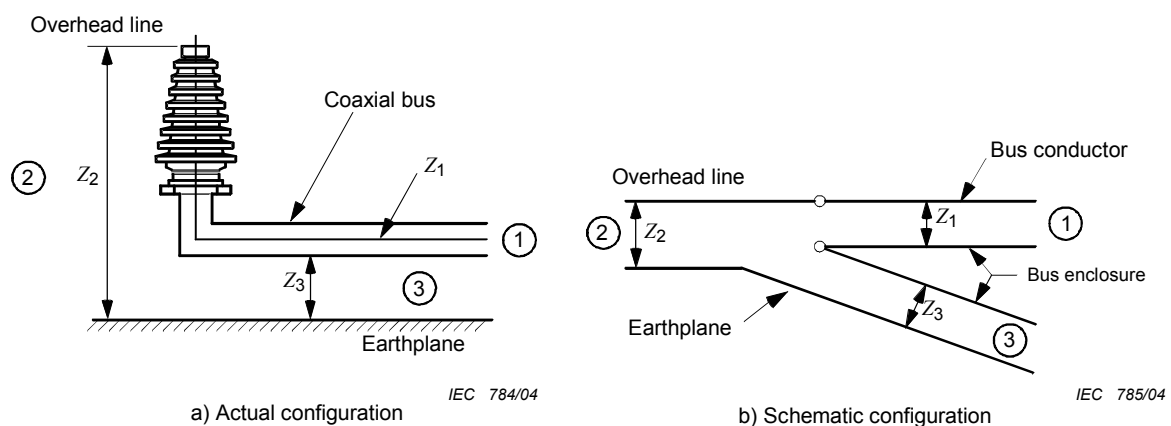
Figure 22 – At the GIS-air interface: coupling between enclosure and earth (Z_3), between overhead line and earth (Z_2) and between bus conductor and enclosure (Z_1) [33]

11.3.5.1 Transient enclosure voltages (TEV)

Transient enclosure voltages are short-duration, high-voltage transients which appear on the enclosure of the GIS through the coupling of internal transients to enclosure at enclosure discontinuities. The usual location for these voltages is the transition GIS-overhead line at an air bushing, such as visual inspection ports, insulated spacers for CTs or insulated flanges at GIS and GIS/cable interfaces. In general, TEV waveforms have at least two components which are damped quickly: the first one has a short initial rise time and is followed by high-frequency oscillations (range of frequency 5 MHz to 10 MHz); the second component is of lower frequency, hundreds of kHz and is often associated with the discharge of capacitive devices to the earthing system. TEV generally persist for a few microseconds. Their magnitude is in the range of 0,1 p.u.to 0,3 p.u.

11.3.5.2 Transients on overhead connections

A portion of the travelling wave incident at a gas-air transition is coupled onto the overhead connections and propagates to other components. In general, it has two different characteristics:

– a fast-front portion having a rise time in the range of 20 ns;

– an overall waveshape having a typical very significant oscillation of frequency in the order of 10 MHz.

11.4 Guideline to perform studies

The main concern from the point of view of insulation co-ordination is related to internal transients. External transients deal with electromagnetic compatibility aspects (transient induction on auxiliary conductors and personnel health and safety). For modern GIS, the main concern is to assess the VFFO occurring when an internal discharge takes place, mainly a disconnector operation.

To perform studies, the system considered is represented using for each component the modelling specified in 7.7.1. The part of the system to be represented in detail is limited to the GIS.

12 Test cases

12.1 General

The aim of this clause is to show how the methodology presented previously can be applied in practical studies. In order to do so, one test case is presented for each type of study.

Supplementary test cases can be found in the annexes .

12.2 Case 1: TOV on a large transmission system including long lines

This section summarizes results of a test case of TOV on a large 735 kV system including long transmission lines. As suggested in 8.3.4, the test case has been performed in two steps:

• Step 1: A stability programme is used to detect the system configurations and events which may lead to severe TOV.

• Step 2: Electromagnetic transient simulations are performed to assess more accurately the level of overvoltages which may appear on the system. Dynamic source models have been used for TOV simulations taking into account the system dynamic behaviour during severe electro-mechanical disturbances that were observed in step 1.

12.2.1 Description of the test-case system

The test-case system, as illustrated in Figure 23, is a long radial system. The three main generating centres, No. 1 (8 100 MW), No. 2 (5 600 MW) and No. 3 (15 600 MW), are far away from the load centre. The length of the two major transmission corridors running from the Nos. 2 and 3 to the load centre is approximately 1 000 km and that from No. 1 to the load centre is about 400 km. The following equipment has been used for reactive power compensation:

- Switched shunt reactors (number of 165/330 MVAr units totalling 25 000 MVAr);
- Synchronous compensators (9×250 MVA);
- Static VAr system (SVS) (11×300 MVAr);
- Series capacitors (32 banks adding up to 11 200 MVAr).

Furthermore, three system-wide automatic switching schemes have also been implemented in this transmission network:

- a shunt reactor automatic switching system called MAIS [40];
- an automatic generation rejection and remote load shedding scheme called RPTC [41];
- an automatic system, namely SPSR, using switched metal-oxide surge arresters (SMOSA) [39], [55].

12.2.2 Step 1: Detection of the system configuration and events leading to severe TOV using a stability programme

System stability study shows that, in case of misoperation of the RPTC, this transmission system could be unstable following a three-phase fault at CHM7 with the loss of three lines: two lines CHM-JCA7 and one line CHM7-SAG7. These disturbances would lead to out-of-phase conditions on the three lines connecting LVD7 to the load centre. Subsequently, the simultaneous tripping of these last three lines by their distance-relay based protections makes the system full-load rejection (or separation). Following a system separation, severe TOV due to Ferranti effects appear on long unloaded lines which are still connected to generating centres. This system separation scenario has been simulated using a stability programme by the following switching sequence:

- At t = 0, the system is under steady-state peak-load flow condition.
- At t = 6 cycles, a three-phase fault at CHM7 is initiated.
- At t = 12 cycles, the three-phase fault at CHM7 is cleared simultaneously with the trip-out of the three lines CHM7-JCA7 and CHM7-SAG7.
- At t = 27 cycles, the total generation of 4 400 MW at TIL7 is successfully rejected by the actions of the RPTC. However, the remote load shedding function is not active due to misoperation of the RPTC.
- At t = 55 cycles, the three lines connecting LVD7 to the load centre are tripped by actions of their distance-relay-based protections under out-of-phase conditions making the system separation.
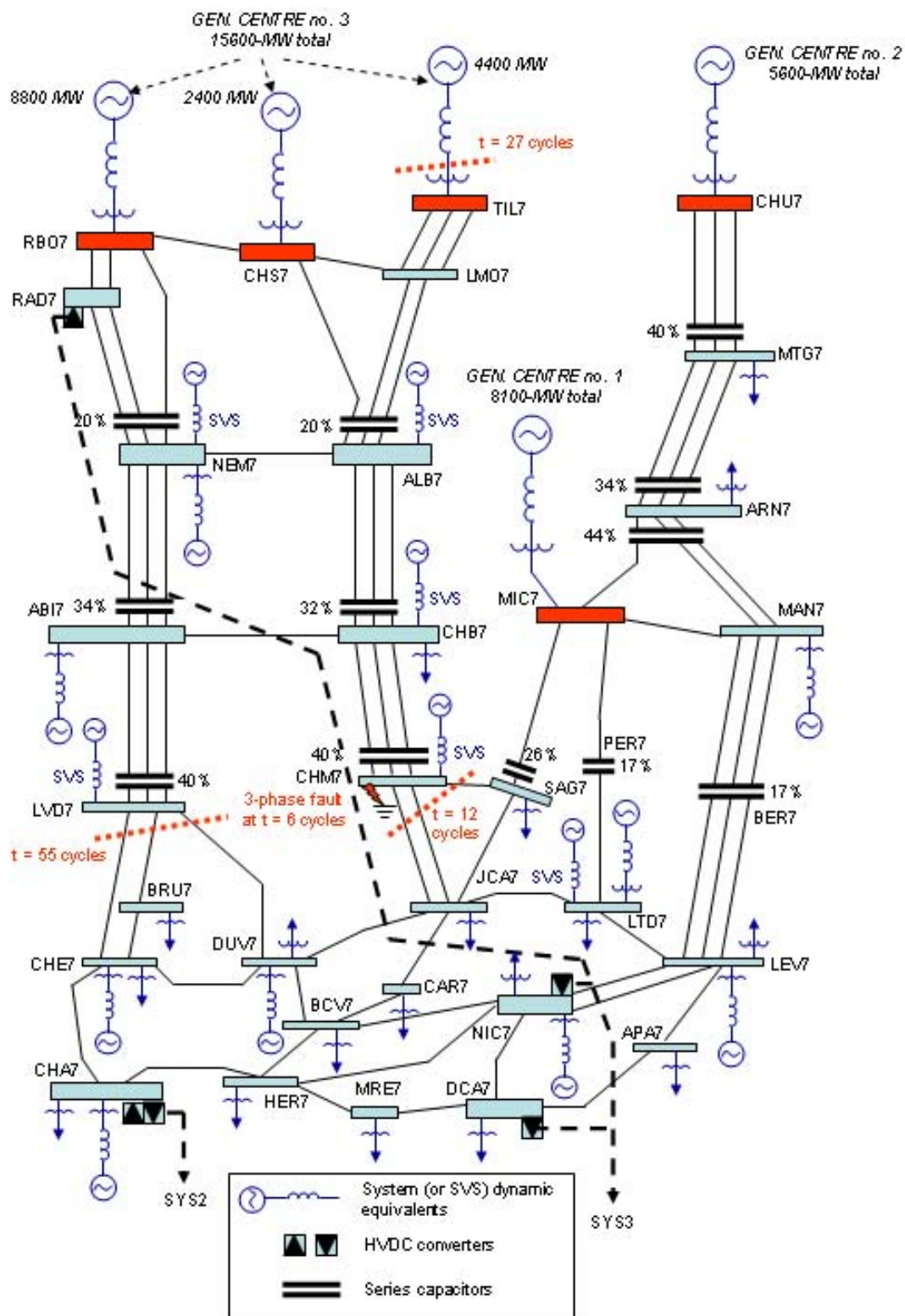
Figure 23 − **Single-line diagram of the test-case system**

IEC   786/04

The results of the stability programme are illustrated in Figures 24 and 25. Following three-phase fault clearing and loss of the three lines CHM7-JCA7 and CHM7-SAG7, the rates of rise in frequency at the various generating centres are not the same. Out-of-phase conditions between No. 3 and Nos. 1 and 2 are reached at t = 55 cycles (0,9166 s) when the difference in frequency of these generating centres is approximately equal to 1,0 Hz or 0,016 p.u., as illustrated in Figure 25. At the same instant, the voltages at LVD7 and CHE7 reach their minimum before the system separation takes place (Figure 24). Following the system separation, very high TOV occur on long unloaded and slightly compensated lines that are left connected to generating centre No. 3. As a result, the prospective TOV of 2,5-2,7 p.u. were observed at LVD7 and CHM7. These prospective TOV are much more severe than those occurring on the sound phases during single phase-to-earth faults. Although voltage regulators in generating centre No. 3 tend to reduce the magnitude of prospective TOV over a time period of 30 cycles, their effects are not sufficient to bring TOV down to a safer level for system equipment (Figure 24). It should be mentioned that the results of the stability programme do not include the non-linear effects of transformer saturation and metal-oxide surge arresters. These effects limit the expected TOV on the real system. Therefore, detailed electromagnetic transient simulation including system dynamic behaviour, transformer saturation and metal-oxide surge arresters is needed in order to obtain more realistic TOV.

IEC   787/04
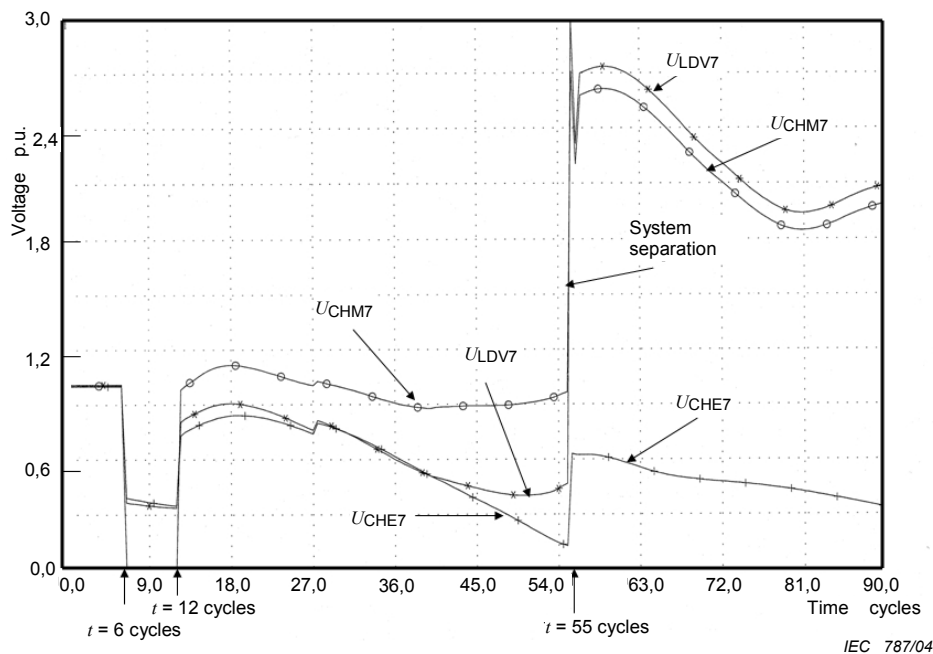
Figure 24 − TOV at CHM7, LVD7 and CHE7 from system transient stability simulation
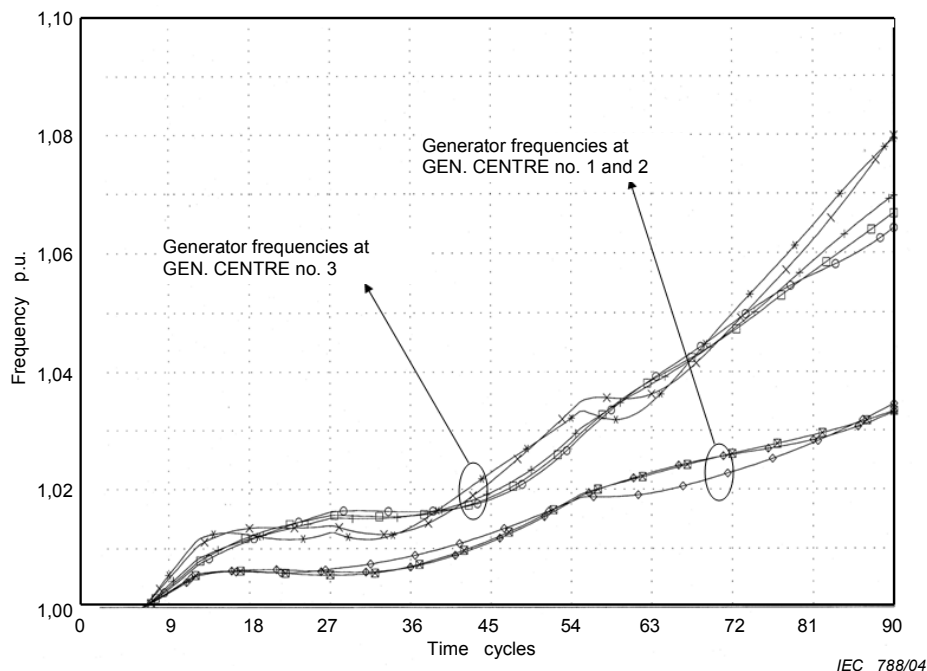
**Figure 25 – Generator frequencies at generating centres Nos. 1, 2 and 3
from system transient stability simulation**

12.2.3 Step 2: Electromagnetic transient simulation

12.2.3.1 System modelling

The system configuration and events leading to severe TOV that were detected in step 1 were represented by detailed three-phase electromagnetic transient simulation using the following models.

• **Dynamic sources**

In order to represent system dynamic behaviour, all generating stations and all Thévenin equivalents were simulated by the dynamic source models described in 7.4.1. The two driving signals $\delta_i(t)$ and $V_i(t)$, as illustrated in Figure 26, were calculated from the results of the stability simulation of step 1. This play-back simulation technique can only be used to include the system dynamic behaviour which was previously predicted by a stability programme. However, with the detailed representation of system non-linear characteristics such as transformer saturation and metal-oxide surge arresters, electromagnetic transient simulation will give more accurate results of TOV on the system.

f = system frequency

$V_0(t) = V_i(t) \, \text{Cos}(2\pi f t) + \delta(t)$, where:

$V_i(t)$ and $\delta(t)$ are magnitude and angle of generator
internal voltage obtained from transient stability simulation
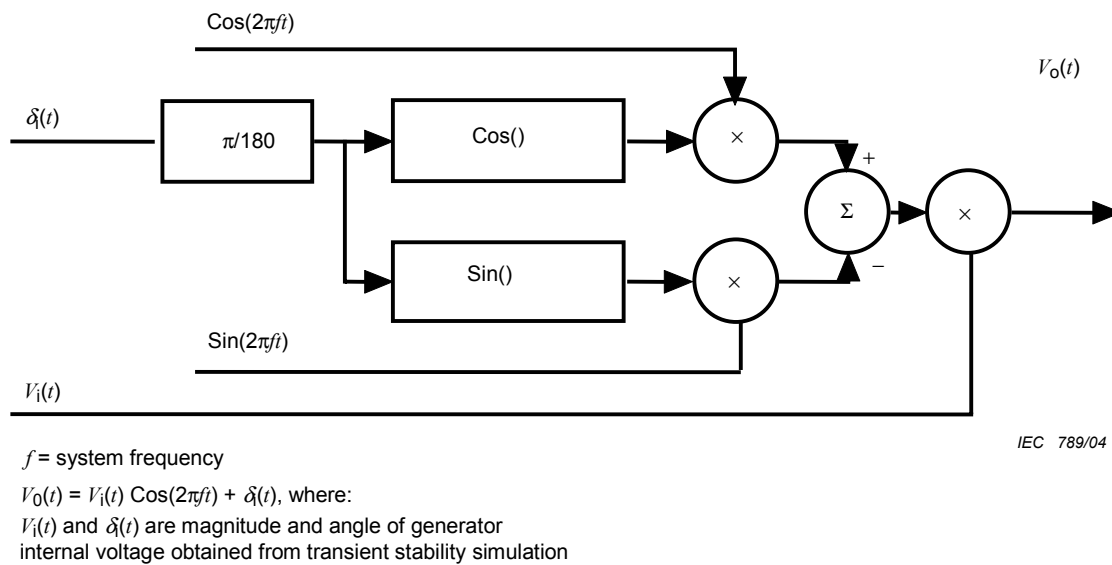
Figure 26 – Block diagram of dynamic source model [55]

- **Transmission lines**

All transmission lines were represented by three-phase distributed line models using positive and zero-sequence line parameters at fundamental frequency.

- **Transformers and auto-transformers**

Saturable transformer models have been used to represent all transformers and auto-transformers in the system. A typical saturation curve having a knee point of 1,2 p.u. and a slope of 30 % in the saturation region has been used to represent transformer saturation characteristics.

- **Loads**

All system active and reactive loads were calculated according to the system pre-fault load flow and were distributed through the sub-transmission systems which is connected to the secondary side of transformers. These loads were represented by constant impedances made up of *R-L-C* branches in parallel.

- **Synchronous compensators**

All synchronous compensators were represented by dynamic source models having equivalent internal impedance. All necessary data to control these dynamic sources was collected from the results of the stability simulation of step 1.

- **Static var systems (SVS) and HVDC interconnection**

All SVS and HVDC interconnection were also represented by equivalent dynamic source models. The internal impedances of these equivalent dynamic source models were set so high that they would not modify the system strength. All necessary data to control these dynamic sources are also collected from the results of the stability simulation of step 1.

- **Metal-oxide varistors protecting series-capacitor banks**

All metal-oxide varistors protecting series-capacitor banks were simulated by non-linear models representing their *V-I* characteristics at low-frequency injected currents (ms wave front).

- **Surge arresters**

Two types of metal-oxide surge arresters have been used in the test case system.

- **Permanent metal-oxide surge arresters having a rated voltage of 588 kV or 612 kV**

The permanent 588 kV or 612 kV surge arresters were installed at different locations in each 735 kV substation such as: shunt reactor terminals, power transformer terminals, line side of line circuit-breakers, etc. Their switching impulse protective levels are approximately 1,90-2,0 p.u.. These metal-oxide surge arresters were simulated by non-linear models representing their *V-I* characteristics at low-frequency injected currents (ms wave front).

- **Automatically switched metal-oxide surge arresters (SMOSA) having a rated voltage of 484 kV [39] [55]**

The SMOSA, which were applied on line terminals of ABI7, CHB7, LVD7, CHM7 and SAG7, limit the magnitude of TOV in case of system full-load rejection (or system separation) to approximatively 1,60 p.u.. Since their rated voltage is too low to be permanently connected to the system, they must therefore be automatically switched in for a short period of time (≈ 15 s) during system disturbances by local power swing detection, by remote detection of over-frequency or by open-corridor condition. These metal-oxide surge arresters were also simulated by non-linear models representing their *V-I* characteristics at low-frequency injected currents (ms wave front).

- **Switching sequence**

Switching sequence leading to severe TOV, as simulated in step 1, has been repeated in electromagnetic transient simulation using time-controlled switches.

12.2.3.2 Results

The results of electromagnetic transient simulations are presented in Figures 27, 28, 29 and 30.

- **Effects of permanent surge arresters**

Figures 27 and 28 show respectively TOV at LVD7 and CHM7 obtained from electromagnetic transient simulation with 588 kV and 612 kV permanent surge arresters. It can be seen that the non-linear characteristics of these system surge arresters limit TOV following the system separation to 1,9-2,0 p.u. compared to those of 2,7 p.u. from stability simulation (see Figure 24).

IEC   790/04
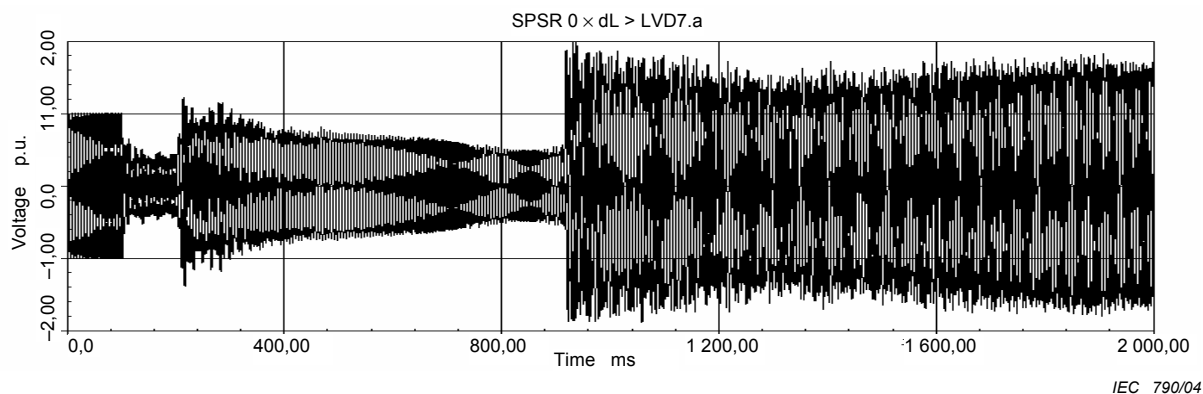
**Figure 27 – TOV at LVD7 – Electromagnetic transient simulation
with 588 kV and 612 kV permanent surge arresters**

SPSR 0 × dL > CHM7.a
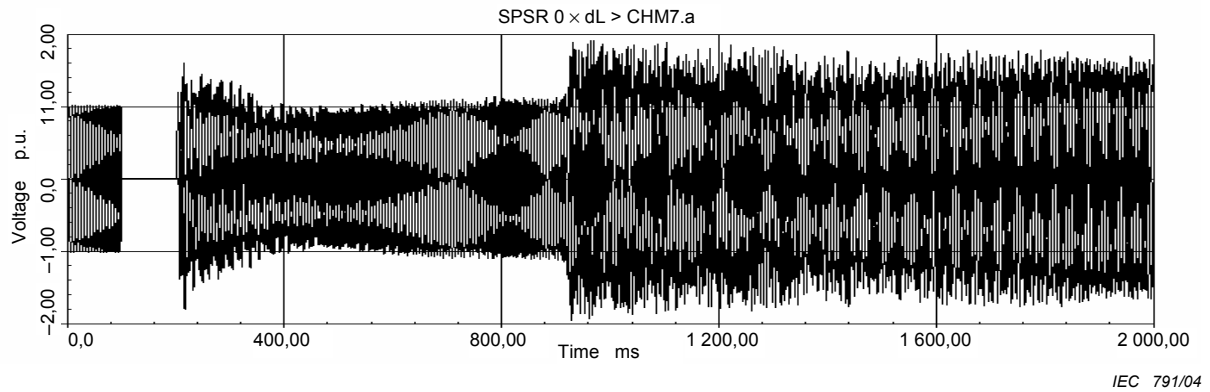
**Figure 28 – TOV at CHM7 – Electromagnetic transient simulation
with 588 kV and 612 kV permanent surge arresters**

- **Effects of automatically switched metal-oxide surge arresters**

The results of electromagnetic transient simulation, as illustrated in Figures 29 and 30, show that TOV at LVD7 and CHM7 were further reduced to less than 1,6 p.u. with the presence of 484 kV automatically switched metal-oxide surge arresters.

SPSR 1996 > LVD7.a
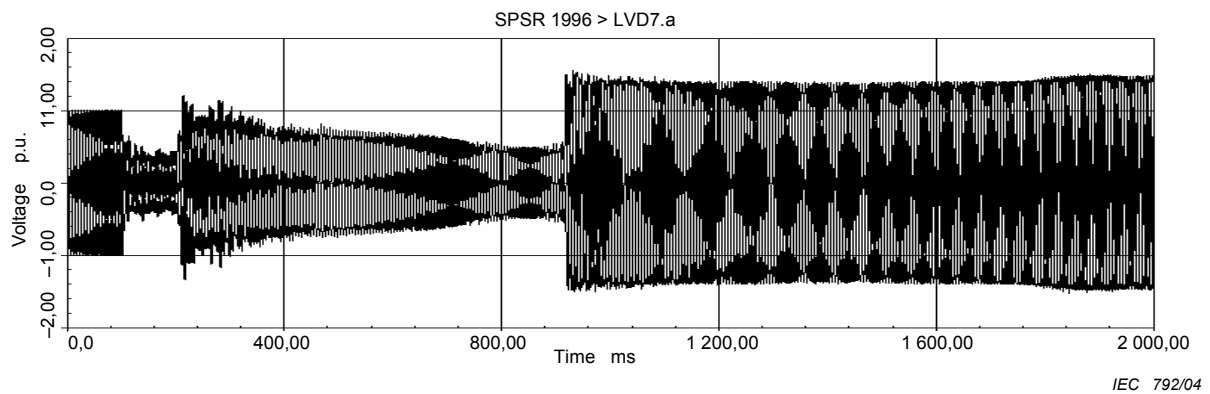
**Figure 29 – TOV at LVD7 – Electromagnetic transient simulation
with 484 kV switched metal-oxide surge arresters**

SPSR 1996 > CHM7.a
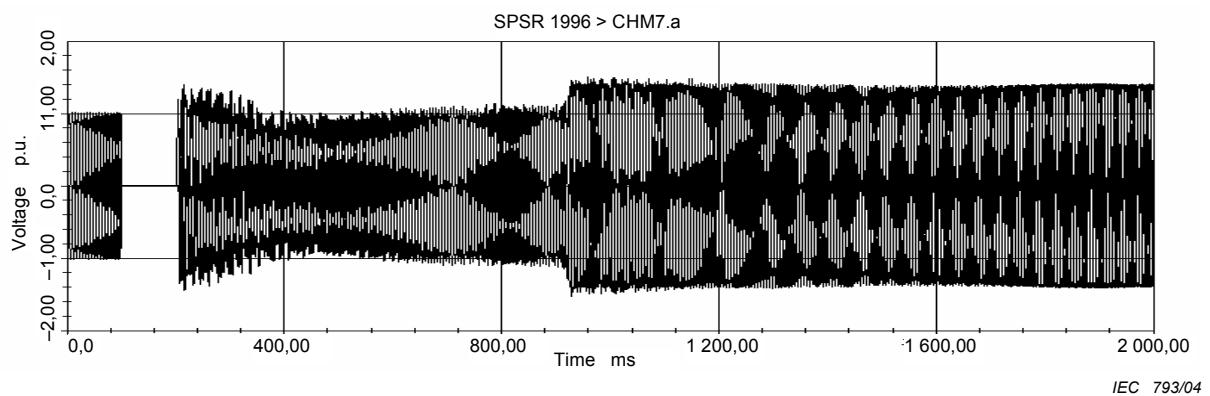
**Figure 30 – TOV at CHM7 – Electromagnetic transient simulation
with 484 kV switched metal-oxide surge arresters**

12.2.4 Concluding remarks in terms of modelling and method

The following concluding remarks could be drawn from the results of this TOV test case:

- On a large transmission system, TOV following a full-load rejection (or a system separation) could be accurately simulated with an electromagnetic transient programme including system dynamic behaviour and system non-linear characteristics such as transformer saturation, metal-oxide surge arresters, etc.
- In order to obtain realistic TOV scenarios, all actions associated to the most relevant protections and automatic switching systems in the network should be predicted and simulated.
- In order to obtain realistic TOV results, the major part of the transmission system where disturbances take place should be represented in detail in electromagnetic transient simulation.

12.3 Case 2 (SFO) – Energization of a 500 kV line

This test case describes the study of a fictitious 500 kV line energization with the semi-statistical method (see 9.4.2). The influence of trapped charges and insertion resistors on overvoltage levels will be studied. Different configurations will be compared with help of the failure rate.

12.3.1 Input data and modelling

12.3.1.1 Diagram (Figure 31)

IEC 794/04
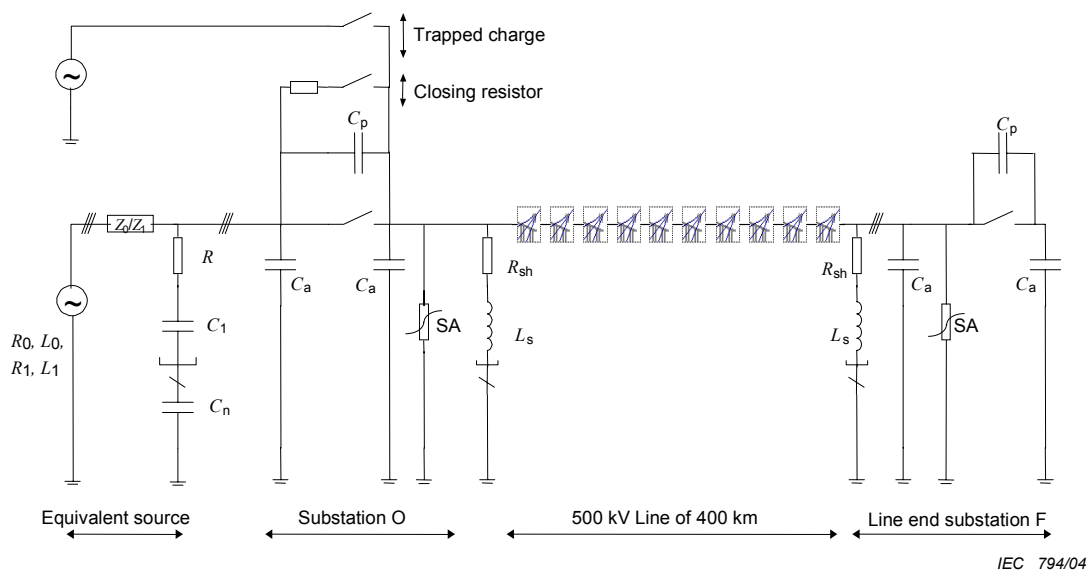
Figure 31 – Representation of the system

12.3.1.2 Short-circuit power

The source is represented by a perfect voltage source and a resonant circuit at a frequency of 1 500 Hz (see Table 14).

Table 14 – Source side parameters

U_n	Nominal voltage (V)	525 000
P_{cc3}	Three-phase short-circuit power (VA)	$3,00\ 10^9$
P_{cc1}	Single-phase short-circuit power (VA)	$9,52\ 10^8$
f	Resonance frequency (Hz)	1500
τ of the source	Time constant (s)	$5,00\ 10^{-2}$
I_{cc3}	Three-phase short-circuit current (A)	3299
I_{cc1}	Single-phase short-circuit current (A)	1047
L_1	Positive-sequence inductance (mH)	9,74
L_0	Zero-sequence inductance (mH)	72,6
R_1	Positive-sequence resistance (Ω)	0,195
R_0	Zero-sequence resistance (Ω)	1,45
C_1	Stray phase capacitance (µF)	1,15
C_n	Stray neutral capacitance (µF)	0,537
R	Damping resistance (Ω)	73,5

12.3.1.3   Substation earthing (7.5.12)

The earth impedance is represented by a 5 Ω resistance.

12.3.1.4   Surge arresters (7.5.11)

Surge arresters are modelled by their $U(I)$ characteristic. Concerning switching transient, they are characterized by their rated voltage U_r, their continuous operating voltage, U_c and their class. U_c depends on steady-state voltages that may appear in the network (see Table 15).

Table 15 – Characteristics of the surge arresters

U_r	Rated voltage (kV)	444
U_c	Continuous operating voltage (kV)	350
Cl	Class (CEI)	5
$U(1kA)$	Residual voltage at 1 kA (kV)	864

12.3.1.5   Shunt reactor

The compensation factor for this study is 70 %, which is a typical value for an EHV line. Fifty per cent of the inductance is connected at each end of the line (see Table 16).

Table 16 – Characteristics of the shunt reactor

C_{line}	Line capacitance (µF)	5,28
α	Compensation factor	0,7
L_s	Compensation coil inductance (H)	5,488
R_{sh}	Damping resistor (Ω)	3,45

12.3.1.6 Line energization circuit-breaker

In order to take into account the standard deviation of the inter-phase closing time, statistical switches have been used (7.5.10.1).

Auxiliary contact closing   Main contact closing

10ms

IEC 795/04
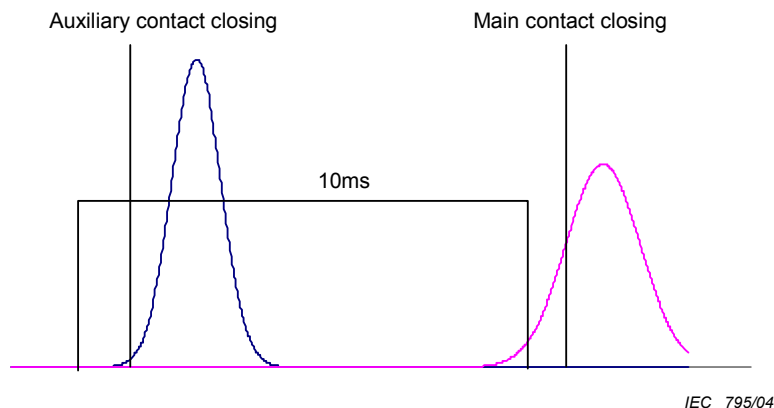
Figure 32 – Auxiliary contact and main

When using a closing resistor (400 Ω), an auxiliary switch is introduced. This switch is also a statistic one whose contacts are closed 10 ms before the main contacts are closed. The standard deviation of the inter-phase time distribution is 0,66 ms for auxiliary contacts and 1 ms for main contacts (see Figure 32).

12.3.1.7 Line-end substation circuit-breaker

This breaker is supposed to be always open and all voltages are studied: phase-to-earth, phase-to-phase and longitudinal.

Phase-to-earth and longitudinal stray capacitance are modelled (see Table 17).

Table 17 – Capacitance of circuit-breaker

C_a	Phase-to-earth stray capacitance (pF)	120
C_p	Longitudinal stray capacitance (pF)	200

12.3.1.8 Line (7.5.2.2)

Lines are modelled with distributed elements, in separate sections of 40 km, in order to get voltages along the line. A very simple model is used to represent the line: the so-called K.C. Lee model [29]. The frequency of modelling is 500 Hz.

12.3.1.9 Trapped charges (7.5.2.1)

During the steady-state calculation, the line is charged by an auxiliary voltage source which is disconnected after the first time-step (see Table 18).

Table 18 – Trapped charges

U_n	Nominal voltage (V)	525 000
I_a	Chopped current (A)	0

12.3.2 Method applied

With a semi-statistical method only one network is considered, for which the only varying parameters are the breakers' closing times. In this case, the method has been applied on four configurations of the system, as shown in Table 19.

Table 19 – System configurations

Network configurations	Shunt compensation	Surge arresters	Trapped charge	Insertion resistance
Base	X	X		
Trapped charge	X	X	X	
Insertion resistor	X	X		X
Trapped charge + Insertion resistor	X	X	X	X

For each system configuration, a batch of 300 simulations is performed.

For each system three subsystems are studied: substation 0, the line, and substation F (Table 20). Each subsystem is a part of the total system and can be made of one or many nodes.

At each closing of the substation 0's circuit-breaker (each simulation) and for each subsystem, two or three kinds of overvoltages are stored: phase-to-earth, phase-to-phase and longitudinal.

Table 20 – Recorded overvoltages

	Phase-earth	Phase-phase	Longitudinal
Substation 0	X	X	
Line	X	X	
Substation F	X	X	X

For each simulation, only the peak values are considered and put into the probability of each sub-networks (see 2.3.3.1 of IEC 60071-2)). Of course, this is done insulation by insulation.

For example, with the base system, three subsystems are considered (substation 0, line and substation F). The "line" sub-network involves 10 three-phase nodes, and so for each simulation and for each insulation, the maximum peak value among the 10 three-phase nodes is added to the voltage distribution.

Then for each distribution of overvoltages the failure rate R is computed.

Document provided by IHS Licensee=Qatar Petroleum/5943408001, 12/08/2004
21:49:44 MST Questions or comments about this message: please call the Document
Policy Group at 303-397-2295.

71

12.3.3 Results and interpretation
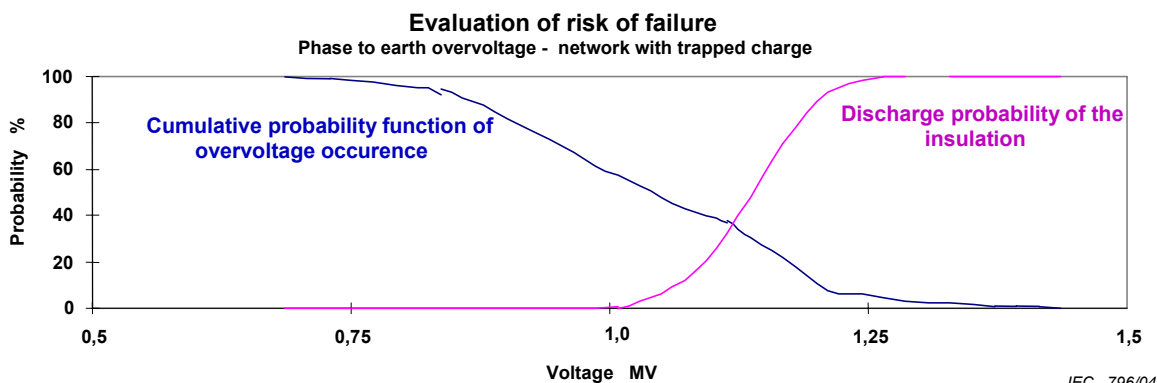
Figure 33 – An example of cumulative probability function of phase-to-earth overvoltages and of discharge probability of insulation in a configuration with trapped charges and insertion resistors

The failure risks shown in Table 21 and Figure 33 have to be analysed comparatively. One can see the influence of an insertion resistor: with or without trapped charges, the insertion resistor reduces drastically the overvoltages, even leading to a null failure rate.

Table 21 – Number of failures for 1 000 operations

Failures for 1 000 operations	Substation 0		Line		Substation F		
	ph-e	ph-ph	ph-e	ph-ph	ph-e	ph-ph	longitudinal
Base case	0,00	0,00	0,39	0,00	0,36	0,22	0,00
Pre-insertion resistor (PIR)	0,00	0,00	0,00	0,00	0,00	0,00	0,00
Trapped charge (TC)	0,00	0,00	318,16	0,00	7,08	81,66	0,00
PIR+TC	0,00	0,00	0,00	0,00	0,00	0,00	0,00
Withstand level (kV)	950	1 615	1 050	2 000	950	1 615	950

This kind of statistical study can be used to optimize the insulation withstand of equipment. It is interesting to study the failure rate versus the insulation withstand. Of course, the number of failures decreases while the withstand level of the insulation increases.

Figure 34 is for the trapped charge case with different assumed withstand voltages for the equipment.
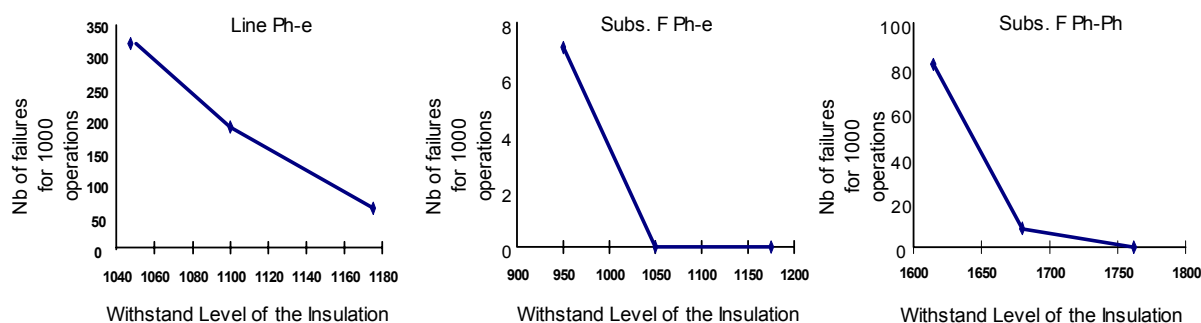
Figure 34 – Number of failure for 1 000 operations versus the withstand voltage of the insulation

This decreasing rate of failure must be compared to the increasing cost of the insulation in order to find the best technical and economical optimum.

12.4 Case 3 (FFO) – Lightning protection of a 500 kV GIS substation

The study presented in this subclause deals with the lightning protection of a GIS against lightning impacting shielding conductors and towers. The semi-statistical method proposed in 10.2 for the estimation of the insulation failure rate per year has been applied. Its approach consists in applying the following steps:

a) determination of the limit distance;

b) evaluation of the number of lightning strokes impacting the line and of the random distribution associated to these lightning strokes;

c) evaluation of the risk of failure of the GIS in one configuration.

This sub-section concentrates mainly on the last step, the first one being presented very briefly. The hypothesis has been voluntary simplified in order to streamline the comprehension of the method.

12.4.1   Input data and modelling

12.4.1.1   Diagram (Figure 35)

Diagram for lightning study of a 500 kV GIS substation in the case of normal operation
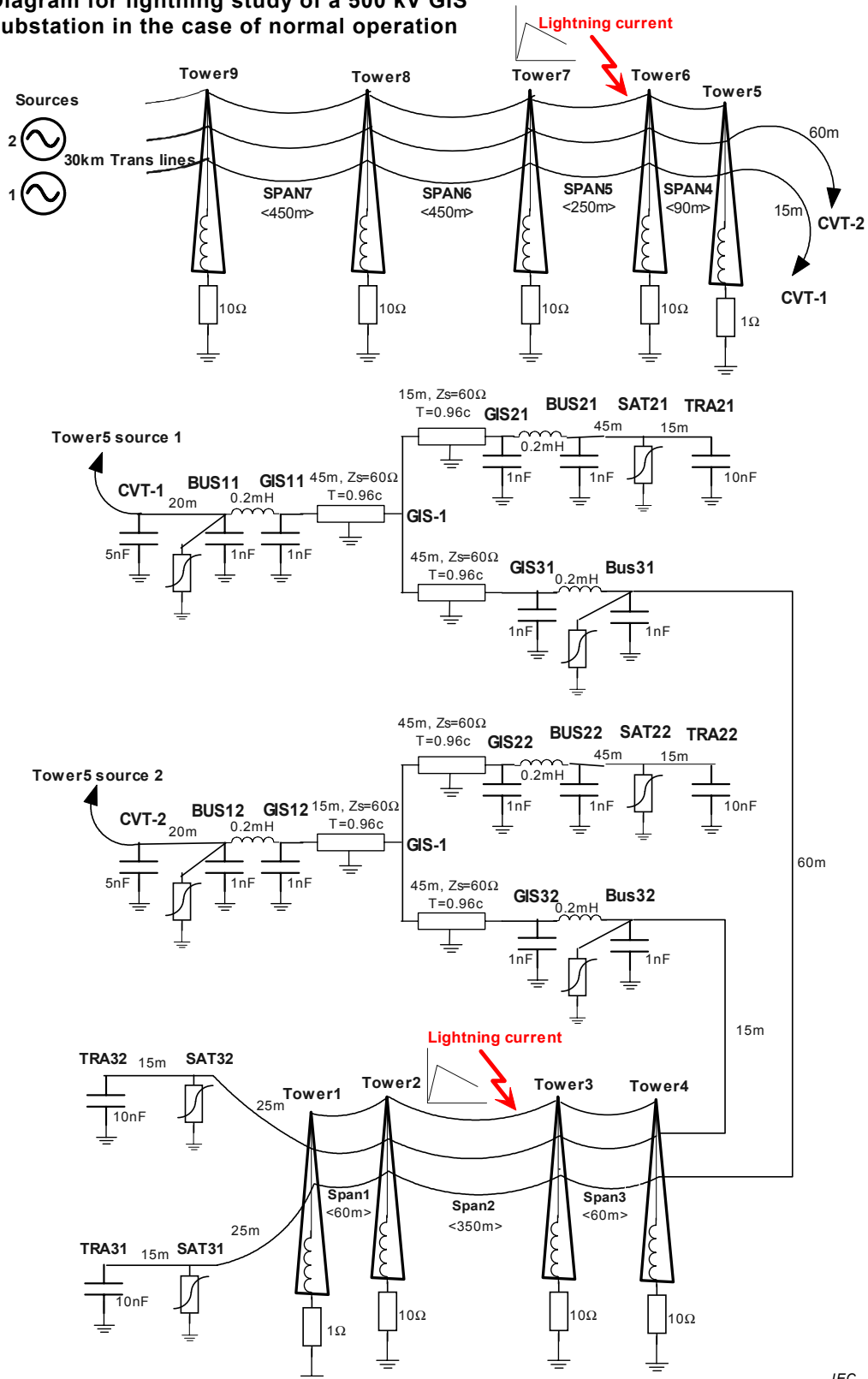
Figure 35 – Schematic diagram of a 500 kV GIS substation intended for lightning studies

12.4.1.2   Lightning stroke current

The lightning stroke is modelled by a double ramp shape for which several crest-current values are simulated.

The time to crest is defined as a function of the crest current given by the following relationship (see Annex C) which gives the minimum equivalent medium time to crest (μs) versus the crest value of the lightning current (kA), considering that the crest value of the current is higher than 20 kA:

$$t_m = 0,154 \times i^{0,624}$$

The lightning tail duration is fixed to 150 μs, irrespective of the crest-current value (Figure 36).

IEC   799/04
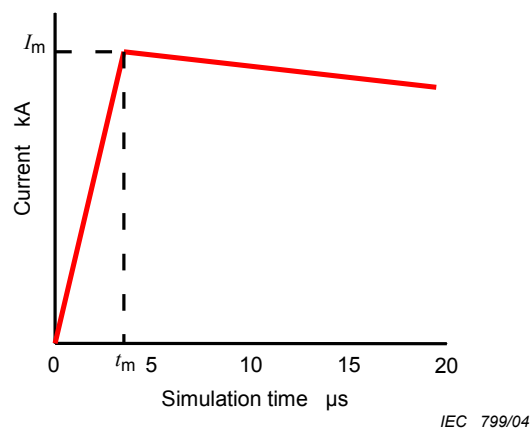
Figure 36 – Waveshape of the lightning stroke current

The limit distance has been determined using numerical simulations. Strikes terminating on the shield wire and strikes terminating on tower tops are assumed to result in the same overvoltage stress as that of the closest simulated point. Therefore, to simplify, points of impact are restricted to the transmission line's tower tops closest to the substation (not including the terminal towers connected to the earthing grid).

The a.c. power voltage at inception time is assumed to be deterministic, and its phase angle is fixed to a value such that the lightning surge voltage would be maximum (conservative case).

12.4.1.3   Modelling of elements

Table 22 gives the modelling of the system.

Table 22 – Modelling of the system

Configuration of the substation	Characteristics See Figure 35	Modelling
Power transformers		Phase-to-earth capacitance of 10 nF (see 7.6.7)
Capacitive voltage transformer		Phase-to-earth capacitance of 5 nF (see 7.6.7)
GIS	Withstand voltage (normal) Median value = 1 550 kV Standard deviation: 10 %	Surge impedance: 60 Ω Velocity of propagation: 0,95 Velocity in vacuum
Connecting conductor in substation		Sections between 3 m and 15 m are modelled like lumped inductance of 1 μH/m
Towers		Propagation element of 150 Ω (see 7.6.3.1)
Span	Double circuit line with two shielding conductors	Frequency-dependent line model (see 7.6.2)
Earthing electrode of towers		A lumped resistance of 10 Ω
Earthing electrode of substation		A null impedance
Surge arrester		It is represented by its 8/20 μs characteristic[1]
Air gaps		Equal area criteria

[1] The surge arrester connections and the height of the arrester itself have been represented by equivalent inductances, but the increase in residual voltage for surges steeper than 8/20μs has been neglected in the present study as a simplification; they could have been included if the corresponding characteristic was known.

12.4.1.4 Data for lightning incidence evaluation

Table 23 gives the data used for the application of the EGM.

Table 23 – Data used for the application of the EGM

Data	Tower height: 57 m
	Shield wire height at mid-span: 45,5 m
	Ground-flash density: four flashes per year per square kilometre
EGM model	Love 's EGM [4]

12.4.2 Method

12.4.2.1 Limit distance evaluation (10.2.3)

This evaluation is performed making transient simulations.

12.4.2.2 Evaluation of the number of lightning strikes impacting the line and of the random distribution associated to these lightning strokes

The number of lightning strikes impacting each section of the line is estimated as shown in Table 25, using the attractive radius-versus-crest value of the stroke current (10.2.4). The density of probability of the crest value of the lightning current on the ground has been calculated using Love electrogeometric model from a log-normal distribution on structures of which the parameters are shown in Table 24.

Table 24 – Crest-current distribution

Median value	33 kA
Logarithmic standard deviation	0,605 kA

Table 25 – Number of strikes terminating on the different sections of the two incoming overhead transmission lines

Section	Tower 2	Tower 3	Tower 6	Tower 7	Tower 8
Number of strokes per year	0,14	0,14	0,11	0,2	0,25

The statistical distribution of the crest value of the lightning stroke current will be the "statistical distribution on structure" given above.

12.4.2.3 Risk estimation

12.4.2.3.1 Limit-state surface formulation

The approximation is made that the GIS insulation will be in a failure state when the lightning overvoltage U is greater than the disruptive voltage U_d. Therefore, the limit state is reached for $U_d = U$.

For each point of lightning strike point of impact, the lightning overvoltages have been simulated as a function of crest-current values i_k. A set of pairwise data (i_k, u_k) of simulated current values and corresponding overvoltages are obtained for each section of the GIS. By interpolation of this set of data, one can get the limit-state function $u_d = u(i)$. See Figure 37.
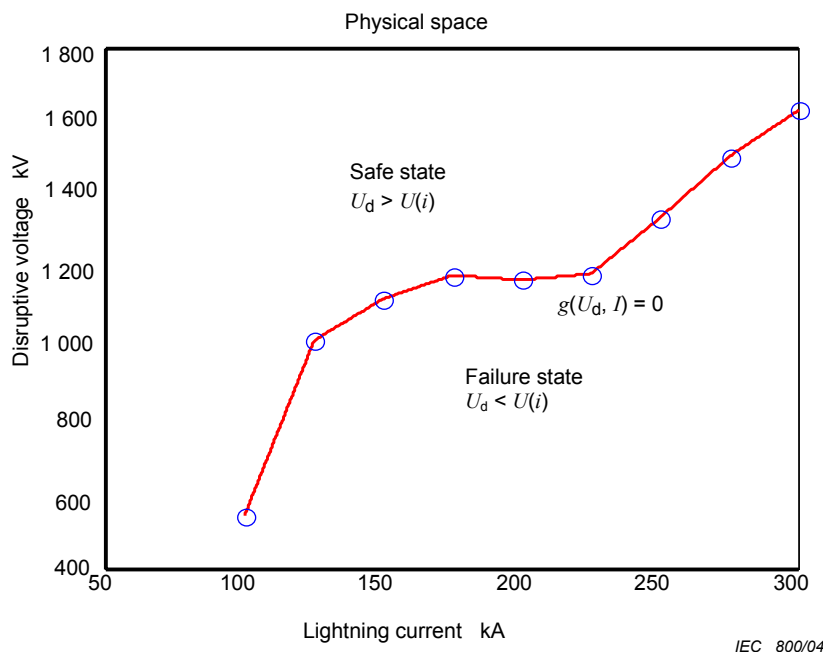
**Figure 37 – Response surface approximation
(failure and safe-state representation for one GIS section (node))**

12.4.2.3.2 Risk of failure formulation (see Annex C and 10.2.5)

The risk of insulation failure is the probability mass of the failure domain:

$$P_F = P(U(I) > U_d) = \iint\limits_{u_d - u\,(i) \leq 0} f_{I,U_d}(i, u_d)\,\mathrm{d}i\mathrm{d}u_d$$

The definition of the variables is given in 10.2.5.

As the crest current and the disruptive voltage of the GIS are independent random variables the joint probability density function $f_{I,U_d}(.,.)$ is simply the product of the crest current marginal probability density function $f_I(.)$ with the one of the disruptive voltage $f_{U_d}(.)$ as follows:

$$f_{I,U_d}(i, u_d) = f_I(i) f_{U_d}(u_d)$$

Hereafter, the crest current and the GIS disruptive voltage are assumed to be respectively log-normally and normally distributed with the parameters given in Table 26.

**Table 26 – Parameters of GIS disruptive voltage distribution
and lightning crest-current distribution**

GIS disruptive voltage distribution	Medium value (kV)	1 550
	Standard deviation (kV)	155 (10 % of the medium value)
Lightning crest-current distribution	Medium value (kA)	33
	Logarithmic standard deviation	0,605
NOTE The standard deviation has been taken equal to 10 % of the medium value for the GIS disruptive voltage, but in practice lower values are usually considered.		

A contour plot of the joint probability density function $f_{I,U_d}(.,.)$ is provided in Figure 38 to help visualize its three-dimensional shape. The drawn curves represent points of constant density values. As it stands to reason, the highly probable values are in the safe domain.
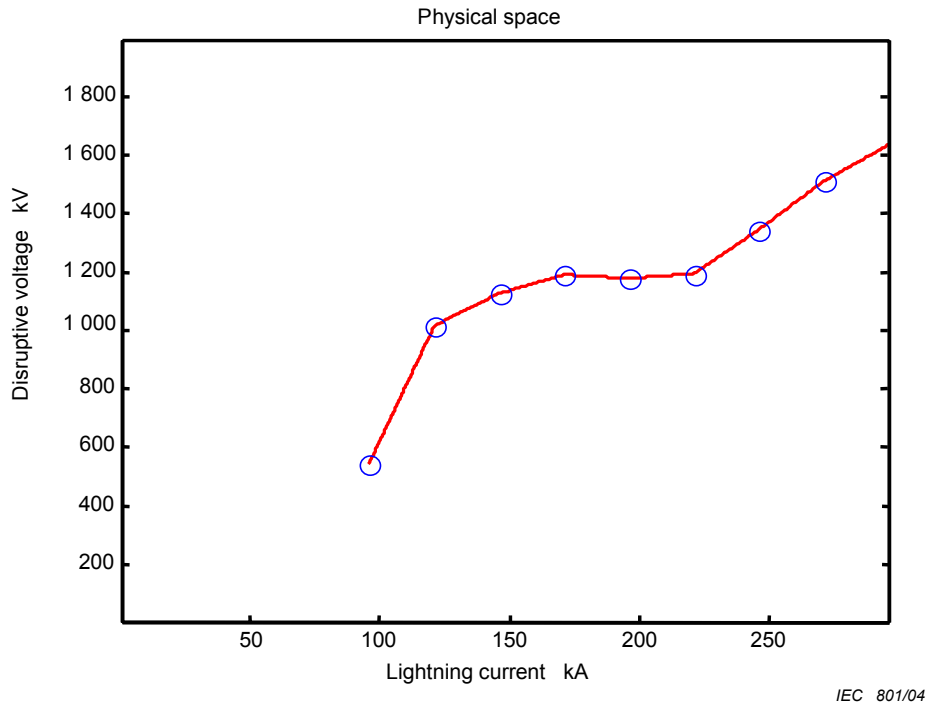
Physical space

NOTE   The dots portray the EMTP simulation results and the line is the interpolated response surface.

**Figure 38 – Limit-state representation in the probability space
of the physical variables risk evaluation**

The evaluation of the risk integral is achieved using FORM technique (see Annex C).

12.4.3   Results and interpretation

12.4.3.1   FORM estimation results for each section and each part of the GIS

Table 27 summarizes the FORM estimation results for the GIS.

Table 27 – FORM risk estimations (tower footing resistance = 10 Ω)

Point of impact / Risk	Tower 2	Tower 3	Tower 6	Tower 7	Tower 8	Tower 9
Risk GIS11	2,5E-5	3,1E-4	1,2E-4	1,9E-4	1,8E-5	9,8E-5
Risk GIS21	1,4E-5	2,3E-4	1,2E-4	1,7E-4	1,8E-5	6,7E-5
Risk GIS31	2,5E-5	5,1E-4	1,4E-4	2,1E-4	1,7E-5	7,4E-5
Risk GIS12	4,6E-6	2,2E-4	1,3E-4	8,5E-5	7,8E-6	4,9E-5
Risk GIS22	4,4E-6	1,9E-4	1,2E-4	6,2E-5	8,7E-6	3,9E-5
Risk GIS32	1,3E-5	2,0E-4	1,5E-4	1,4E-4	1,4E-5	6,2E-5
Risk GIS1	2,0E-5	2,7E-4	1,3E-4	2,E-4	1,7E-5	8,0E-5
Risk GIS2	6,5E-6	2,2E-4	1,3E-4	1,0E-4	9,5E-6	4,9E-5

12.4.3.2 Total failure rate for each part of the GIS

The GIS insulation failure rate for one part of the GIS considered for one specific configuration is the sum of the individual failure rates associated to the different points of impact, each of which is the product of the frequency of lightning strokes with the risk of failure given this point (see Table 28).

Table 28 – Failure rate estimation for the GIS11

Strokes to	Tower 2	Tower 3	Tower 6	Tower 7	Tower 8
Number of strokes per year	0,14	0,14	0,11	0,2	0,25
Risk of failure	2,5E-5	3,1E-4	1,165E-4	1,9E-4	1,8E-5
Failure rate associated to each line section	0,34E-5	0,43E-4	0,1E-4	0,4E-4	0,45E-5
Total failure rate (number of failures/year)	1,019E-4/year				

The total failure rate is 1,0E-4/year. It is equal to the sum of the failure rates corresponding to each of the contributions to the risk of a section of the line.

Remark: if the failure rate of one part of the GIS is one order higher than that of the other parts, this risk of failure can be assumed as being the risk of the total station; if this condition is not fulfilled, the total risk may be conservatively approximated by the arithmetic sum of the partial risks.

12.5 Case 4 (VFFO) – Simulation of transients in a 765 kV GIS [51]

This test case presents some aspects of a study which has been performed to check the modelling to be used for GIS representation [51]. It is illustrated by results from digital simulation in a 765 kV substation.

12.5.1 Input data and modelling

Figures 39 and 40 show the one-line and the connectivity diagram of a 765 kV test bay. Models used to represent components of this case are presented in Table 29. Representation of components was made following the recommendations of 7.7.1.

IEC 802/04
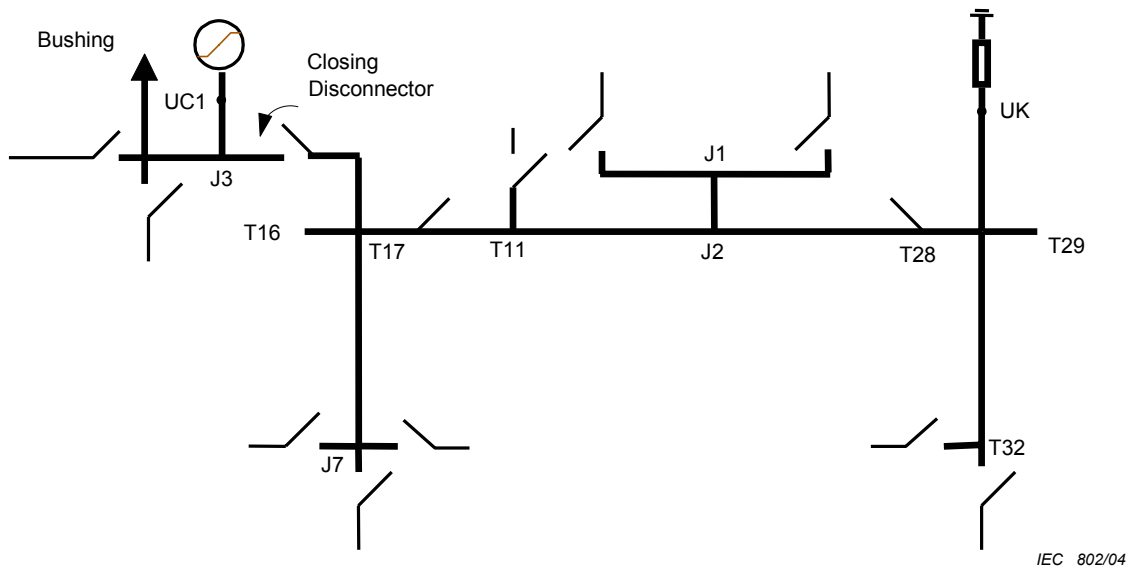
Figure 39 – Single-line diagram of a 765 kV GIS with a closing disconnector
(only the GIS part in thick lines is of interest for the transient phenomena simulated here;
some points that are in Figure 40 are also shown here)

IEC 803/04
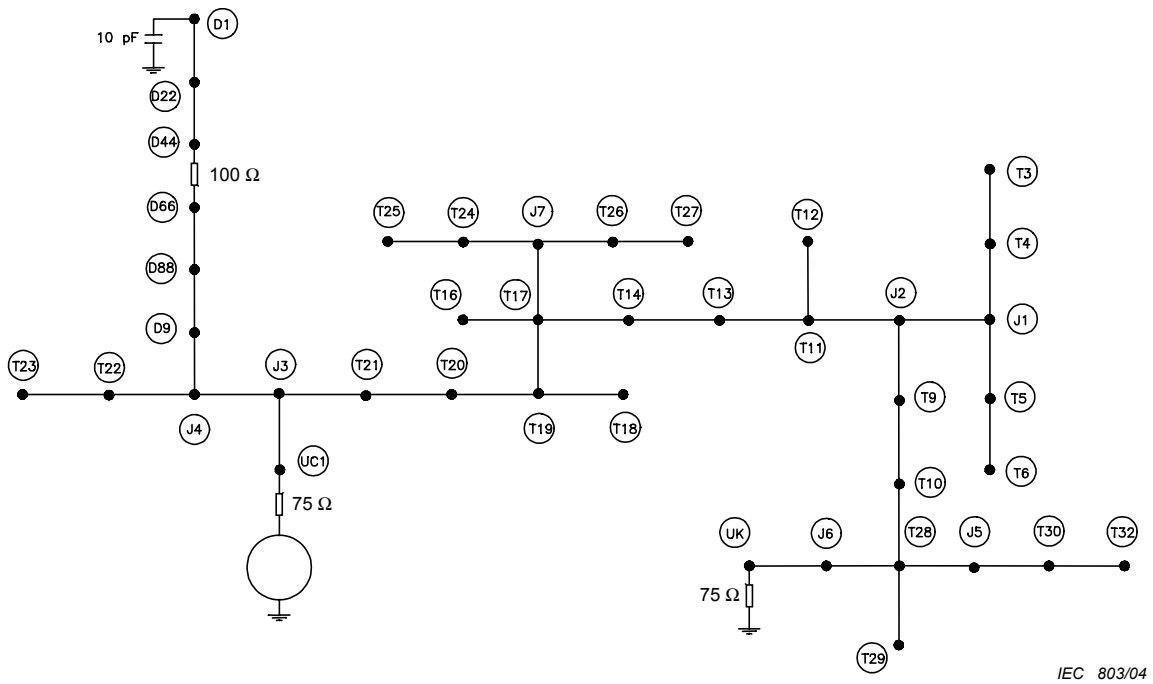
**Figure 40 – Simulation scheme of the 765 kV GIS part
involved in the transient phenomena of interest**

Table 29 – Representation of GIS components – Data of the 765 kV GIS

Branch	Z (Ω)	Travel time (ns)
UC1 – J3	75	6,40
J3 – J4	75	48,0
J4 – T22	75	2,20
T22- T23	51	1,90
J4 – D9	78	2,20
D9 – D88	68	1,80
D88 – D66	59	4,20
D44 – D22	33	5,80
D22 – D1	330	9,10
J3 – T21	75	2,20
T21 – T20	51	1,90
T20 – T19	160	0,67
T19 – T18	65	1,70
T19 – T17	75	6,80
T17 – T16	65	1,70
T17 – J7	75	8,50
J7 – T24	75	2,20
T24 – T25	51	1,90
J7 – T25	75	2,20
T26 – T27	51	1,90
T17 – T14	160	0,67
T14 – T13	51	1,90
T13 – T11	75	9,90
T11 – T12	65	1,70
T11 – J2	75	7,50
J2 – T9	75	2,20
T9 – T10	51	1,90
T10 – T28	160	0,67
T28 – J6	75	7,10
J6 – UK	75	6,40
T28 – T29	65	1,70
T28 – J5	75	8,80
J5 – T30	75	2,20
T30 – T32	51	1,90
J2 – J1	75	6,70
J1 – T4	75	2,20
T4 – T3	51	1,90
J1 – T5	75	2,20
T5 – T6	51	1,90

12.5.2 Method applied to validate modelling

A deterministic study was made to validate GIS modelling. A summary of the procedure followed is listed below:

– low-voltage simulations on individual components were performed using waves with fronts of 4 ns and 20 ns;

– the parameters of the models corresponding to all elements of the system were calculated on the basis of physical dimensions. Simulations were performed assuming a propagation velocity equal to 0,96 that of light in vacuum.

For normal studies, the input wave would be one of three forms:

– a ramp voltage with a magnitude determined by the voltage across the switch;
– two ramp currents on opposite sides of the switch such that the voltage across the switch is equal to zero at the crest of the inputs;
– charge both sides of the switch to the desired value and close the switch.

12.5.3   Results and interpretation

In the configuration of Figure 40, a low voltage step was injected at UC1 location through a 75 Ω matching impedance and digital simulations were performed using two different source models for the step voltage:

– in the first one, a ramp voltage saturating at 100 V is applied at t = 0;
– in the second case, the ramp voltage source saturating at 100 V is also used but the transient starts after closing a switch at the instant the ramp reaches its maximum value.

Waveforms obtained for both cases at two nodes are shown in Figures 41 and 42. It can be observed that, for both cases, they are essentially the same, except for the first nanoseconds in the vicinity of the input node UC1. These simulation results did match very well actual low-voltage measurements [51].

Voltage at location UC1
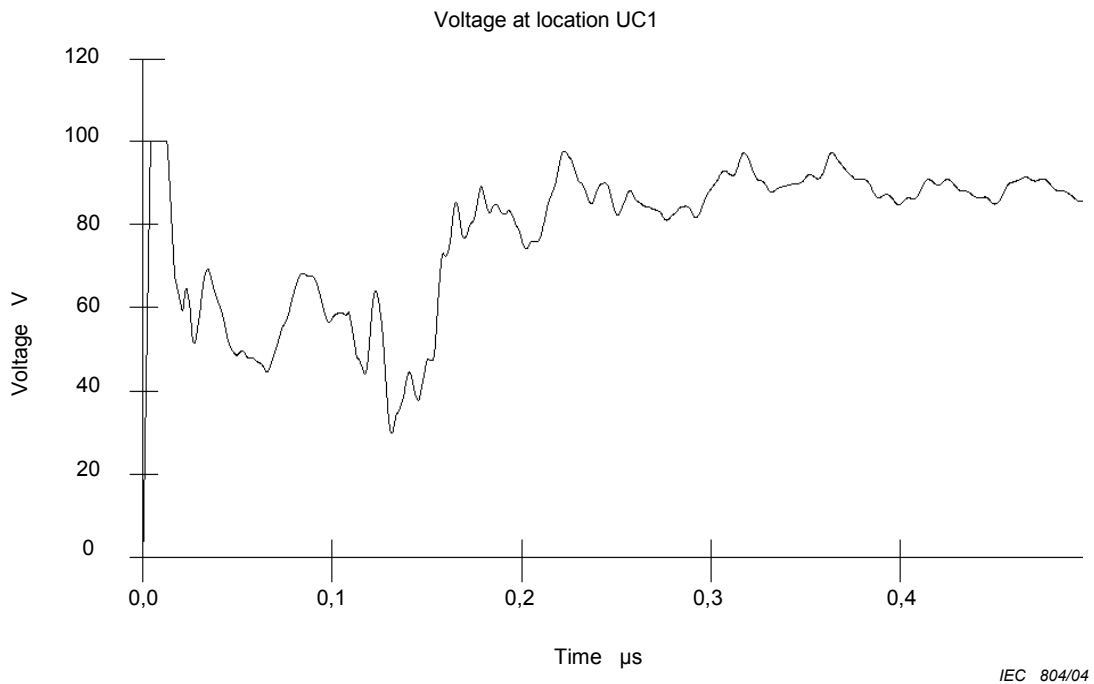
Figure 41a – Simulation results – Voltage at location UC1

Voltage at location UK
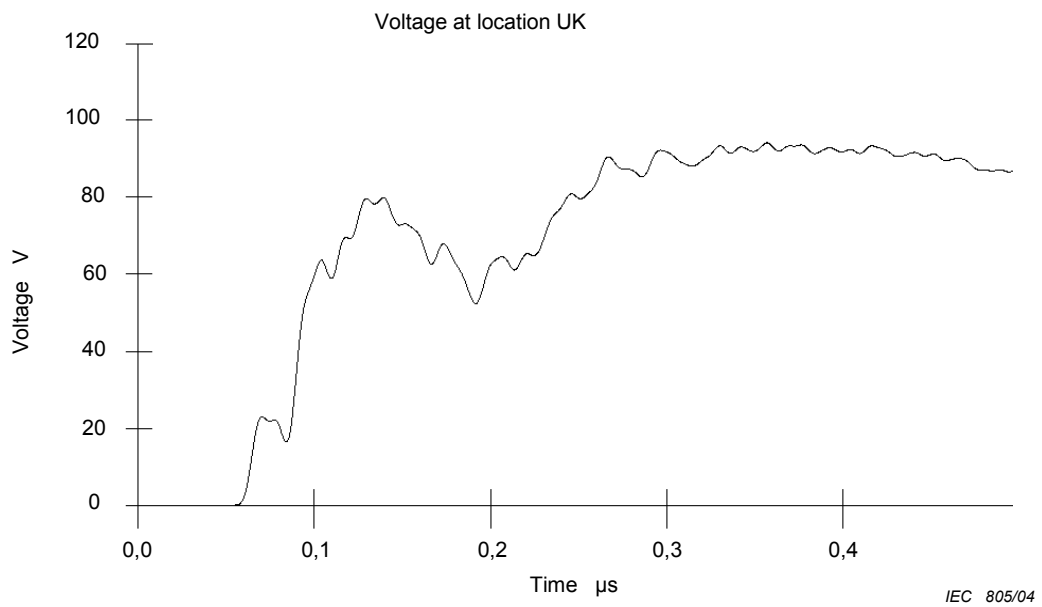
Figure 41b – Simulation results – Voltage at location UK

Figure 41 – 4 ns ramp
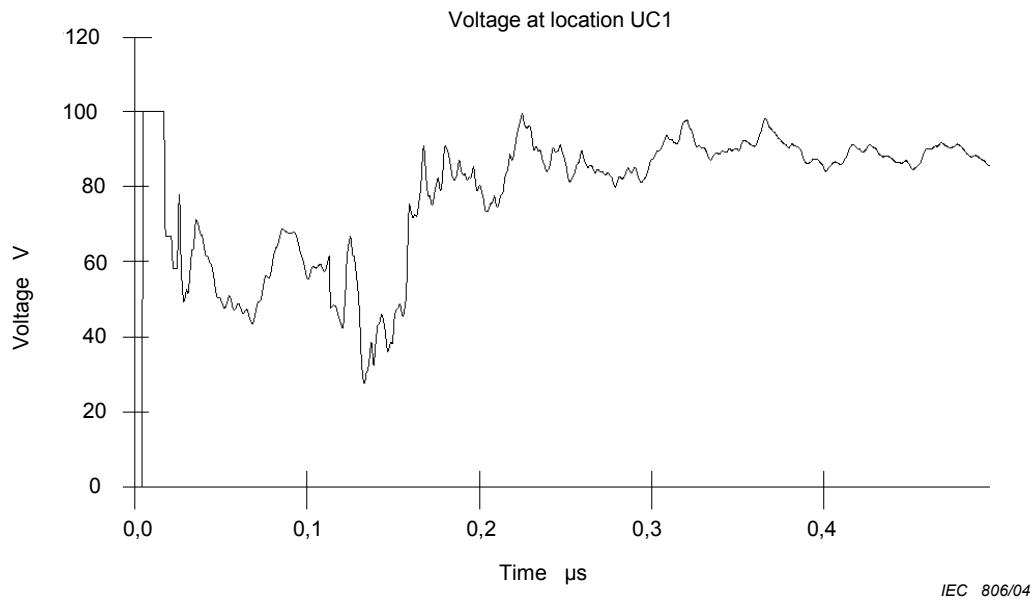
Figure 42a – Simulation results – Voltage at location UC1
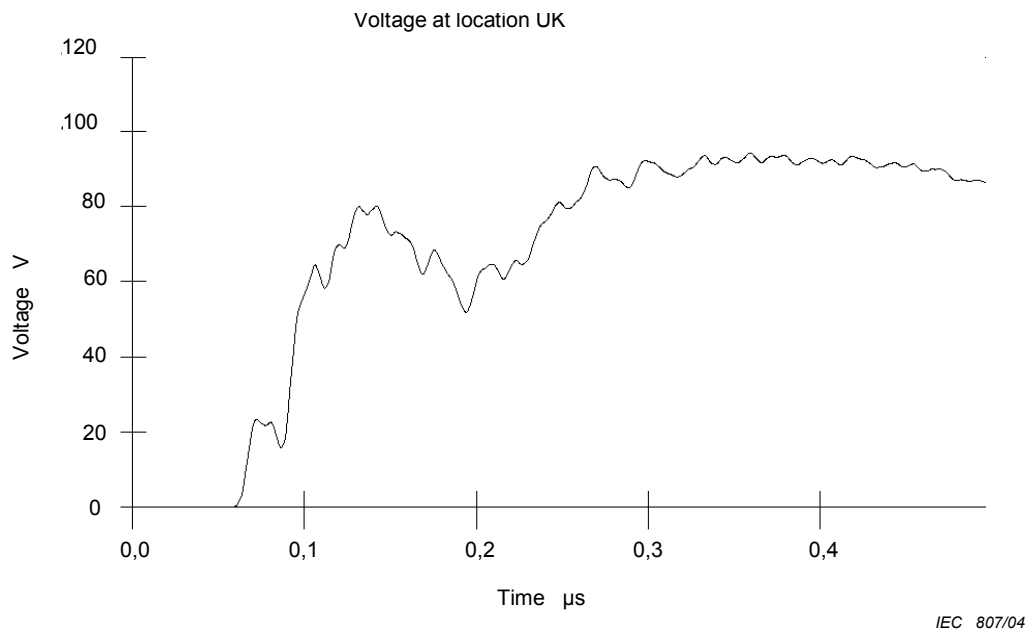
Figure 42b – Simulation results – Voltage at location UK

Figure 42 – Switch operation

Annex A
(informative)

Representation of overhead lines and underground cables

The same electrical models apply for both overhead lines and underground cables. The models used to calculate the waves propagating along electric lines are based on the so-called wave equations:

$$-\frac{\partial V}{\partial x} = RI + \frac{\partial (LI)}{\partial t}$$

$$-\frac{\partial I}{\partial x} = GV + C\frac{\partial V}{\partial t}$$

where

R, L, C and G are the resistance, inductance, capacitance and conductance matrices per unit length of the line, x is the distance from one end of the line and t is the time. In overhead lines G is usually not taken into account unless the decrease of trapped charges is to be considered.

A.1   Exact Pi model for a single conductor electric line (see Figure A.1)

IEC 808/04
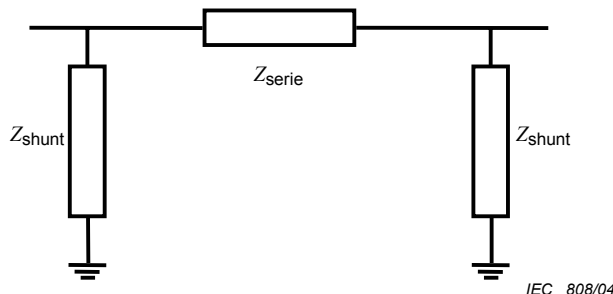
Figure A.1 – Pi-model

One line of length l can be represented by a Pi-model, whose parameters are as follows:

$$Z_\text{shunt} = \frac{Z_\text{c}}{\tanh(\frac{\gamma l}{2})} \qquad \text{and} \qquad Z_\text{serie} = Z_\text{c}\sinh(\gamma l)$$

where Z_c, the surge impedance of the line, and γ, the propagation constant, are given by the following formulae:

$$Z_\text{c} = \sqrt{\frac{R + \text{j}L\omega}{G + \text{j}C\omega}} \qquad \text{and} \qquad \gamma = \sqrt{(R + \text{j}L\omega)(G + \text{j}C\omega)}$$

This model is very efficient for programmes based directly on the frequency or on the Laplace domain because the variation of line resistance and inductance with frequency can be directly accounted for. In most time-domain-based programmes, the parameters of this model are calculated at a single frequency.

A.2   Nominal Pi-circuit

If γl is small the series impedance and the shunt admittance can be approximated by

$$Z_{\text{serie}} = (R + jL\omega)l \qquad \text{and} \qquad Y_{\text{shunt}} = \frac{1}{2}jC\omega l = \frac{1}{Z_{\text{shunt}}}$$

A line can be represented by a cascade of π circuits. For steady-state solutions, this model is accurate if each part of the line represented by a π circuit is not too long (for overhead lines <150 km at 60 Hz, <15 km at 600 Hz). However, it cannot represent the frequency dependence of R and L in case of harmonics.

This model can be used for transient calculations.

A.3   Travelling wave method: Single-phase lossless line with constant L

In this particular case, the wave equations have a solution proposed by d'Alembert:

$$I = F_1(x - v\,t) - F_2(x + v\,t)$$

$$V = Z_c\,(F_1(x - v\,t) + F_2(x + v\,t))$$

This solution leads to the following equation:

$$V(t) + Z_c\,I(t) = 2 \times Z_c\,F_1(x - vt)$$

which can be written, if ι = line length/v is the travel time along the line:

$$V(t) + Z_c\,I(t) = 2 \times Z_c\,F_1(-v(t - \iota))$$

$V(t)$ and $I(t)$ at one end of a line are calculated using a historical term calculated from previously computed values of $V(t)$ and $I(t)$ at the remote end of the line.

The losses can be taken into account by including equivalent lumped resistances at the line ends and in the middle of the line, directly proportional to its length. Therefore, the length of a line modelled this way should be limited to avoid unrealistic reflections on these resistances.

A.4   The frequency-dependent line model for a single conductor line (Figure A.2)
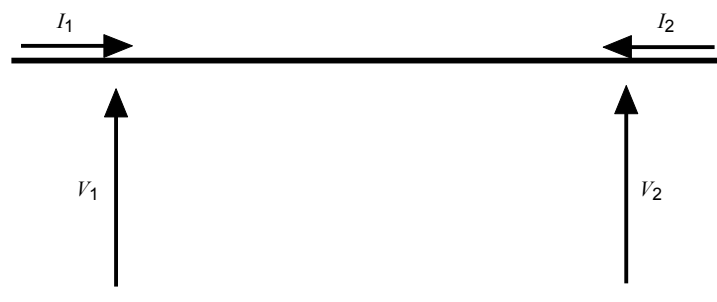
IEC 809/04

Figure A.2 – Representation of the single conductor line

$$V_1(t) - F^{-1}(Z_c) * I_1(t) = F^{-1}(e^{-\gamma l}) * (V_1(t) + F^{-1}(Z_c) * I_2(t))$$

where

F is the Fourier transform;

* is the convolution operator.

$e^{-\gamma l}$ is the so-called propagation function. It includes both an attenuation factor and a phase-shift factor, which are functions of frequency.

To perform the computing of the equation, $Z_c(p)$ can be approximated by a rational function of p and $e^{-\gamma l}$ by a rational function of p multiplied by $e^{-\tau p}$. In mathematical terms, it corresponds to a linearization of the problem.

This model takes into account the effect of variation versus frequency of the attenuation and characteristic impedance on a wide range of frequency.

A.5 The representation of multi-conductor lines

A.5.1 The modal parameters

In the case of multi-conductor lines $V(x)$ and $I(x)$ are vectors. Each coordinate of $V(x)$ and $I(x)$ corresponds respectively to the voltage and the current of one conductor at the distance x from the end of the line.

The wave equations

$$-\frac{dV(p,x)}{dx} = Z(p)I(p)$$

$$-\frac{dI(p,x)}{dx} = Y(p)V(p)$$

can be transformed into

$$\frac{d^2V(p,x)}{dx^2} = Z(p)Y(p)V(p,x)$$

$$\frac{d^2I(p,x)}{dx^2} = Y(p)Z(p)I(p,x)$$

To solve the system of equations it is possible to linearly transform the quantities $V(p,x)$ and $I(p,x)$ into quantities $V_{mod}(p,x)$ and $I_{mod}(p,x)$ in such a way that the equations become decoupled. $V_{mod}(p,x)$ and $I_{mod}(p,x)$ are called modal quantities. $V_{mod}(p,x) = T_v(p) \times V(p,x)$ and $I_{mod}(p,x) = T_i(p) \times I(p,x)$. T_v and T_i are called transformation matrices.

A.5.2 The approximation of the transformation matrices

If T_v and T_i are approximated as constant matrices, the approach used for a single-phase line applies directly for each mode. In the case of multiphase balanced lines, the transformation from phase-to-mode quantities can be done exactly with $\alpha\beta0$ components, and there is no error introduced in the transformation. In the case of untransposed multiphase lines, in many programmes, T_i and T_v are approximated as real which could be inappropriate in some cases. This remark is valid for all the models which are presented in the previous subclauses.

This approximation is usually considered to be accurate enough except for the representation of underground cables and multiple-circuit overhead lines at low frequencies. For cable representation, T_v and T_i could be usually considered as constant after a value of 2 kHz. For lower values of the frequency, variations are very severe.

In the case of overhead lines, variation of the above-mentioned matrices versus frequency is important in the case of conductors disposed vertically. This is not the case if the conductors are disposed horizontally.

If the variation of T_v and T_i versus frequency is taken into account, the calculation of the quantities in the phase domain from the quantities in the Laplace domain lead to the evaluation of $n \times n$ convolutions. The method of the approximation of each coefficient by a rational function of p applies for this evaluation.

There are other methods to represent lines. For instance, a phase-domain solution can be used directly [7], [36], [37] or antenna theory can be applied.

Annex B
(informative)

Arc modelling: the physics of the circuit-breaker

B.1 The steps in interruption

Prior to breaking a circuit, a circuit-breaker is in the closed position, i.e. the contact ensures the electrical continuity of the network. When an abnormally high current is detected, the circuit-breaker receives the order to "break" the network.

To break the current, a circuit-breaker separates the two touching conductive elements at any moment in the power-frequency wave, thus creating an electric arc. Electric arcs are currently the main circuit-breaking "device" in power networks. As the contacts move apart, the current drops to zero and the arc is extinguished, at the same time establishing an electrical separation between both parts of the electrical network. Arc extinction is accompanied by substantial thermal phenomena that have to be taken into account in good circuit-breaker simulation.

As soon as the current drops to zero, there is a race against time between the increasing dielectric strength of the circuit-breaker and the transient recovery voltage (TRV). The TRV is the voltage across the terminals of the circuit-breaker when the arc is extinguished, i.e. the difference of the upline and downline voltages of the network. For the circuit-breaker to "hold" the break, its TRV must remain lower than its dielectric strength. Otherwise, the gap breaks down, i.e. a new electric arc is created, and another attempt at breaking the circuit will be made when the current next drops to zero.

There are, in fact, different types of circuit-breaking, depending on the amplitude of the currents to be cut and the physical characteristics involved, i.e. the thermal and dielectric aspects. For high currents, one speaks of "power arc breaking", and the thermal aspect of the break is of major importance, as is the case with line fault breaks; but, for low currents, it is above all the dielectric aspect of the break that is taken into account, as in the case of breaking of low-induction currents. The two cases that will be studied as examples for validation of the circuit-breaker model illustrate these two aspects, but, in all cases, the model relies chiefly on modelling the behaviour of the electric arc as accurately as possible.

B.2 Mathematical models of an arc

Most mathematical models are based on energy balances between the electric arc and the surrounding environment when the current drops to zero. The two equations most used are the Mayr and Cassie equations [13]:

Mayr
$$\frac{\mathrm{d}g}{\mathrm{d}t} = \frac{1}{T}\left(\frac{i^2}{P} - g\right)$$
(B.1)

Cassie
$$\frac{\mathrm{d}g}{\mathrm{d}t} = \frac{1}{T}\left(\frac{iu}{U_0^2} - g\right)$$
(B.2)

where

g is the conductance of the electric arc;

T is its time constant;

u and i are the arc voltage and arc current;

P is the power loss of the arc;

U_0 is the stationary arc voltage.

These two equations and all those derived from them describe the evolution of the conductance (or resistance) of the arc in accordance with the behaviour of the voltage and current. For a high arc current, the resistance is very low, at around a few ohms, but as the current gets closer to zero, the resistance increases quickly, along a very steep gradient, until it reaches as much as, or more than, $10^8\ \Omega$, which is equivalent to an open circuit. These two equations are not classical electrical equations. Therefore, they have to be implemented in a general-purpose solver which is interfaced with the electrical network solver step by step.

B.3   Special cases of circuit interruption

B.3.1   Breaking line faults

Line-fault interruptions involve high currents and therefore entail important thermal phenomena. When a line fault is detected, the circuit-breaker receives the instruction to open and the break occurs in accordance with the scenario described previously.

But following the first extinction of the arc, the dielectric strength of the space between the contacts must be quickly re-established in order to prevent the arc re-appearing. This can be done by modifying several parameters: the temperature (arc blast) and the pressure (vacuum or air-blast circuit-breaker) of the insulating gas, the contact opening speed, etc.

Thus, for example, if the arc blast is insufficient, the arc heats up, thereby increasing the conductivity of the plasma of which it is made, and increases the energy dissipated by the Joule effect: this results in re-establishment of the arc. This phenomenon is called thermal re-ignition.

Just after the break, a post-arc current of about 1 A is created in the circuit-breaker in the first few micro-seconds after arc extinction. It decreases to zero after a few micro-seconds if the break succeeds, or increases in the event of thermal failure [26].

B.3.2   Breaking small induction currents (see Figure B.1)
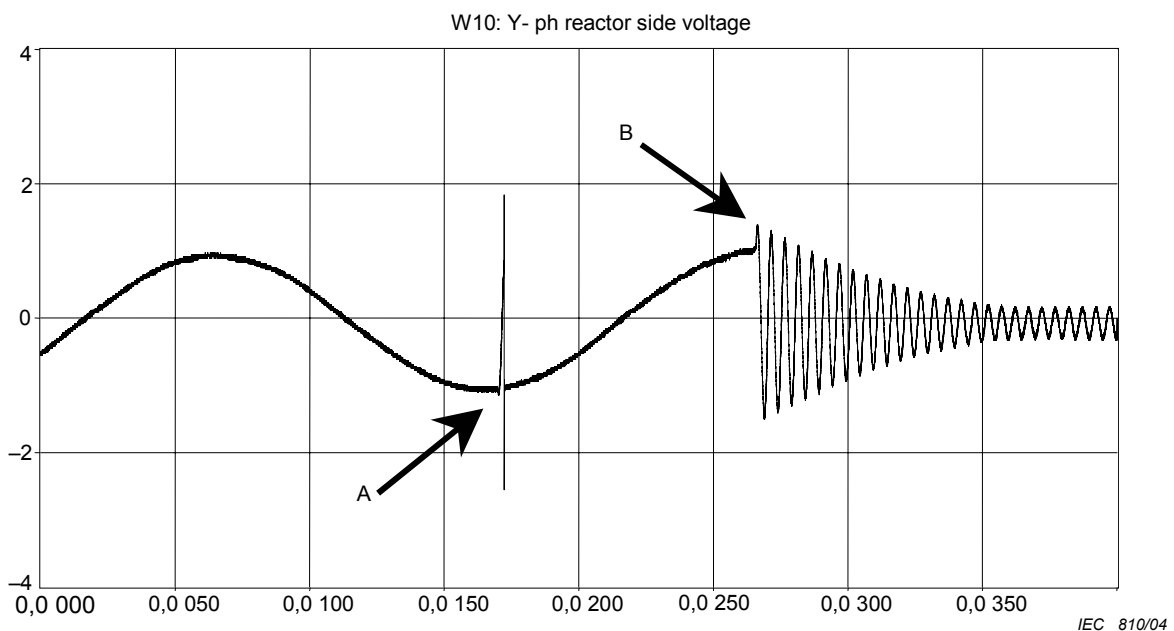
Key

A   Re-ignition overvoltage (VFFO).

B   Suppression overvoltage (SFO).

Figure B.1 – SF$_6$ circuit-breaker switching

In the particular case of low-current breaks, it is the dielectric aspect which counts most. This type of break occurs, for example, during disconnection of unload transformers compensation inductors or motors. It produces considerable overvoltage in the network on the element side, principally as a result of chopping current and breakdown. Modelling this type of break therefore helps to understand the appearance of overvoltage which can damage equipment.

As in the general case, opening of the contacts creates arcing in the circuit-breaker. When the current declines to close to zero, interaction of the arc with the circuit engenders high-frequency current variations which, on top of the power-frequency component, cause the current to drop to zero more rapidly. This phenomenon is called chopping current.

As soon as the current reaches zero, the arc is extinguished and both sides of the electrical circuit evolve freely. Since the element switched has inductive energy at the time the circuit-breaker opens, the current begins to oscillate at an amplitude of 1 p.u or more, depending on the chopping current. The transient recovery voltage (TRV) is the difference of the voltages at both sides of the breaker. If the TRV exceeds the dielectric strength of the circuit-breaker, there will be breakdown. The current will be re-established across the circuit-breaker and there will be a high-frequency transient in the circuit on top of the power-frequency current. This phenomenon can occur several times in swift succession before the current is finally broken for good, which may happen the next time the power-frequency current reaches zero [14].

Annex C
(informative)

Probabilistic methods for computing lightning-related risk
of failure of power system apparatus

C.1   Introduction

Lightning strike events can be characterized by different sets of random variables; therefore, estimating the risk of failure of a power system apparatus due to lightning should first begin by selecting the most relevant random variables and formulating probability distributions for them. These can constitute input random variables for the numerical simulations that need to be run for evaluating the corresponding lightning stresses (output random variable).

The risk of failure evaluation process includes the following three steps:

a) definition of a probabilistic model to account for the possible scenarios of lightning strokes to the transmission;

b) simulation of the system response to some user-defined lightning strokes in order to identify those leading to a failure;

c) integration of the risk integral over the identified failure domain.

Each step is detailed hereafter.

C.2   Definition of a probabilistic model

The first step in predicting the risk of failure of a power-system apparatus due to lightning is to define a probabilistic model which aims at giving a mathematical representation of the possible scenarios of lightning strokes to the power line. The probabilistic model consists of a set of random variables and of their probability distributions. Typically, those random variables should account for

–   the natural variability of the lightning stroke current waveshape, which is commonly described by its peak value, time-to-crest and tail duration,

–   the possible points of impact along the incoming lines,

–   the fluctuation of the a.c. voltage of the power line,

–   the fluctuation of the withstand capability of the apparatus.

On the one hand, considering so many random variables permits the precise modelling of the natural fluctuations of some parameters, although it may not be consistent with the scarcity of lightning data but, on the other hand, it imposes the running of many time-consuming electromagnetic transient programme simulations in order to determine the response of the system to the various lightning stroke scenarios defined.

Moreover, it overcomplicates the risk integral evaluation problem as conventional numerical integration techniques become quickly impractical for problems with more than two random variables. In such a case, more dedicated computational methods such as Monte Carlo simulation techniques or approximation methods (first- or second-order reliability methods) may be used.

As a consequence, some simplifications have to be made. Basically, one can focus only on the most influential and significant random variables and assume other random parameters as deterministic quantities (fixed values). A list of the practical simplifying assumptions proposed is given below.

C.2.1 Stroke point of impact

The point of impact can be considered to be a discrete random variable denoted by X whose values (x_1, x_2, x_n) are chosen by the user along the line. Its probability distribution (probability mass function), $P_x(x)$ is given by the proportion of lightning strokes terminating at the different points of impact, which is estimated by applying the electro-geometrical concepts in three dimensions.

For substations protected by a surge arrester, a limit distance is proposed by IEC 60071-2 and can be of help to the user for defining the points of impact along the line. It is often considered appropriate to use a limited number of points of impact on the spans within the limit distance.

C.2.1.1 Lightning stroke current waveshape

The lightning stroke current is generally represented as an ideal current source having a double ramp or CIGRE concave waveshape for which the following characterizing parameters are considered:

– The peak current amplitude, I, is supposed to be a continuous random variable. The user may choose between two probability distributions:

a) a log-normal distribution $f_I(i)$ given by $f_I(i) = \dfrac{1}{\sqrt{2\pi}\sigma_I i} e^{-\frac{1}{2}\left(\frac{\ln(i/\mu_I)}{\sigma_I}\right)^2}$ with parameters μ_I

and σ_I defined by the user. The default value could be those given by [4]

	$3 \le I \le 20$ kA	$I > 20$ kA
Median value μ_I (kA):	61,1	33,3
Logarithmic standard deviation σ_I (kA)	1,33	0,605

b) conditional probability distributions $f_{I/X}(i,x)$ given the points of impact X as obtained after applying the electro-geometric theory.

It should be noted that it is more accurate to consider the conditional probability distribution, especially when studying shielding failures.

– The time to crest is supposed to be a function of the peak current amplitude given by its conditional median value: $T_m = 0,0834 \times I^{0,828}$ for and $T_m = 0,154 \times I^{0,624}$ for $I > 20$ kA.

– The tail duration can be characterized by its time-to-half value T_d which it is proposed to consider as

i) a deterministic quantity fixed to its median value 77,5 µs if the lightning stresses under study are overvoltages;

ii) either a fixed value or a continuous random variable log-normal distribution with parameters μ_{Td} = 77,5 µs and σ_{Td} = 77,5 if one is focusing on the lightning energy stresses experienced by surge arresters.

With regard to the waveshape, it is often considered as preferable to use the CIGRE concave waveshape. The double-ramp waveshape may be used too but, most of the time, it gives more conservative results.

C.2.1.2 AC power voltage

It is proposed to consider by default only one value of phase angle for the a.c. power voltage. However, the user can consider several values, in which case the a.c. power-voltage angle becomes a discrete random variable denoted q which values (J_1, J_2 .., J_n) will be equiprobably distributed.

C.2.1.3   Strength or withstand capability of the apparatus

According to the type of lightning stresses one will look at, either voltage or energy stresses, the strength or withstand capability W of the apparatus will be respectively characterized by its disruptive voltage denoted by U_d or its energy absorption capability E_c, either defined by a fixed value or a random variable. In the latter case, the user will have to choose between two distributions, a normal or a Weibull distribution, for which he will have to stipulate the parameters. The probability distribution functions will be denoted respectively by $f_W(.)$, $f_{U_d}(.)$

and $f_{E_c}(.)$ for the random variables W, U_d and E_c.

C.2.1.4   Representative overvoltages

The crest values of the overvoltages evaluated by numerical simulations are usually considered as the representative overvoltages.

C.3   Evaluation of the stress function and determination of the failure domain (see Figure C.1)

When the probabilistic model has been defined, one has to evaluate which are the lightning stroke events that would lead to a failure of the apparatus in order to delimit the domain of integration of the risk integral (failure domain). This would be achieved by running a large number of EMTP simulations. For each point of impact $X = x_k$ and for each phase-angle value $\theta = \vartheta_t$, the user will define a set of lightning current values $(i_1, i_2 ..., i_n)$ and eventually a set of time-to-half values for the tail duration $(t_{d_1}, t_{d_2} ..., t_{d_n})$ that should be simulated by the programme.

By interpolating the simulation results (a piece-wise linear interpolation is precise enough), it is then possible to obtain a representation of the apparatus 'stress function' $h_{X,\theta}(.)$, given a point of impact $X = x_k$ and an a.c. power-voltage phase-angle value of $\theta = \vartheta_t$:

if T_d is assumed fixed to a specific value

$$S = h_{X,\theta}(I) \qquad \text{(C.1)}$$

if T_d is considered as a random variable

$$S = h_{X,\theta}(I, T_d) \qquad \text{(C.2)}$$

where I, T_d and S are respectively the input random variables 'lightning crest current' and 'time-to-half value of the tail duration' and the output random variable 'lightning stresses at the apparatus terminals'.

The region of the probability space for which the values of overvoltages are greater than those of apparatus withstand capability $\{h_{X,\theta}(i, t_d) > w\}$ gives the failure domain. The domain defined by $\{h_{X,\theta}(i, t_d) < w\}$ gives the safe domain and the boundary $\{h_{X,\theta}(i, t_d) = w\}$ is the limit state.
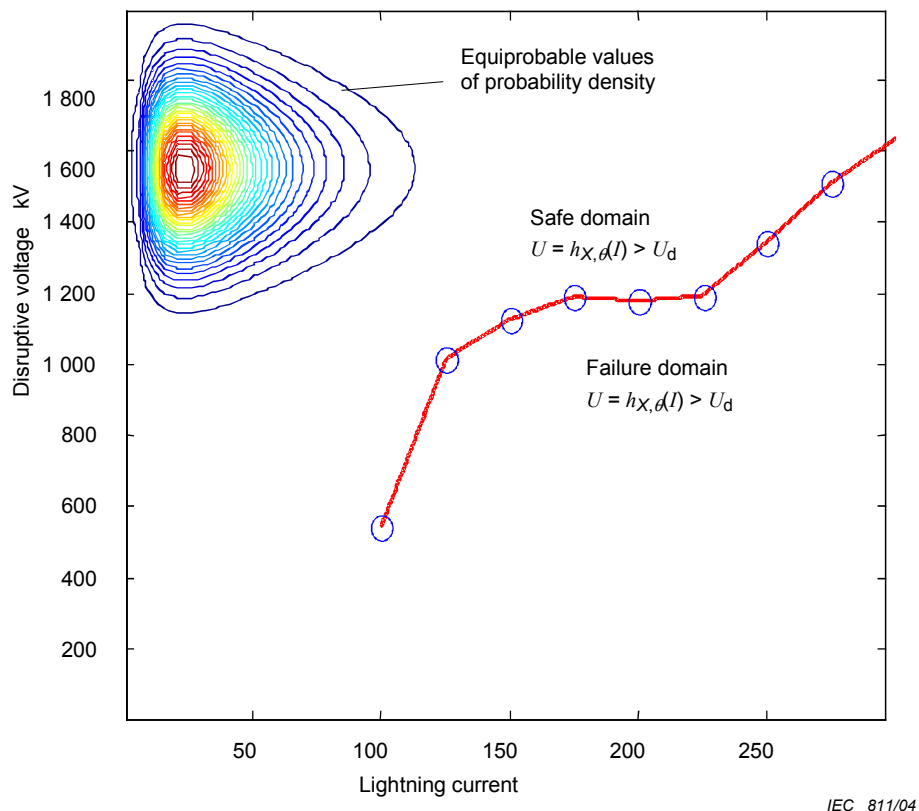
Figure C.1 – Example of a failure domain
(the dots represent the EMTP simulation results and the line is the interpolated function
$U = h_{X,\theta}(I)$)

C.4 Risk integral computation

When the stress function $h_{X,\theta}(.)$ has been obtained for each point of impact and all values of phase angle, the risk of failure $R_{X,\theta}(x_k, \vartheta_t)$ of the apparatus given that the line is struck at point $X = x_k$ and for an a.c. power-voltage angle $\theta = \vartheta_t$ is given by the following integral:

$$R_{X,\theta}(x_k, \vartheta_t) = \iiint\limits_{\left\{h_{x_k,\theta_t}(i,t_d) > w\right\}} f_W(w) f_I(i) f_{T_d}(t_d) \mathrm{d}w \mathrm{d}i \mathrm{d}t_d \tag{C.3}$$

if the apparatus withstand capability is defined by a random variable, or by

$$R_{X,\theta}(x_k, \vartheta_t) = \iint\limits_{\left\{h_{x_k,\theta_t}(i,t_d) > w_0\right\}} f_I(i) f_{T_d}(t_d) \mathrm{d}i \mathrm{d}t_d \tag{C.4}$$

if the apparatus withstand capability is deterministic and fixed to w_0.

If the time-to-half value of the tail duration T_d is not considered as a random variable, then the above equations would be respectively simplified to

$$R_{X,\theta}(x_k,\vartheta_t) = \iint\limits_{\{h_{x_k,\theta_t}(i)>w\}} f_w(w)f_I(i)\,\mathrm{d}w\,\mathrm{d}i \tag{C.5}$$

and

$$R_{X,\theta}(x_k,\vartheta_t) = \int\limits_{\{h_{x_k,\theta_t}(i)>w_0\}} f_I(i)\,\mathrm{d}i \tag{C.6}$$

Then the discrete variable 'a.c. power-phase angle' can be eliminated using the equiprobably distributed property of its values:

$$R_X(x_k) = \frac{1}{n_\theta}\sum_{t=1}^{n_\theta} R_{X,\theta}(x_k,\vartheta_t) \tag{C.7}$$

where

$R_X(x_k)$ is the risk of failure of the apparatus if a lightning stroke hits the line section; x_k

n_θ is the number of phase-angle values.

It should be noted that three major computational techniques are available for evaluating the above risk integrals:

– standard numerical integration techniques;

– FORM/SORM approximation methods;

– Monte Carlo simulation or numerical experimentation.

The first technique is straightforward and easy to implement for simple problems with few primitive random variables. However, for higher order problems, it often proves to be inappropriate as the required computational time becomes quickly excessive, and the accuracy may be affected by the numerical noise, especially for a very low risk of failure.

The second technique gives an estimate of the probability of failure by considering the geometry of the region of integration. It is based on a first-order (FORM) or a second-order (SORM) approximation of the limit state, after transposition of the latter into a standard probability space. The main advantage of this technique is that it does not depend greatly on either the level of reliability or the number of primitive random variables. It also permits the identification of the region of the failure domain mostly contributing to the risk.

In the third technique, many lightning stroke scenarios would be randomly generated. After a large set of simulations, the results would be surveyed and an estimate of the probability of failure would be given by the ratio of observed failures over the number of simulations. The advantages are that it is a convergent process with a well-defined error estimate and that the complexity of the limit state does not affect the accuracy of the estimation. The disadvantage is that it is a computationally expensive technique as it imposes many simulations.

Greater details of the two latter techniques can be found in academic books about reliability theory. The first technique will, however, prove to be sufficient in most case studies.

C.5 Expected annual number of failures

Let us denote by

N_k the number of lightning strokes that are annually captured by the line section corresponding to the discrete point of impact $X = x_k$,

R_X the resulting risk of failure for the power-system apparatus.

The expected annual number of failures N due to lightning is calculated as follows:

$$N = \sum_{k=1}^{n} N_k \times R_X(x_k) \qquad\qquad (C.8)$$

and the expected time-to-failure T by

$$T = \frac{1}{N} \qquad\qquad (C.9)$$

Annex D
(informative)

Test case 5 (TOV) – Resonance between a line and a reactor in a 400/220 kV transmission system

This test case describes the energization of a long line during restoration of service. This kind of switching implies energization of lines (sometimes long) with weak short-circuit power feeding, thus increasing the probability of obtaining high overvoltages.

In the case shown, the overvoltages obtained during normal energization are so high that a reactor must be connected to the end of the line prior to energization (Figure D.1). In the receiving end substation a reactor is installed to perform voltage control in the area, thus this reactor is used to solve this problem.

The parameters of the line and reactor are such that a resonance was found during energization, in the case that a malfunction of a breaker pole occurred. This suggested the use of a different operation scheme to energize the line (Figure D.2).

The physical phenomena can be understood with Figure D.3. The phase whose breaker pole malfunctioned (phase A in the example) is fed through the capacitive coupling with the other phases. This way, a series resonant circuit is made with the corresponding reactor, having the possibility of achieving high voltages at the point where the reactor connects to the line.

A study has been conducted to evaluate the magnitude of the overvoltages. This test case gives an example of application of the third step of the method presented in Clause 8. The event considered is an "uneven breaker pole operation".

D.1   Input data and modelling

D.1.1   Scheme
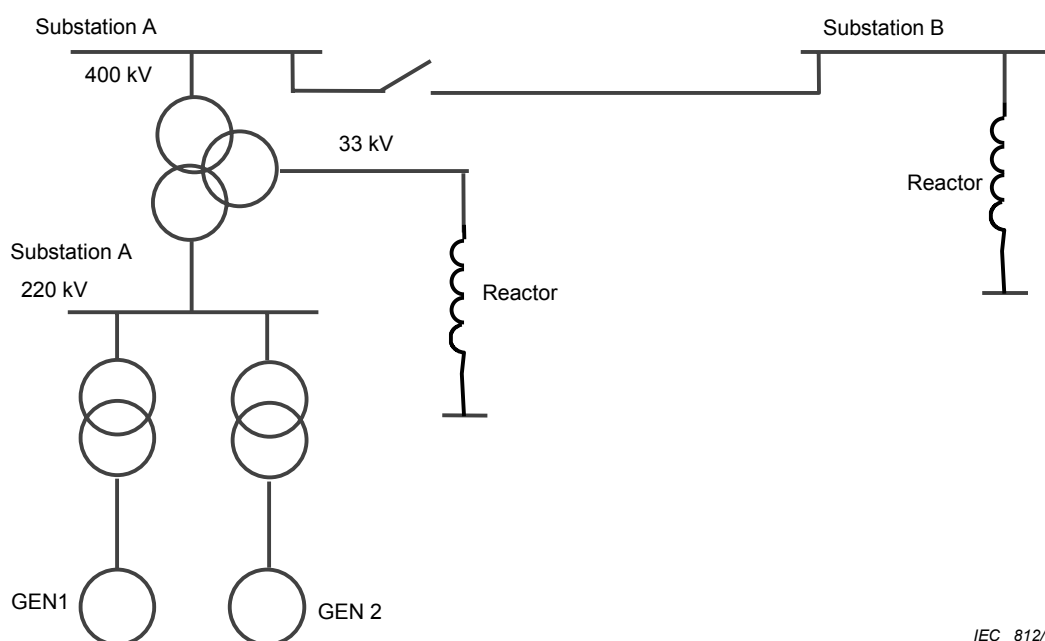
IEC   812/04

Figure D.1 – The line and the reactance are energized at the same time
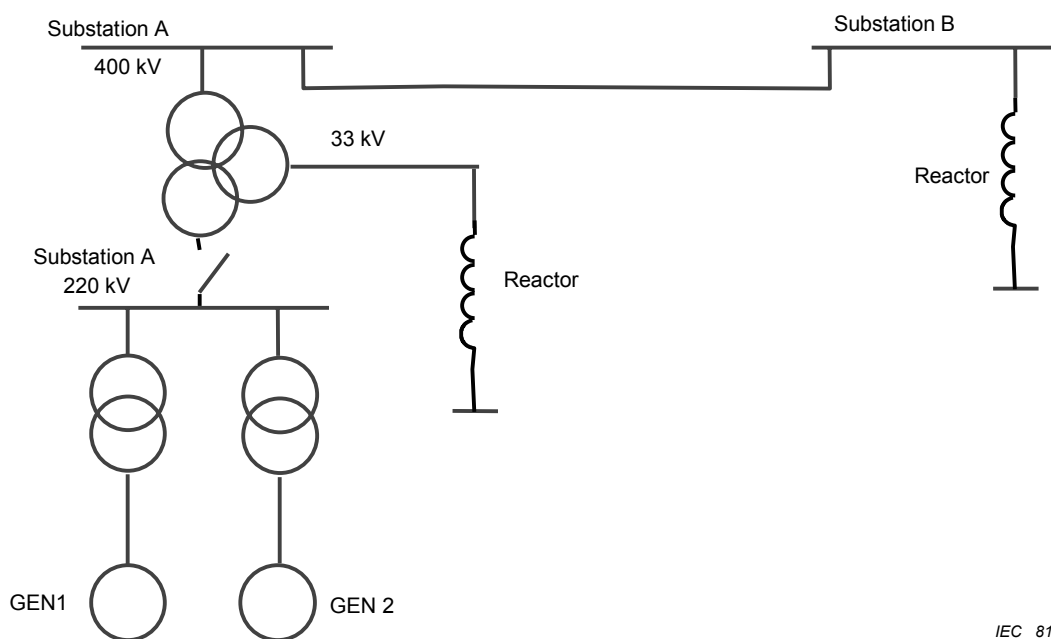
IEC   813/04

**Figure D.2 – Energization configuration of the line minimizing the risk
of temporary overvoltage**

As the energization configuration proposed in Figure D.1 has a resonance problem, another energization configuration, as proposed in Figure D.2, can be studied. Before energization, the line and the reactor in substation B are connected to the secondary side of the transformer and then the primary side of the transformer is energized in order to limit the risk of temporary overvoltages. In Figure D.6 we can see the voltage in the phase where the breaker failed to close. The impedance of the transformer included is enough to avoid the resonance situation.

D.1.2   Line parameters

The line has been represented with a distributed parameters model and the following characteristics, as shown in Table D.1:

Table D.1 – Line parameters

	Resistance Ω	Inductance mH	Capacitance µF
Zero sequence	87,4	819	2,23
Positive sequence	9,25	299	3,27
NOTE The line length is 276 km.			

D.1.3   Generators

Two generators of 113 MVA and equal characteristics are considered. They have been modelled as Thevenin equivalents with the following parameters:

Voltage (phase-to-earth):	11 kV
Inductance:	1,72 mH
Resistance:	85,6 Ω

The inductance and resistance have been modelled in parallel. This way numerical oscillations (see 7.2.4) caused by the sudden energization of the reactance are avoided.

D.1.4 Transformers

Each of the three transformers has been modelled by three single-phase units, as shown in Tables D.2 and D.3.

Table D.2 – 400 /220/33 kV transformer

Winding kV	Resistance Ω	Inductance mH
400	0,16	107
220	0,0484	−4
33	0	3,8

Table D.3 – 220 /13,8 kV transformer

Winding kV	Resistance Ω	Inductance mH
220	0,5566	90
13,8	0,0066	1,06

For configuring the magnetizing impedance of the 400/220/33 kV transformer, two points of current and flux are known (peak values), as shown in Table D.4:

Table D.4 – Points of current and flux of 400 /220/33 kV transformer

Current A	Flux V.s
2,67	148
8	163

These values are calculated to be coupled in the tertiary.

For configuring the magnetizing impedance of the 220/13,8 kV transformer, two points of current and flux are known (peak values), as shown in Table D.5:

Table D.5 – Points of current and flux of 220 /13,8 kV transformer

Current A	Flux V.s
6,4	62
19	68

D.1.5 Reactor

The 400 kV/150 MVAr reactor has been modelled by a saturable reactance in parallel with a resistance (losses) and a capacitance (stray capacitance).

For configuring the inductance, two points of current and flux are known (peak values), as shown in Table D.6:

Document provided by IHS Licensee=Qatar Petroleum/5943408001, 12/08/2004
21:49:44 MST Questions or comments about this message: please call the Document
Policy Group at 303-397-2295.

101

Table D.6 – Points of current and flux of 400 kV /150 MVAr

Current A	Flux V.s
367	1 248
5 000	6 612

$$R = 400 \text{ k}\Omega$$
$$C = 6 \text{ nF}$$

D.2   Method

In order to discover the possibility of appearance of resonance, the malfunction of one pole of the energization breaker has been simulated. The phase whose pole has not closed is fed through the coupling with the other phases constituting a series resonance circuit with the reactor (Figure D.3).
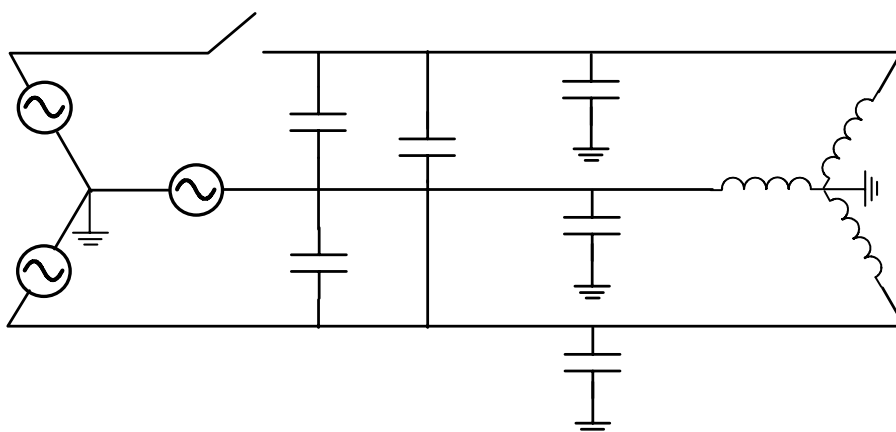
IEC   814/04

Figure D.3 – Malfunction of a circuit-breaker pole during energization of a transformer

A deterministic study is carried out with only two switching procedures considered. The first one is the energization of the line together with the reactor (Figure D.1), the second one is the energization of the 400 /220 kV transformer together with the line and reactor (Figure D.2).

D.3   Results and interpretation

In Figures D.4 and D.5 the evolution of the voltage in substation B can be seen in two of the three phases. In Figure D.4, the phase whose pole has not closed (phase A) is presented, and in Figure D.5 a phase whose pole closed correctly is presented (phase B). These figures correspond with Figure D.1. Due to a resonance between the line and the reactor, the voltage reaches steady state around 1,4 p.u. of its original value.
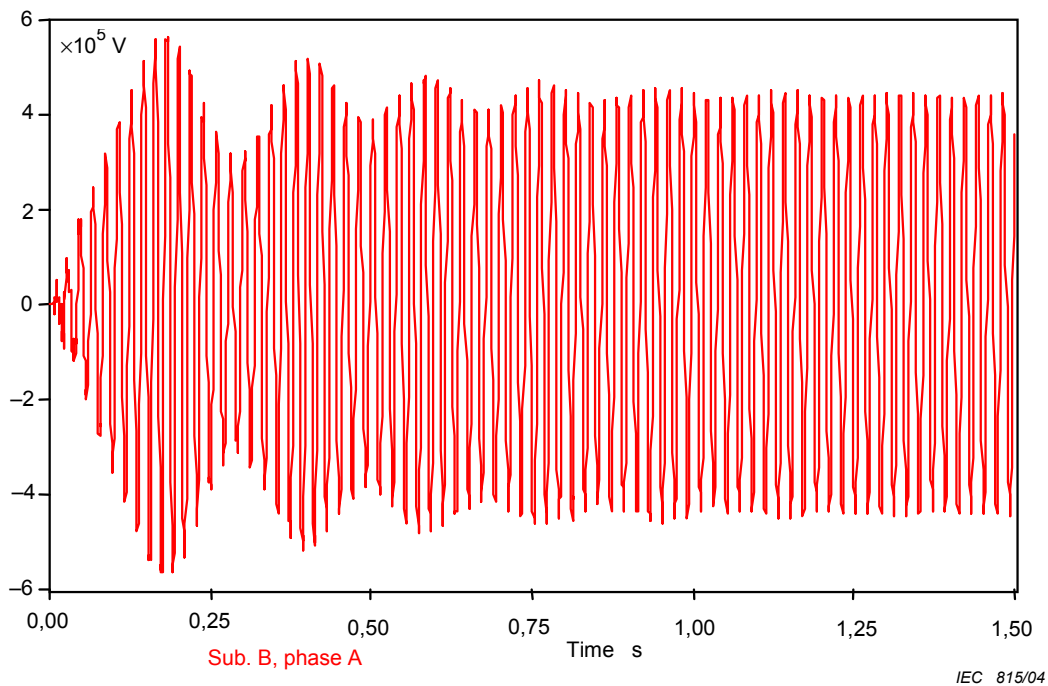
Figure D.4 – Voltage in substation B phase A whose pole has not closed
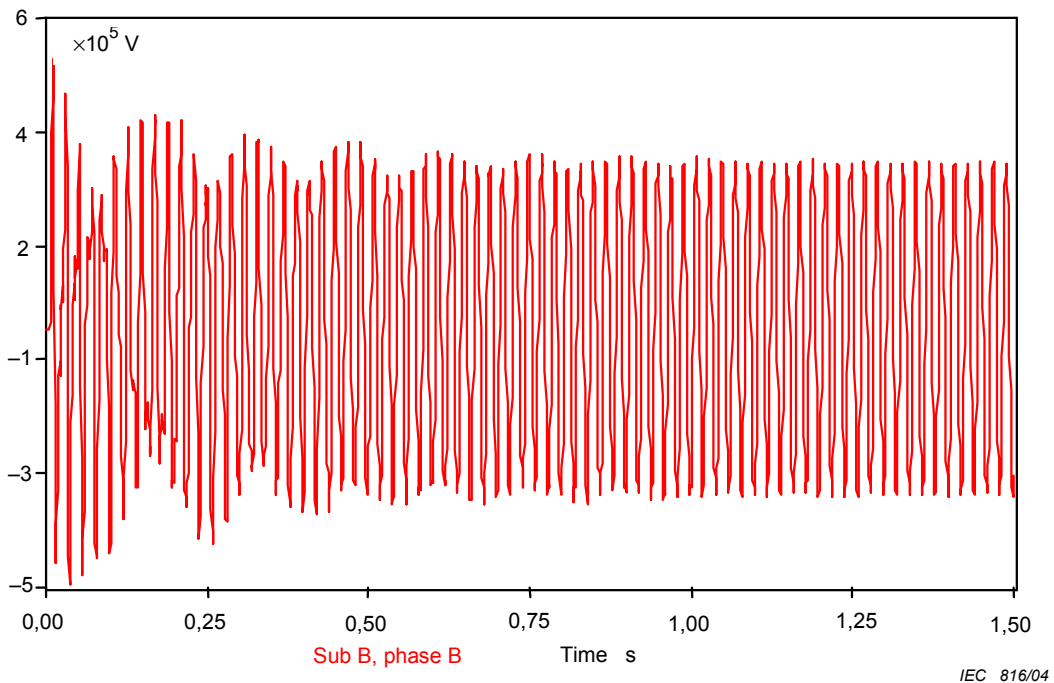
Figure D.5 – Voltage in substation B phase B whose pole closed correctly

As the switching operation proposed in Figure D.1 has a resonance problem, the switching proposed in Figure D.2 is studied. In Figure D.6 we can see the voltage in the phase where the breaker failed to close. The impedance of the transformer included is enough to avoid the resonance situation.

Sub. B, phase A

IEC 817/04
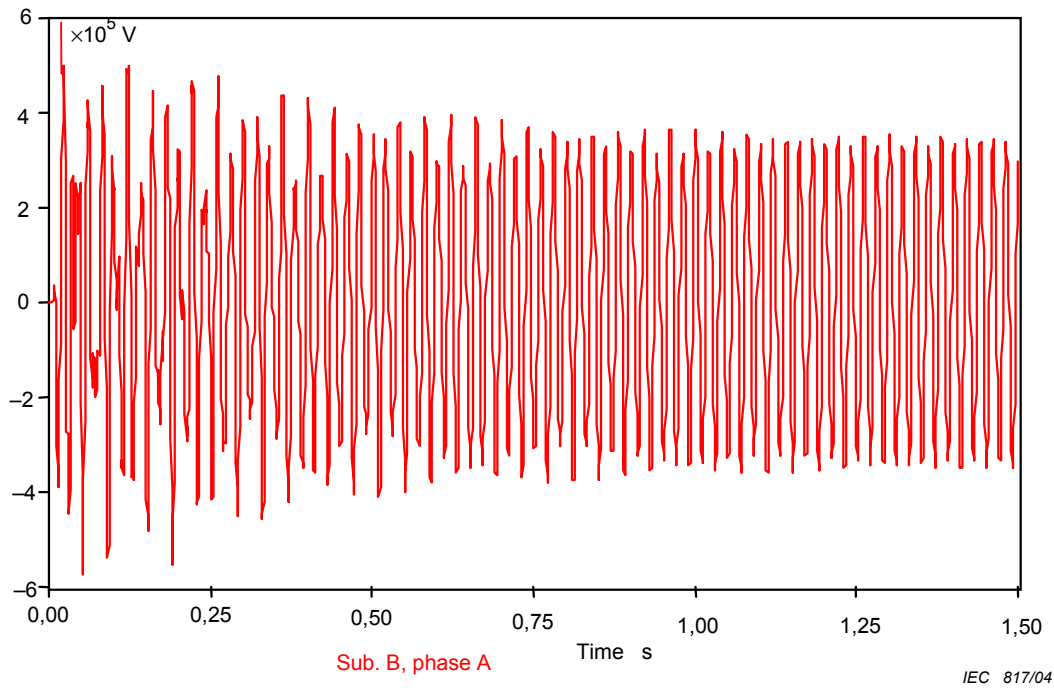
**Figure D.6 – Voltage in substation B phase A where the breaker failed to close
(configuration of Figure D.2)**

<div align="center">

Annex E

(informative)

Test case 6 (SFO) –
Evaluation of the risk of failure of a gas-insulated line due to SFO

</div>

This test case is an example of a statistical study performed in order to calculate the risk of failure due to FFO. This example includes a 420 kV line energization with and without trapped charges in presence of a gas insulated line (GIL). A risk calculation is performed in order to allow a failure rate associated to dielectric constraints. Several configurations and parameters may be studied: short-circuit current, overhead line length and GIL length. The objectives are to show a classical application of a risk calculation method for M-insulations in parallel, to estimate overvoltages ($U_{2\%}$) magnitude and to estimate the performances according to the SIWV.

E.1   Input data and modelling

E.1.1   Diagram (Figure E.1)

<div align="center">
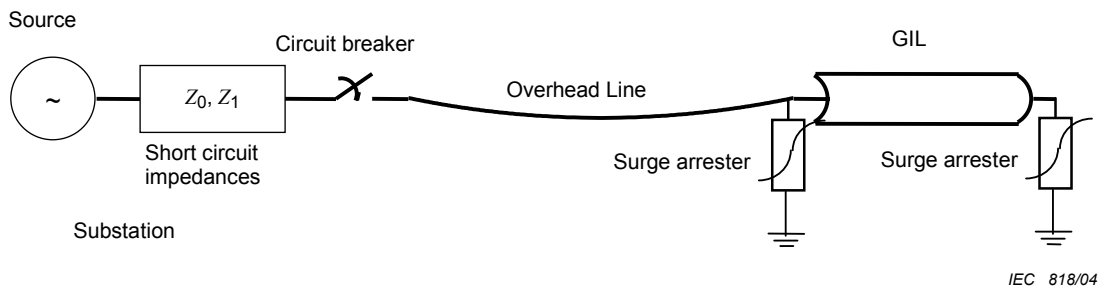
Figure E.1 – Electric circuit used to perform closing overvoltage calculations

</div>

To reclose overvoltage calculations, a 50 Hz source is connected before the transient in order to model the trapped charges in the circuit (7.5.2.1). To close overvoltages in presence of a single-phase-to-earth fault, a switch connecting one phase conductor to earth is modelled immediately after the circuit-breaker (between the circuit-breaker and the overhead line).

E.1.2   Power supply

The model used for the substation is presented in 7.4.1. It corresponds to a particular type of modelling of the source for SFO.

The parameters are given in Table E.1.

<div align="center">

Table E.1 – Parameters of the power supply

U_n	Phase-to-phase voltage service (r.m.s.)	420 000 V
Icc3	Three-phase short-circuit current	63 kA and 36 kA depending on the configuration
Z_0 / Z_1	Zero-positive impedance ratio	Three for all configurations
f	Resonance frequency	2 000 Hz for all configurations
τ	Time constant	0,07 s for all configurations

</div>

E.1.3 Surge arresters (7.5.11)

Surge arresters are installed at both ends of the GIL. They are modelled by their $V(I)$ characteristic. The rated voltage is 360 kV r.m.s. The maximum operating voltage is 267 kV and TOV is 418 kV (1 s). The residual voltage at 1 kA is 650 kV. From the point of view of a system designer, the energy may be estimated by numerical calculation as for the overvoltages.

E.1.4 Circuit-breaker

To simulate three-pole closure, three statistical switches were used as shown in 7.5.10. All three poles have the same Gauss standard deviation with closing times comprised between $\pm 3\sigma$, with σ = 1,5 ms. For each configuration, 500 simulations were performed.

The closing time for the three poles is driven by a "mean time pilot" that is increased by Δt (20 ms/500) with the number of simulations over one 50 Hz period. For each simulation, all three poles have the same "mean time pilot", which corresponds to $t_{50\,\%}$, but different random closing times according to each Gauss distribution. This procedure allows a complete systematic variation of the closing times over the 50 Hz period.

E.1.5 Overhead line and GIL

The models used for overhead lines and for gas-insulated lines are frequency-dependent models (7.5.2). In both models the frequency of the transformation matrices was fixed at 5 kHz. In this test case, overhead line and GIL parameters (Y(s) and γ(s)) were calculated between 0,1 Hz and 200 kHz (frequency limits must be chosen according to the system studied). Several lengths were used according to the configuration. Physically, the overhead line surge propagation velocity of the aerial modes are near the velocity of light. For GIL the same velocity is obtained. The GIL was modelled using several portions in series in order to measure the voltage distribution in the GIL. The sheaths are connected to earth by a 2 Ω at each extremity.

E.1.6 Trapped charges (7.5.2)

An auxiliary voltage source of 1 p.u. was used to simulate maximum trapped charges scenario (PhA + 1 p.u., PhB – 1 p.u., PhC + 1 p.u.). This source is connected to the overhead line at the initial steady-state calculation and is disconnected at the first time step. Zero chopping current was considered.

E.2 Method employed

A statistical method is used to calculate voltage probability density function and then to perform risk calculation. A pseudo-random routine is used to control each simulation according to pole switch closing time. Each of the studied configurations consists of 500 simulations. $U_{2\,\%}$ and $U_{10\,\%}$ or $U_{16\,\%}$ as proposed in IEC 60071-2 can be directly obtained. The phase overvoltage distribution used to calculate the risk is the one that has the higher $U_{2\,\%}$ (according to 2.3.3.1 of IEC 60071-2, the so-called phase-peak method). Only phase-to-earth overvoltages were studied.

To perform a risk calculation for a uniform voltage distribution, the following general formula is used:

$$R = \int_{\pm 4\sigma} f(u)P(u)\mathrm{d}u$$

These two functions are

– $f(u)$: overvoltages probability density function obtained,

– $P(u)$: probability of flashover of the insulation under an impulse of value u.

The first one is obtained by random numerical calculation(Figure E.2 presents an example of overvoltage distribution with two different fitting critiera). The second one is estimated and should be confirmed by laboratory testing if possible. This estimation must reflect an experienced knowledge of the equipment.

Proposed simplified fitting for switching overvoltage distributions
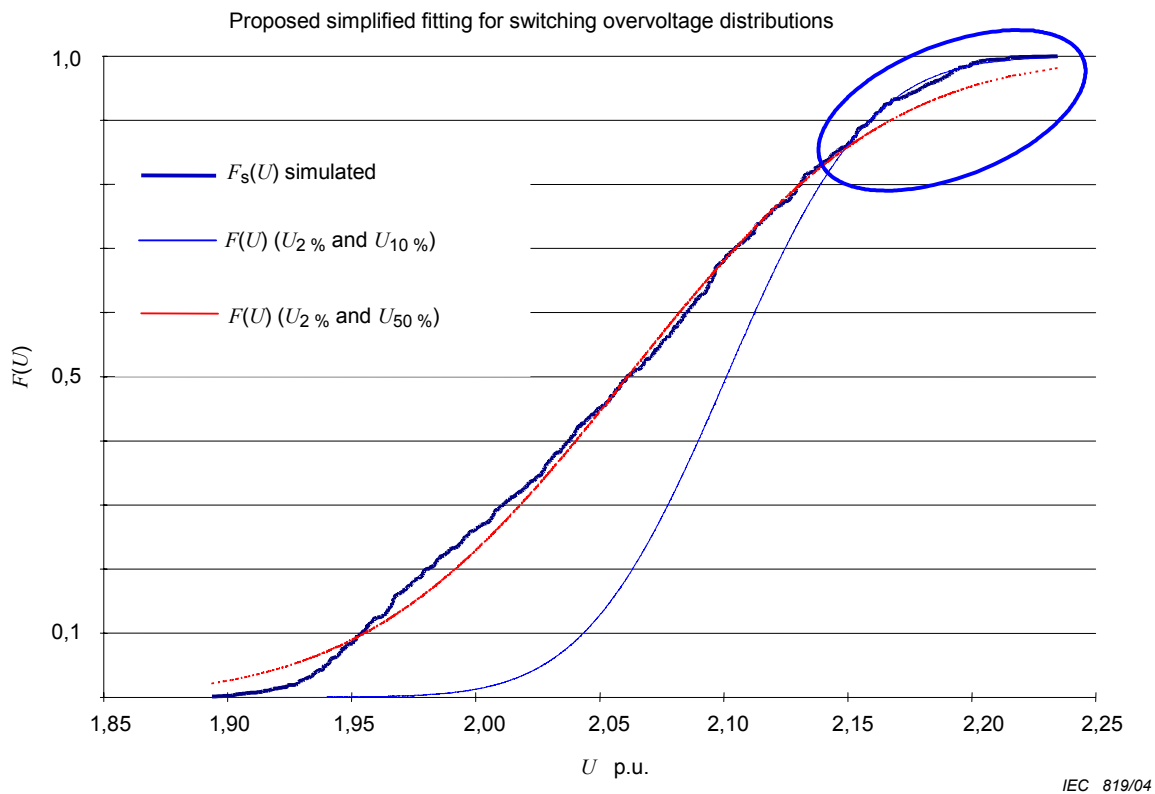
Figure E.2 – Calculated overvoltage distribution – Two estimated Gauss probability functions resulting from two different fitting criteria (the $U_{2\,\%}$ and $U_{10\,\%}$ guarantees a good fitting of the most dangerous overvoltages)

Thus, GIL can be considered as a parallel of M-insulation, M being the number of elementary portions of tested GIL on site. On this basis, one may consider a standard deviation of 3 % (based on past dielectric tests) for a 100 m GIL elementary portion (site tests are generally performed on 500 m to 1 000 m portions). The other hypothesis that must be made concerns the on-site guaranteed withstand voltage. One may consider that $U_{10\,\%}$ (100 m) = 80 % SIWV. The next two equations may help to estimate the equivalent probability function of the total GIL length (see formula (C.12) of IEC 60071-2):

$$Z_{\text{M}} = \frac{Z}{\sqrt[5]{M}} \qquad \text{and} \qquad U_{50\text{M}} = U_{50} - 4Z\left(1 - \frac{1}{\sqrt[5]{M}}\right)$$

where

Z is the value of the standard deviation of the discharge probability of one elementary portion;

Z_{M} is the value of standard deviation of M elementary portions in parallel;

U_{50} is the value of the 50 % discharge voltage of one elementary portion;

U_{50M} is the value of the 50 % discharge voltage of M elementary portions in parallel.

The formulae given are valid just in the case of a flat voltage profile of the overvoltage along the GIL.

The following Tables E.2 to E.4 resume the parameters used (standard deviation and $U_{50\%}$ for the lengths considered):

$$U_{10\%}(100\ m) = 80\ \%\ SIWV = 0,8 \times 1\ 050\ kV = 840\ kV$$

Table E.2 – Standard deviation and U_{50M} for different lengths (SIWV = 1 050 kV)

SIWV = 1 050 kV	Standard deviation % of U_{50}	U_{50M} kV
100 m	3 %	874
0,6 km	2,1 %	842
1,4 km	1,8 %	830
3 km	1,5 %	821
5 km	1,4 %	817
10 km	1,2 %	810

$$U_{10\%}(100\ m) = 80\ \%\ SIWV = 0,8 \times 950\ kV = 760\ kV$$

Table E.3 – Standard deviation and U_{50M} for different lengths (SIWV = 950 kV)

SIWV = 950 kV	Standard deviation % of U_{50}	U_{50M} kV
100 m	3 %	790
0,6 km	2,1 %	762
1,4 km	1,8 %	752
3 km	1,5 %	744
5 km	1,4 %	739
10 km	1,2 %	733

$$U_{10\%}(100\ m) = 80\ \%\ SIWV = 0,8 \times 850\ kV = 680\ kV$$

Table E.4 – Standard deviation and U_{50M} for different lengths (SIWV = 850 kV)

SIWV = 850 kV	Standard deviation % of U_{50}	U_{50M} kV
100 m	3 %	707
0,6 km	2,1 %	682
1,4 km	1,8 %	672
3 km	1,5 %	665
5 km	1,4 %	661
10 km	1,2 %	656

Using a Weibull probability function for the GIL insulation characterization and a Gauss fitting of the simulated overvoltages, it is possible to obtain the equivalent density function for the overvoltages.

E.3   Configurations

Several GIL lengths were considered: 600 m, 1 400 m, 3 km, 5 km, and 10 km.

Configuration A

Short-circuit current 63 kA + GIL (several lengths)

Configuration B

Short-circuit current 36 kA + 58 km of single-circuit overhead line + GIL (several lengths)

Configuration C

Short-circuit current 63 kA + 84 km of double circuit overhead line + GIL (several lengths)

E.4   Results and interpretation

Figure E.3 gives an example of overvoltage obtained on two phases of the GIL. Figure E.4 gives an example of the repartition of overvoltages obtained along the GIL. Because of the presence of surge arresters at both ends of the GIL, the voltage distribution along the GIL may not be uniform. Depending on the GIL length, the ratio between the maximum and the minimum voltage may vary. For a GIL of less than 10 km, this ratio is lower than 1,01, and for 50 km this ratio is 1,10. For these reasons, uniform voltage distribution can be considered for GIL smaller than 10 km. Otherwise, the risk calculation method will need to take into account the non-uniform voltage distribution along the GIL.
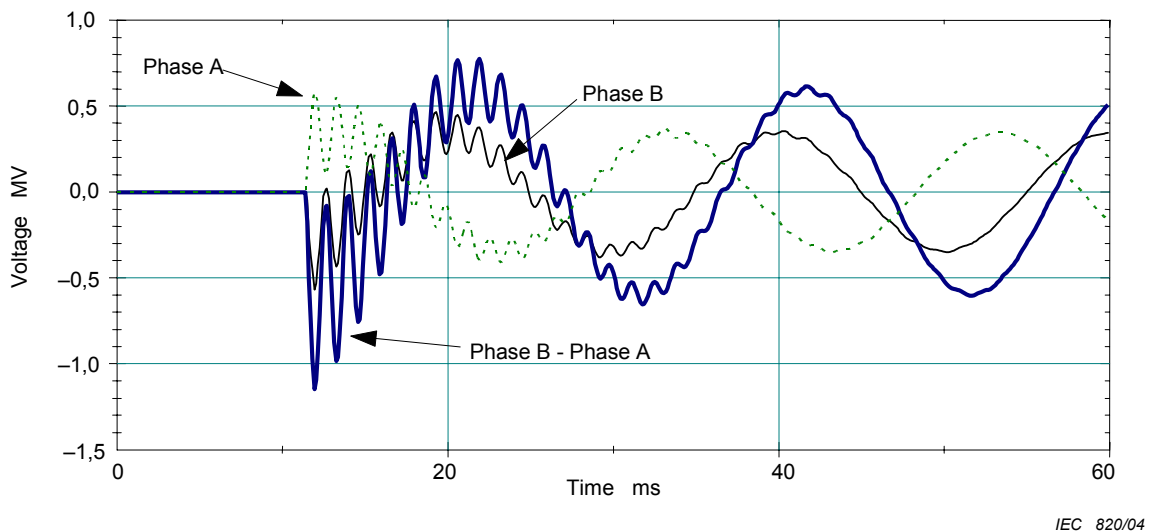

IEC 820/04

**Figure E.3 – Example of switching overvoltage between phases A and B
and phase-to-earth (A and B)**

Voltage distribution along the 10 km GIL
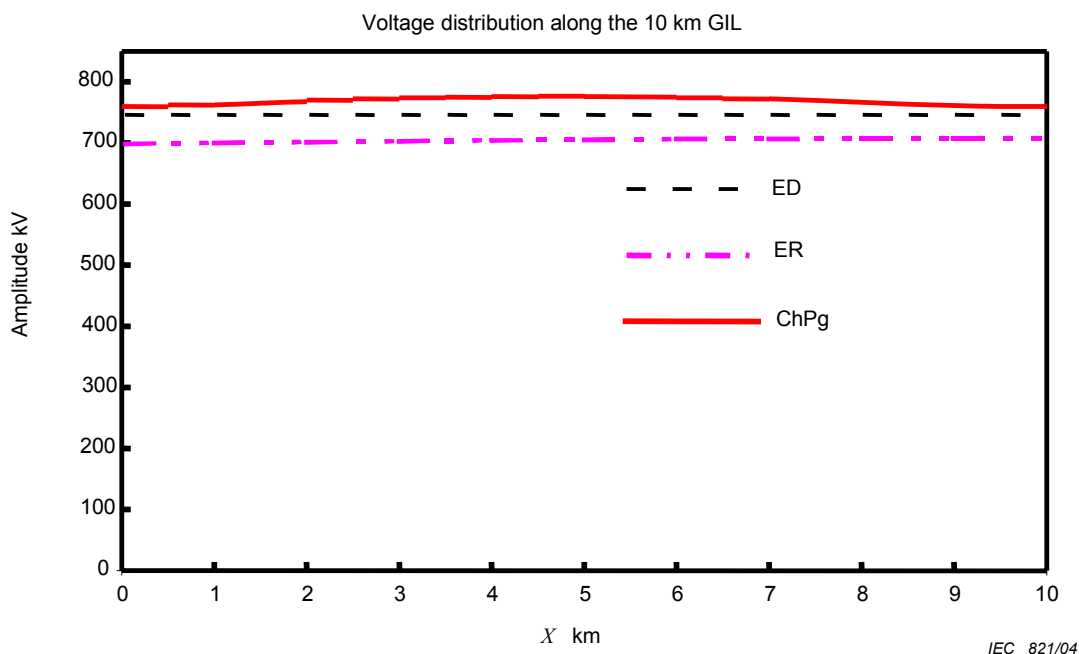

IEC 821/04

Figure E.4 – Voltage distribution along the GIL (ER-energization ED-energization under single-phase fault ChPg-trapped charges)

In Table E.5 the statistical overvoltage calculations results are given under the $U_{2\%}$ and $U_{10\%}$ for every considered configuration. The surge arrester energy can also be obtained from the same simulations.

Table E.5 – Statistical overvoltages $U_{2\%}$ and $U_{10\%}$ for every considered configuration

GIL length	600 m			1400 m			3 km			5 km			10 km		
Configuration (energizing with trapped Charges)	A	B	C	A	B	C	A	B	C	A	B	C	A	B	C
$U_{10\%}$	1,18	1,34	2,07	1,47	1,68	2,05	1,87	1,94	2,06	1,96	1,99	2,07	2,04	2,05	2,08
$U_{2\%}$	1,28	1,44	2,09	1,63	1,83	2,07	1,93	1,96	2,09	2,00	2,02	2,09	2,09	2,09	2,10
Configuration(single phase-to-earth fault)	A	B	C	A	B	C	A	B	C	A	B	C	A	B	C
$U_{10\%}$	1,59	1,71	2,02	1,77	1,86	2,03	1,92	1,95	2,02	1,99	1,99	2,03	2,03	2,06	2,05
$U_{2\%}$	1,62	1,73	2,04	1,80	1,89	2,04	1,94	1,96	2,05	1,99	2,00	2,06	2,04	2,07	2,06
Configuration (energizing)	A	B	C	A	B	C	A	B	C	A	B	C	A	B	C
$U_{10\%}$	1,17	1,23	1,94	1,32	1,39	1,94	1,47	1,58	1,94	1,55	1,73	1,95	1,77	1,83	1,95
$U_{2\%}$	1,21	1,31	1,97	1,39	1,53	1,97	1,58	1,71	1,97	1,71	1,80	1,98	1,84	1,89	1,99

The magnitude and oscillation frequency of the overvoltages depend on many factors: network topology (degree of interconnection of the network, number of overhead lines connected to the busbars, short-circuit power of the busbars Z_0/Z_1, overhead line lengths, circuit-breaker characteristics, surge arrester protection distance, etc.)

The overvoltage oscillations result from the conjunction of the source side resonance frequency and the natural frequency of lines or other equipment of the circuit.

Some conclusions concerning switching overvoltages in the GIL resulting from this short test case are as follows:

– the longer the overhead line, the bigger the overvoltages in the GIL;

– the longer the overhead line, the less important the GIL length. On the contrary, for short-length overhead lines, the GIL length becomes very important. The longer the GIL, the higher the overvoltages.

E.5   Risk calculation

The overvoltages due to single phase-to-earth faults were not considered because a very small probability is concerned. If one desires to take this operation into account, one should estimate or assume the probability of closing the circuit-breaker under fault conditions (see Table E.6).

Table E.6 – Risks for every considered configuration

Risk	SIWV = 1 050 kV $U_{10\%}$ = 840 kV		SIWV = 950 kV $U_{10\%}$ = 760 kV		SIWV = 850 kV $U_{10\%}$ = 680 kV	
Risk (configuration A)	R En	R_En_TCh	R En	R_En_TCh	R En	R_En_TCh
0,6	0,0E+00	6,0E-25	0,0E+00	7,7E-19	4,5E-27	2,5E-13
3	1,7E-13	1,5E-11	2,4E-09	4,3E-06	6,0E-06	2,7E-02
10	7,0E-12	5,8E-07	9,3E-07	1,0E-02	4,7E-03	7,0E-01
Risk (configuration B)	R En	R_En_TCh	R En	R_En_TCh	R En	R_En_TCh
0,6	1,0E-28	5,0E-19	2,0E-21	7,0E-14	7,0E-15	3,0E-09
3	2,0E-09	3,0E-14	2,0E-06	9,8E-07	4,6E-04	2,2E-01
10	6,0E-13	1,5E-07	7,0E-07	9,5E-03	1,6E-02	8,4E-01
Risk (configuration B)	R En	R_En_TCh	R En	R_En_TCh	R En	R_En_TCh
0,6	2,0E-13	5,8E-10	9,8E-07	6,6E-04	4,4E-02	8,3E-01
3	7,0E-13	4,8E-09	3,4E-06	3,0E-03	1,4E-01	9,6E-01
10	1,0E-11	3,0E-08	3,4E-05	2,5E-02	4,0E-01	9,9E-01

The risk of failure may be interpreted as the risk of failure of each $1/R$ operation. Risks less than $10E^{-8}$ do represent zero risk. The previous risk calculation may help the system designer in choosing the desired SIWV. The accepted failure rate must be fixed.

Considering the possibility of trapped charges for a 10 km GIL (re-closing), the estimated failure rate can be obtained as a function of the chosen SIWV. In the decision, the performance criteria and another possible problem not treated in this exercise dealing with the energy absorption of the surge arresters must be taken into account. The same type of analysis can be made. If surge-arrester breakdown dielectric characteristics are unknown and no good estimation is available, one can perform $E_{2\%...}$ If $F_E(.)$ is the cumulative probability distribution of the energy stress, $F_E(E_{2\%}) = 0{,}02$ and $E_{10\%}$ calculations and compare with the specified energy withstand.

As an example, Table E.7 presents the number of dielectric breakdowns over 20 000 operations (N), and the following results can be deduced:

Document provided by IHS Licensee=Qatar Petroleum/5943408001, 12/08/2004
21:49:44 MST Questions or comments about this message: please call the Document
Policy Group at 303-397-2295.

111

**Table E.7 – Number of dielectric breakdowns over 20 000 operations
for every configuration**

Length in km	SIWV = 1 050 kV $U_{10\%}$ = 840 kV	SIWV = 950 kV $U_{10\%}$ = 760 kV	SIWV = 850 kV $U_{10\%}$ = 680 kV
Length (configuration A)	N	N	N
0,6	1,2E-20	1,5E-14	5,0E-09
3	3,0E-07	8,6E-02	5,4E+02
10	1,2E-02	2,0E+02	1,4E+04
Length (configuration B)	N	N	N
0,6	1,0E-14	1,4E-09	6,0E-05
3	6,0E-10	2,0E-02	4,3E+03
10	3,0E-03	1,9E+02	1,7E+04
Length (configuration C)	N	N	N
0,6	1,2E-05	1,3E+01	1,7E+04
3	9,5E-05	6,0E+01	1,9E+04
10	6,0E-04	5,0E+02	2,0E+04

According to the performance criteria and to a technical and economic analysis, one may choose the optimal SIWV.

E.6   Recommendations

–   The choice of the method: case peak or phase peak may give different results.

–   To optmize the choice of the SIWV of a GIL (considered as self-restoring insulation) or an overhead line, statistical failure rate calculations must be performed. IEC 60071-2 proposes a risk calculation method for M-insulations in parallel. If the voltage distribution along the GIL is uniform, a simplified method can be used (as in this test case). On the contrary, if voltage distribution along GIL is non-uniform, the elementary risk calculation formulation must be used for each regular spaced measurement point i of the GIL. The final risk of failure is a function of the M-calculated risks of failure.

–   The way one interpolates the overvoltage profile must not be relevant in the final result. In other words, the choice of a Gauss or Weibull function, or the choice of $U_{2\%}$, $U_{10\%}$, $U_{16\%}$ or $U_{50\%}$ must be optimized in order to keep a good fitting of the simulated overvoltage distribution.

–   Resonance frequency of each element of the network must be as precise as possible in order to obtain the best results. Some models are usually very difficult to obtain without measurements (transformer, rotating machines). In this case, literature-based assumptions may be made for equivalent equipment.

Annex F
(informative)

Test case 7 (FFO) –
High-frequency arc extinction when switching a reactor

This test case shows a simulation of high-frequency arc extinction phenomena experienced when switching a reactor.

F.1   Experiment

A gas circuit-breaker (GCB) model in Figure F.1 was opened from a closed state, and an impulse voltage generator IG was started synchronously (point A in Figure F.2). A breakdown occurred at point B of Figure F.2. This caused a high-frequency current IHF to flow in circuit C-L-GCB.

The charge in IG was released in the circuit IG-R-L-GCB and a quasi-d.c. current I_0 flowed in the GCB. The GCB current is the sum of I_{HF} and I_0. This I_0 corresponds to the power-frequency current component in actual reactor interruption. At point C in Figure F.2, an arc extinction occurred.

IG Impulse voltage generator (2 µF 100 kV × 12)

C Capacitor (5 000 pF-40 000 pF)

R Resistor (18 kΩ -36 kΩ)

L Reactor (180 µH -870 µH)

  GCB SF$_6$ 300 kV circuit breaker model

B_g Bushing
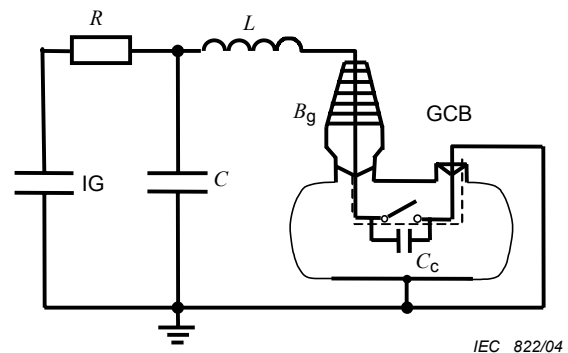
C_c Capacitor between circuit breaker electrodes

IEC 822/04

Figure F.1 – Test circuit (Copyright1998 IEEE [48])
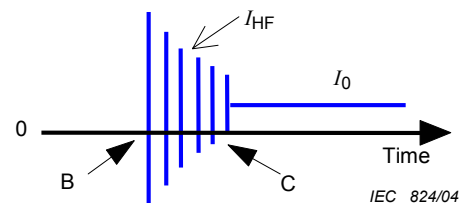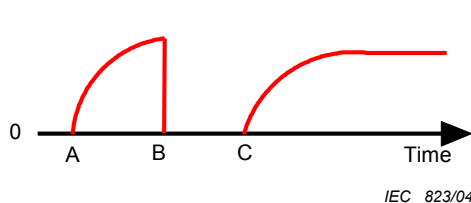

IEC 823/04

IEC 824/04

Figure F.2a – Terminal voltage V_{GCS} of GCB model | **Figure F.2b – Current I_{GCS} of GCB model**

Figure F.2 − Terminal voltage and current of GCB model (Copyright 1998 IEEE [48])

F.2 Input data and modelling for simulation

F.2.1 Arc model and arc parameter

The Mayr arc equation (see Clause B.2) was used to simulate the measured results. Figure F.3 shows arc time constant theta (T in (1) in Clause B.2) and arc power loss N_0 (P in Clause B.2) measured for the GCB model. These parameters are a function of both frequency and the stroke length of the movable electrode of the circuit-breaker (this is expressed in p.u. in the figure).

F.2.2 Circuit for simulation

Figure F.4 shows a circuit used for simulation.

Non-linear equations, including the arc equation that uses arc parameters shown in Figure F.3, for the circuit shown in Figure F.4 were solved by the Runge-Kutta-Gill method.
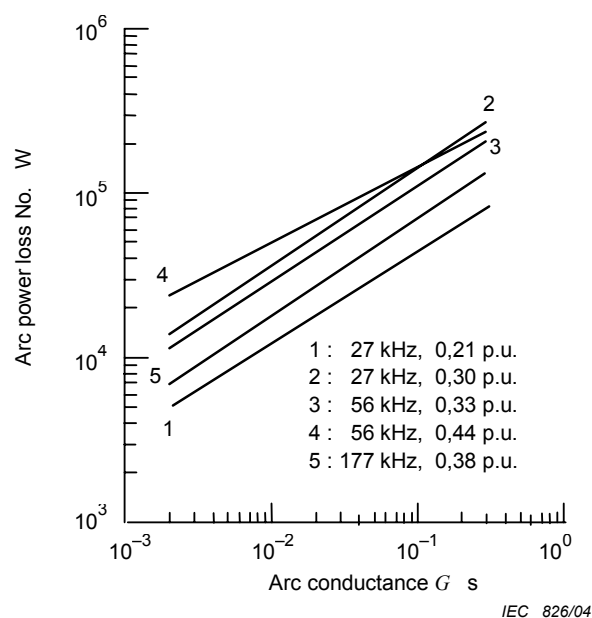

IEC 825/04

IEC 826/04
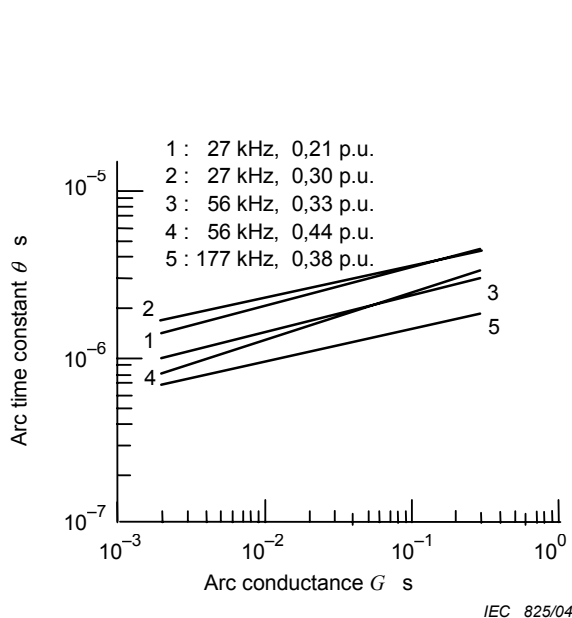
Figure F.3a – Arc time contant θ

Figure F.3b – Arc power loss N_0

Figure F.3 – Measured arc parameter (Copyright 1998 IEEE [48])
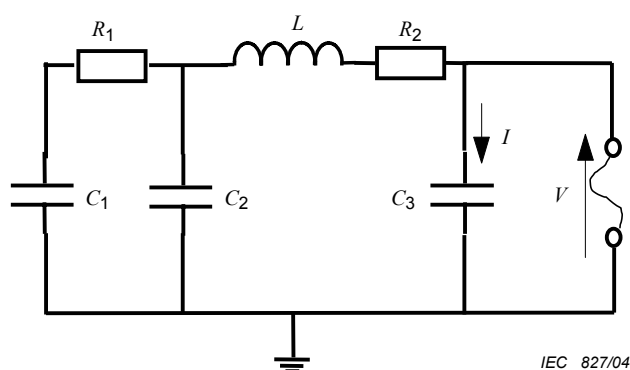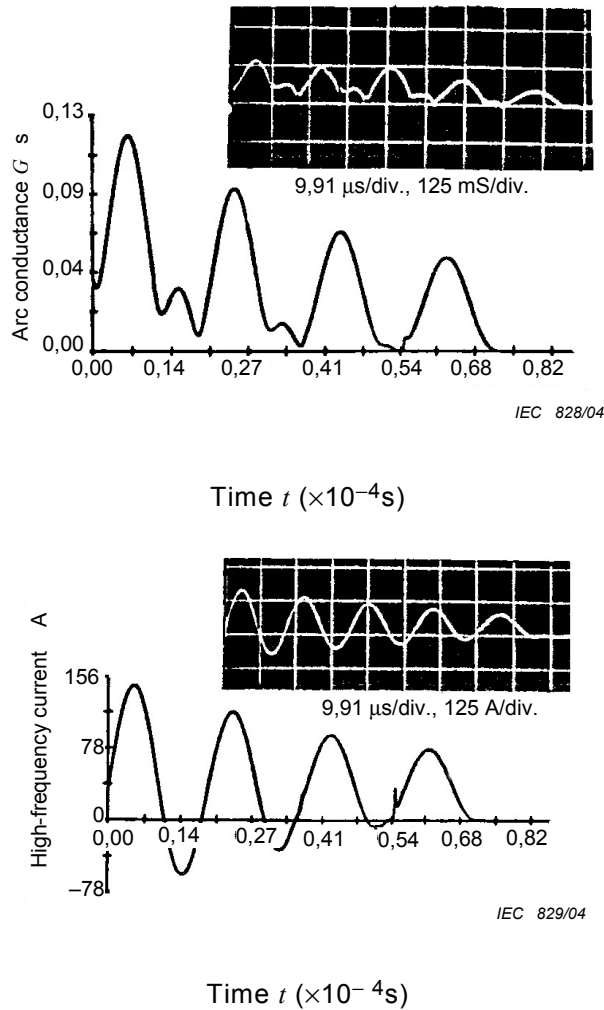

C_1 Capacitance of IG in Figure F.1

C_2 C in Figure F.1

C_3 C_c in Figure F.1

L L in Figure F.1

R R in Figure F.1

R_2 Attenuation resistance of high-frequency current

V, I Arc voltage and arc current

IEC 827/04

Figure F.4 – Circuit used for simulation

F.3   Result and interpretation

Figure F.5 is an example of a comparison between measured and calculated results. This case is for 56 kHz and 0,44 p.u. of stroke length and corresponds to the case where high-frequency arc extinction occurred in the test.

It is said that the possibility of high-frequency arc extinction occurrence can be calculated. However, it should be noted that corresponding arc parameters, which differ from one circuit-breaker to another and depend on conditions such as frequency and strokes, should be used.

9,91 μs/div., 125 mS/div.

IEC 828/04

Time t ($\times 10^{-4}$s)

9,91 μs/div., 125 A/div.

IEC 829/04

Time t ($\times 10^{-4}$s)

**Figure F.5 – Comparison between measured and calculated results
(Copyright 1998 IEEE [48])**

Bibliography

[1] IEC multilingual dictionary, ISBN 2-8273-0003-6, 1983

[2] "Temporary overvoltages: causes, effects and evaluation", CIGRE 1990 session, Paris, WG 33-10- Report 33-210, 1990

[3] "Monograph on GIS Very Fast Transients", CIGRE report, Working Group 33/13.09, 1988

[4] "Guide to procedures for estimating the lightning performance of transmission lines", CIGRE report, reference 63, Working Group 33-01, 1991-10

[5] "Guidelines for representation of network elements when calculating transients", type: CIGRE report, reference 39, Working Group 33-02, 1991-10

[6] Eriksson A.J., Anderson R.N., "A summary of lightning parameters for engineering applications -", CIGRE, 33-06, 1980

[7] "A universal model for accurate calculation of electromagnetic transients on overhead lines and underground cables", IEEE Trans on Power Delivery, Vol 14, No 3, July 1999- A. Morched, B. Gustavsen, M. Tartibi,

[8] "Electrical Transients in Power Systems", Greenwood A., Wiley-Interscience, 1991, ISBN 0-471-62058-0

[9] "Temporary overvoltages – Test Case Results ", Electra Nbr 188, February 2000

[10] "Lightning Performance of Transmission Lines", Anderson J. G., Chapter 12, Transmission Line Reference Book, Electric Power Research Institute, Palo Alto, CA.

[11] "A simplified method for estimating lightning performance of transmission lines", IEEE Working Group on lightning performance of transmission lines, 1985, IEEE Trans. PAS-104, pp 919-932, April 1985.

[12] "Sumer: a software for overvoltage Surges Computation Inside Transformers", MOREAU O., Guillot Y., ICEM 1998

[13] "Practical application of arc physics in circuit breakers " CIGRE WG 13-01 Electra N°118, 1988.

[14] "Interruption of Small Inductive Currents" CIGRE WG 13-02 Electra N° 72, 1980

[15] "A new approach for the calculation of the lightning performance of transmission lines III-a, simplified method: stroke to tower", C.F. Wagner and A.R. Hileman, AIEE trans. (Powers Apparatus and Systems), vol 79, October 1960

[16] "Multistory transmission tower model for lightning surge analysis" IEEE Transactions on Power Delivery, Vol 6, No 3, July 1991 – Masaru Ishii, Eiichi Ohsaki, Tatsuo Kawamura, Kaneyoshi Murotani, Teruya Kouno, Takemitsu Higuchi

[17] "Number of sections necessary for transmission line model used for transient network analyzer" Electrical Engineering of Japan Vol. 95, No 5, 1975 – T. Ono, H. Matsubara

[18] "Lightning Surge Response of Transmission Towers" IEEE Transactions on Power Apparatus and Systems, Vol PAS-102, No 9, September 1983 – W. A. Chisholm, Y. L. Chow

[19] "Travel Time of Transmission Towers" – IEEE Transactions on Power Apparatus and Systems, Vol PAS-104, No 10, October 1985 – W. A. Chisholm, Y. L. Chow

[20] "An investigation on the Closing Dispersion of Circuit Breaker, the Decay Time Constant of Residual Line Voltage and Surge Impedance" – CRIEPI report No. 178012, September 1978 – T. Ono, H. Matsubara

[21] "L'effet de couronne en tension alternative – Pertes et perturbations radioélectriques engendrées par les lignes de transport d'énergie électrique" – 1976, Eyrolles n°24 – C. GARY, M. MOREAU

[22] "Probability Concepts in Engineering Planning and Design – Volume I – Basic Principles", A. Ang, W. H. Tang, 1975, John Wiley and Sons

[23] "Les propriétés de l'air" – Eyrolles n°51 – C. GARY and al.

[24] "EDF Reports on Turbogenerator Saturation Models, DC Converter Station Energization Transients, Airgap Models, Substation Models, Low-Frequency Corona Models, and High-Frequency Corona Models", EPRI document TR-103642s

[25] "Dynamic arc Modeling in EMTP" – July 1985, EMTP Newsletter – M. KIZILCAY

[26] "EMTP-based Model for Grounding System Analysis" – IEEE Winter meeting New-York 1994 – F.E. Menter, L. Grcev

[27] Juan A. Martinez-Velasco: "Computer Analysis of Electric Power System Transients: Selected Readings", IEEE first edition 1997 (ISBN: 0-7803-2318-1)

[28] "Modeling Guidelines for fast front transients" IEEE Transactions on Power Delivery, Vol 11, No 1., January 1996

[29] EMTP Theory Book – Hermann Dommel – University of British Columbia, 1992

[30] "Guidelines for the Evaluation of the Dielectric Strength of External Insulation" – CIGRE Report, Reference 72, Working Group 33-07

[31] "Observation and Analysis of Multiphase Back Flashover on the Okushishiku Test Transmission Line caused by Winter Lightning" – IEEE PE 304 PWRD 0 12 97 – Hideki Motoyama, Kazuo Shinjo, Yasuhiro Matsumoto, Naoki Itamoto .

[32] "Experimental Study and Analysis of Breakdown Characteristics of Long Air Gaps with Short Tail Lightning Impulse" – IEEE Transactions on Power delivery, Vol 11, No 2, April 1996 – H. Motoyama

[33] "Very fast transient phenomena associated with gas insulated substations", CIGRE paper 33/13-09, 1988"

[34] "Switching surges: Part IV – Control and reduction on A.C. transmission lines" – IEEE PS 101, No 8, August 1982 – IEEE Working Group on Switching Surges

[35] "Fast and Accurate Switching Transient Calculations on Transmission Lines with Ground Return Using Recursive Convolutions" – A. Semlyen, A. Dabuleanu – IEEE Transactions on Power Apparatus and Systems, vol PAS-94, n° 2, March/April 1975

[36] "Phase Domain Modeling of Frequency-Dependent Transmission Lines by Means of an ARMA Model" – T. Noda, N. Nagaoka, A. Ametani – IEEE Transactions on Power Delivery, Vol 11, No 1, January 1996

[37] "Direct Phase-Domain Modelling of Frequency-Dependent Overhead Transmission Lines" – H.V. Nguyen, H.W. Dommel, J. R. Marti – IEEE Transactions on Power Delivery – 96 SM 458-0 PWRD

[38] "Damping of numerical noise in the EMTP solution" – V. Brandwajn – EMTP Newsletter, vol 2, Feb 1982.

[39] Solution to the problem of separation of the Hydro-Québec 735-kV system by switchable metal-oxide surge arresters. By G. Saint-Jean, Y. Latour, M. Landry, J. Bélanger (IREQ) and H. Huynh, P. Czech (Hydro-Québec). CIGRÉ 1986 Session. Paper n° 33-01.

[40] A 735-kV Shunt reactor automatic switching system for Hydro-Québec network. By S. Bernard, G. Trudel, G. Scott (TransÉnergie – Hydro-Québec). IEEE, 96 WM 283-2 PWRS.

[41] Hydro-Québec's defence plan against extreme contingencies. By G. Trudel, S. Bernard, G. Scott (TransÉnergie – Hydro-Québec). IEEE, PE-211-PWRS-0-06:1998.

[42] "Estimating the Probability of failure of Equipment as a Result of Direct Lightning Strikes on Transmission Lines" – M. A. Ismaili, P. Bernard, R. Lambert, A. Xemard – PE-071-PWRD-0-01:1999

[43] "A high Frequency Transformer Model for the EMTP" – A. Morched, L. Marti, J. Ottevangers – IEEE TPD, Vol 8, No3, July 1993

[44] "Guide to Lightning Protection Design of Power Stations, Substations and Underground Transmission Lines" – CRIEPI REPORT No 40 – December 95

[45] "Some fundamentals on Capacitance Switching" I B Johnson *et al.*, IEEE August 1955, pp 727-736

[46] "Accurate Modeling of Capacitively Graded Bushing for Calculation of Transient Overvoltages in GIS" – A. Ardito, R. Iorio, G. Santagostino, A. Porrino

[47] "A study of Predischarge Current Characteristics of Long Air Gaps" – T. Shindo and al – IEEE Trans, Vol PAS-104,pp.3262-3268, 1985

[48] "Application of dynamic arc equations to high-frequency arc extinctions in SF_6 gas circuit breakers" – E. ZAIMA, S. Nishiwaki, *et al.* – IEEE TPD Vol 8, No 3, July 1993, pp 1199-1205

[49] "Modeling of metal oxyde surge arresters" – IEEE working Group 3.4.11 – IEEE TPD, Vol 7, January 1992

[50] "Analysis of faulted power systems" P.M. Anderson – IOWA State University Press – 1978

[51] "VFFT in a 765 kV substation" – J. Grandl, A. Eriksson, J. Meppelink, C. Van Der Merwe – CIGRE 33.12 – session 1988

[52] "Principles and recent practices of insulation coordination in Japan" – T. Kawamura, S. Sasaki, T. Ueda, T. Kouno, E. Zaima, Y. Kato – CIGRE Session 2000, 33-109

[53] "Some fundamentals on Capacitance Switching" I. B. Johnson and al, IEEE Aug 1955 pp 727-736

[54] "High Frequency Transformer Models" C. R. Zani *et al.*, CIGRE SC33-97 WG 11 4 IWD

[55] "Control of Overvoltages on Hydro-Quebec 735-kV Series-Compensated System During a Major Electro-Mechanical Transient Disturbance" – Que Bui-Van *et al.* – International Conference on Power Systems Transients 2001.

[56] "Harmonics, characteristic parameters, methods of study, estimates of existing values of the network" – CIGRE study committee 36 – Electra nbr 77 – July 81

[57] "The calculation of switching surges – III. Transmission line representation for energization and re-energization studies with complex feeding networks" – CIGRE study committee 13 – Electra Nbr 62

[58] "The design of specially bonded cable systems" – CIGRE study committee 21 – Electra Nbr 28 – May 73

[59] "Experimental and analytical studies of the effect of non-standard waveshapes on the impulse strength of external insulation" – R.O. Caldwell, M. Darveniza – IEEE Trans, Pwr App and Syst, Vol 90, pp 1909-1915, 1979

[60] "Metal oxide surge arresters in A.C. systems" – CIGRE brochure 60.

[61] "Phase-to-Phase Insulation Co-ordination", Electra Nbr 64, May 1979

[62] "Temporary Overvoltages: causes, effects and evaluation", CIGRE 1990, Report 33-210

[63] "Energization of a no-load transformer for power restoration purposes: modeling and validation by on site tests", IEEE Winter meeting Singapor 2000 – M. Rioual, C. Sicre

[64] IEC 60071-5:2002, *Insulation co-ordination – Part 5: Procedures for high-voltage direct current (HVDC) converter stations*

[65] IEC 62271-100:2001, *High-voltage switchgear and controlgear – Part 100: High-voltage alternating-current circuit-breakers*

[66] IEC 62271-102: 2001, *High-voltage switchgear and controlgear – Part 102: Alternating current disconnectors and earthing switches*

—————

**PD IEC TR
60071-4:2004**

BSI — British Standards Institution

BSI is the independent national body responsible for preparing British Standards. It presents the UK view on standards in Europe and at the international level. It is incorporated by Royal Charter.

Revisions

British Standards are updated by amendment or revision. Users of British Standards should make sure that they possess the latest amendments or editions.

It is the constant aim of BSI to improve the quality of our products and services. We would be grateful if anyone finding an inaccuracy or ambiguity while using this British Standard would inform the Secretary of the technical committee responsible, the identity of which can be found on the inside front cover.
Tel: +44 (0)20 8996 9000. Fax: +44 (0)20 8996 7400.

BSI offers members an individual updating service called PLUS which ensures that subscribers automatically receive the latest editions of standards.

Buying standards

Orders for all BSI, international and foreign standards publications should be addressed to Customer Services. Tel: +44 (0)20 8996 9001.
Fax: +44 (0)20 8996 7001. Email: orders@bsi-global.com. Standards are also available from the BSI website at http://www.bsi-global.com.

In response to orders for international standards, it is BSI policy to supply the BSI implementation of those that have been published as British Standards, unless otherwise requested.

Information on standards

BSI provides a wide range of information on national, European and international standards through its Library and its Technical Help to Exporters Service. Various BSI electronic information services are also available which give details on all its products and services. Contact the Information Centre.
Tel: +44 (0)20 8996 7111. Fax: +44 (0)20 8996 7048. Email: info@bsi-global.com.

Subscribing members of BSI are kept up to date with standards developments and receive substantial discounts on the purchase price of standards. For details of these and other benefits contact Membership Administration.
Tel: +44 (0)20 8996 7002. Fax: +44 (0)20 8996 7001.
Email: membership@bsi-global.com.

Information regarding online access to British Standards via British Standards Online can be found at http://www.bsi-global.com/bsonline.

Further information about BSI is available on the BSI website at http://www.bsi-global.com.

Copyright

Copyright subsists in all BSI publications. BSI also holds the copyright, in the UK, of the publications of the international standardization bodies. Except as permitted under the Copyright, Designs and Patents Act 1988 no extract may be reproduced, stored in a retrieval system or transmitted in any form or by any means – electronic, photocopying, recording or otherwise – without prior written permission from BSI.

This does not preclude the free use, in the course of implementing the standard, of necessary details such as symbols, and size, type or grade designations. If these details are to be used for any other purpose than implementation then the prior written permission of BSI must be obtained.

Details and advice can be obtained from the Copyright & Licensing Manager.
Tel: +44 (0)20 8996 7070. Fax: +44 (0)20 8996 7553.
Email: copyright@bsi-global.com.

BSI
389 Chiswick High Road
London
W4 4AL